

MUSE-BB: A Decomposition Algorithm for Nonconvex Two-Stage Problems using Strong Multisection Branching

Marco Langiu^{a,b} , Manuel Dahmen^b , Dominik Bongartz^c , Alexander Mitsos^{d,b,a,*} 

^a Process Systems Engineering (AVT.SVT), RWTH Aachen University, Aachen 52074, Germany

^b Institute of Energy and Climate Research, Energy Systems Engineering (IEK-10), Forschungszentrum Jülich GmbH, Jülich 52425, Germany

^c Department of Chemical Engineering, KU Leuven, 3001 Leuven, Belgium

^d JARA-ENERGY, Jülich 52425, Germany

Abstract: We present MUSE-BB, a branch-and-bound (B&B) based decomposition algorithm for the deterministic global solution of nonconvex two-stage stochastic programming problems. In contrast to three recent decomposition algorithms, which solve this type of problem in a projected form by nesting an inner B&B in an outer B&B on the first-stage variables, we branch on all variables within a single B&B tree. This results in a higher convergence order of the lower bounding scheme, avoids repeated consideration of subdomains, inherent to the nesting of B&B searches, and enables the use of cheaper subproblems. In particular, when branching on second-stage variables, we employ a multisection variant of strong-branching, in which we simultaneously consider one candidate variable from each scenario for branching. By our decomposable lower bounding scheme, the resulting subproblems are independent and can be solved in parallel. We then use strong-branching scores to filter less promising candidate variables and only generate child nodes corresponding to a multisection involving the remaining variables by combining the appropriate subproblem results. We prove finite ε_f -convergence, and demonstrate that the lower-bounding scheme of MUSE-BB has at least first-order convergence under the mild assumption of Lipschitz continuous functions and relaxations. MUSE-BB is implemented and made available open source, as an extension of our deterministic global solver for mixed-integer nonlinear programs, MAiNGO, with OpenMP-parallelization of the decomposable subroutines. Numerical results show that MUSE-BB requires less CPU time than solving the deterministic equivalent using the standard version of MAiNGO; moreover, the parallelized decomposition allows for further reduction in wall time.

Keywords: two-stage stochastic programming, decomposition, multisection, convergence analysis, clustering

1 Introduction

A standard formulation for optimization under uncertainty is two-stage stochastic programming (Birge and Louveaux, 2011), typically applied when long-term (“here and now”) decisions are taken prior to the realization of uncertain scenarios, and then recourse (“wait and see”) decisions are taken in response to the realized scenario. This paradigm may also be applied in situations where future events can be expected to occur with a particular *frequency*, i.e., the scenarios do not represent an uncertain, but rather time-variable future, as in design and operation problems in process engineering (Yunt et al., 2008; Langiu, Dahmen, and Mitsos, 2022). In the following we will not distinguish between the two cases and treat both via “probabilities”.

1.1 Problem Formulation and Notation

The overall two-stage problem (TSP) takes the form

$$\begin{aligned} f^{\mathcal{X},\mathcal{Y}} := \min_{\mathbf{x} \in \mathcal{X}} f_{\text{I}}(\mathbf{x}) + \sum_{s \in \mathcal{S}} w_s f_{\text{II},s}^{\mathcal{Y}_s}(\mathbf{x}) \\ \text{s. t. } \mathbf{g}_{\text{I}}(\mathbf{x}) \leq \mathbf{0}, \end{aligned} \quad \text{TSP}^{\mathcal{X},\mathcal{Y}}$$

where $\mathcal{X} \subseteq \mathbb{R}^{N_x}$, $\mathcal{Y}_s \subseteq \mathbb{R}^{N_y}$, for each $s \in \mathcal{S}$, and $\mathcal{Y} \subseteq \mathbb{R}^{N_s N_y}$, such that \mathcal{X} and $\mathcal{Y} := \times_{s \in \mathcal{S}} \mathcal{Y}_s$, are bounded hyperrectangles, and thus compact sets. The set of considered scenarios \mathcal{S} is assumed to have finite cardinality $N_s := |\mathcal{S}| \geq 1$, and each element $s \in \mathcal{S}$ is assigned a probability $w_s \in (0, 1]$, $\sum_{s \in \mathcal{S}} w_s = 1$. Throughout this work, we omit variable domains and other parameters in references to optimization problems, if they are irrelevant, e.g., as in TSP. The limitation to values in $(0, 1]$ makes the sum in the objective a convex combination, allowing for more concise definitions and proofs. Other weights can be equivalently used via appropriate scaling and redefinition of the objective.

*Alexander Mitsos, Process Systems Engineering (AVT.SVT), RWTH Aachen University, Aachen 52074, Germany
E-mail: amitsos@alum.mit.edu

For each scenario s , the value of *second-stage optimal value function* $f_{\text{II},s}^{\mathcal{Y}_s}$, also known as *optimal recourse function* corresponds to the optimal objective value of the following recourse problem (RP) for a fixed value of \mathbf{x} , and second-stage domain \mathcal{Y}_s :

$$\begin{aligned} f_{\text{II},s}^{\mathcal{Y}_s}(\mathbf{x}) &:= \min_{\mathbf{y}_s \in \mathcal{Y}_s} f_{\text{II},s}(\mathbf{x}, \mathbf{y}_s) \\ &\text{s. t. } \mathbf{g}_{\text{II},s}(\mathbf{x}, \mathbf{y}_s) \leq \mathbf{0}. \end{aligned} \quad \text{RP}_{\mathcal{Y}_s}^{\mathcal{Y}_s}(\mathbf{x})$$

The decisions that need to be made in the first and second stage are captured by the variable vectors \mathbf{x} and \mathbf{y}_s , respectively. As a result, the problem $\text{TSP}^{\mathcal{X},\mathcal{Y}}$ and its optimal value $f^{\mathcal{X},\mathcal{Y}}$ are parameterized by the domains \mathcal{X} and \mathcal{Y} , whereas $\text{RP}_{\mathcal{Y}_s}^{\mathcal{Y}_s}(\mathbf{x})$ and its optimal value $f_{\text{II},s}^{\mathcal{Y}_s}(\mathbf{x})$ are parameterized by fixed first-stage variable values \mathbf{x} and the domain \mathcal{Y}_s . $f_{\text{I}} : \mathcal{X} \mapsto \mathbb{R}$ and $f_{\text{II},s} : \mathcal{X} \times \mathcal{Y}_s \mapsto \mathbb{R}$ denote the scalar-valued first- and second-stage objective functions, and $\mathbf{g}_{\text{I}} : \mathcal{X} \mapsto \mathbb{R}^{N_{\text{I}}}$ and $\mathbf{g}_{\text{II},s} : \mathcal{X} \times \mathcal{Y}_s \mapsto \mathbb{R}^{N_{\text{II}}}$ the vector-valued first- and second-stage constraint functions. Note that we assume the number of second-stage variables N_{y_s} , and second-stage constraints $N_{\text{II},s}$, to be equal for all scenarios. This assumption is naturally satisfied in many applications of two stage problems, e.g., system design and operation. While the generalization to different numbers N_{y_s} , and $N_{\text{II},s}$, for each scenario s does not pose substantial complication, we only consider the simpler case for ease of exposition.

For conciseness, we aggregate the vectors \mathbf{y}_s into the overall vector of second-stage variables $\mathbf{y} \in \mathcal{Y}$:

$$\mathbf{y} := \begin{pmatrix} \mathbf{y}_1 \\ \vdots \\ \mathbf{y}_{N_s} \end{pmatrix} = \begin{pmatrix} y_{1,1} \\ \vdots \\ y_{1,N_y} \\ \vdots \\ y_{N_s,N_y} \end{pmatrix} \quad (\mathbf{y})$$

We denominate any scalar element $y_{s,i}$ of \mathbf{y} or \mathbf{y}_s as a *second-stage variable* and refer to the collection of elements at the same position i in \mathbf{y}_s for different values of s as *instances of a second-stage variable*. Furthermore, we define the *scenario objective functions* $f_s : \mathcal{X} \times \mathcal{Y}_s \mapsto \mathbb{R}$

$$f_s(\mathbf{x}, \mathbf{y}_s) := f_{\text{I}}(\mathbf{x}) + f_{\text{II},s}(\mathbf{x}, \mathbf{y}_s) \quad (f_s)$$

and the *overall objective function* $f : \mathcal{X} \times \mathcal{Y} \mapsto \mathbb{R}$

$$\begin{aligned} f(\mathbf{x}, \mathbf{y}) &:= f_{\text{I}}(\mathbf{x}) + \sum_{s \in \mathcal{S}} w_s f_{\text{II},s}(\mathbf{x}, \mathbf{y}_s) \\ &= \sum_{s \in \mathcal{S}} w_s (f_{\text{I}}(\mathbf{x}) + f_{\text{II},s}(\mathbf{x}, \mathbf{y}_s)) \\ &= \sum_{s \in \mathcal{S}} w_s f_s(\mathbf{x}, \mathbf{y}_s), \end{aligned} \quad (f)$$

where the equalities follow from our assumptions on the weights w_s .

Using these definitions, $\text{TSP}^{\mathcal{X},\mathcal{Y}}$ can be equivalently stated as the following single-stage optimization problem, also known as the ‘*extensive form*’ or the ‘*deterministic equivalent*’:

$$\begin{aligned} f^{\mathcal{X},\mathcal{Y}} &= \min_{\substack{\mathbf{x} \in \mathcal{X} \\ \mathbf{y} \in \mathcal{Y}}} f(\mathbf{x}, \mathbf{y}) \\ &\text{s. t. } \mathbf{g}_{\text{DE}}(\mathbf{x}, \mathbf{y}), \end{aligned} \quad \text{DE}^{\mathcal{X},\mathcal{Y}}$$

where the vector-valued constraint function $\mathbf{g}_{\text{DE}} : \mathcal{X} \times \mathcal{Y} \mapsto \mathbb{R}^{N_g^{\text{DE}}}$, groups all $N_g^{\text{DE}} := N_{\text{I}} + N_s N_{\text{II}}$ constraints in DE, and is defined as

$$\mathbf{g}_{\text{DE}}(\mathbf{x}, \mathbf{y}) = \begin{pmatrix} g_{\text{DE},1}(\mathbf{x}, \mathbf{y}) \\ \vdots \\ g_{\text{DE},N_g^{\text{DE}}}(\mathbf{x}, \mathbf{y}) \end{pmatrix} := \begin{pmatrix} g_{\text{I},1}(\mathbf{x}) \\ \vdots \\ g_{\text{I},N_{\text{I}}}(\mathbf{x}) \\ g_{\text{II},1,1}(\mathbf{x}, \mathbf{y}_1) \\ \vdots \\ g_{\text{II},N_s,N_{\text{II}}}(\mathbf{x}, \mathbf{y}_{N_s}) \end{pmatrix}. \quad (\mathbf{g}_{\text{DE}})$$

The two problems $\text{TSP}^{\mathcal{X},\mathcal{Y}}$ and $\text{DE}^{\mathcal{X},\mathcal{Y}}$ are equivalent in the sense that their globally and locally optimal solution points and optimal objective values coincide if they exist, whereas if one of the formulations is infeasible or unbounded, so is the other, see e.g., (Yunt et al., 2008). We are interested in the case where all functions in DE may be nonconvex. We limit the theoretical considerations, implementation, and numerical results to continuous variables. Thus, we do not explicitly address issues pertaining to discrete variables in the following. The presence of discrete variables would however not pose substantial complication.

1.2 Literature Overview

Solving $\text{TSP}^{\mathcal{X},\mathcal{Y}}$ by applying general-purpose branch and bound (B&B) solvers (e.g., Androulakis, Maranas, and Floudas, 1995; Vigerske and Gleixner, 2017; Bongartz et al., 2018; Belotti, 2019; Sahinidis, 2024) to $\text{DE}^{\mathcal{X},\mathcal{Y}}$ is possible, typically amounting to solution of relaxations of $\text{DE}^{\mathcal{X}^n,\mathcal{Y}^n}$ in every B&B node. Here $\mathcal{X}^n \in \mathbb{IX}$ and $\mathcal{Y}^n \in \mathbb{IY}$, where \mathbb{IX} and \mathbb{IY} denote the sets of nonempty, compact interval subsets of \mathcal{X} and \mathcal{Y} . However, as B&B is intrinsically exponential in the number of (branched) variables, this approach has worst-case exponential runtime in the number of scenarios. This has motivated the development of decomposition algorithms capable of exploiting the special structure of TSP for a more efficient solution. In these algorithms, multiple independent subproblems are solved instead of instances of DE , which can result in a reduction of computational time required for the solution, as the subproblems are generally much smaller and thus cheaper to solve. In the best case, such decomposition algorithms achieve linear scaling with the number of scenarios N_s , i.e., an arithmetic complexity of $\mathcal{O}(N_s)$. Furthermore, the subproblems are independent and may thus be solved in parallel, resulting in significant additional reductions of wall time.

Historically, decomposition strategies have predominantly been developed for certain subclasses of TSP , e.g., those restricted to linear functions and either only continuous (e.g., Dantzig and Wolfe, 1960; Benders, 1962) or mixed-integer variables (e.g., Laporte and Louveaux, 1993; Carøe and Schultz, 1999), or those restricted to convex nonlinear functions (e.g., Generalized Benders Decomposition (GBD) Geoffrion, 1972). More recently, algorithms addressing subclasses of TSP allowing for certain nonconvexities, but imposing additional structural assumptions have also been proposed (e.g., Li, Tomaszgard, and Barton, 2011; Li, Sundaramoorthy, and Barton, 2014; Karuppiyah and Grossmann, 2007; Khajavirad and Michalek, 2009; Li and Cui, 2024). In the most general case, any of the functions in TSP may be nonconvex, and no additional structural assumptions are imposed. Two algorithm variants addressing this case are proposed by Ogbe and Li, 2019, however, both variants consider elements of \mathbf{y} which introduce nonconvexity as complicating variables in addition to \mathbf{x} . Thus, in the worst case subproblems have a similar size as the original problem, diminishing the benefits of decomposition.

Three further recent algorithms all employ B&B exclusively on the first-stage variables: (i) Kannan, 2018 propose a modified Lagrangian relaxation in which so called nonanticipativity constraints (cf. Section 2) are dualized. The resulting Lagrangian problem is thus still a nonconvex two-stage problem but exhibits additional structure and can thus be solved in a decomposable manner using the algorithm proposed by Li, Tomaszgard, and Barton, 2011; Li, Sundaramoorthy, and Barton, 2014. As a result, only the continuous first-stage variables need to be branched. (ii) Cao and Zavala, 2019 propose another B&B algorithm that obtains lower bounds in each node via global solutions to separate, but generally nonconvex scenario subproblems, resulting from simply dropping the nonanticipativity constraints. (iii) Li and Grossmann, 2019 use mixed integer linear or convex mixed integer nonlinear relaxations based on DE as lower bounding problems, which are solved via GBD. Cuts from Lagrangean subproblems are added to a Benders master problem and cutting planes for convexification are added to the Benders subproblems. All three algorithms (Kannan, 2018; Cao and Zavala, 2019; Li and Grossmann, 2019), solve N_s independent subproblems on $\mathcal{X}^n \times \mathcal{Y}_s$ at each B&B node n , where $\mathcal{X}^n \in \mathbb{IX}$. While this implies that the computational work of the bounding operation scales linearly in N_s , and further, that the subproblems can be solved in parallel, linear scaling of the overall algorithms with N_s would additionally require that the number of nodes in the outer B&B search is independent of the number of scenarios. Note, however, that within a family of problems with variable number of scenarios, the quality of the lower bounds can be expected to depend on the number of scenarios. Thus for a given tolerance, the number of nodes visited by the outer B&B search may well depend on the number of scenarios, despite branching only on \mathbf{x} . Thus while these types of algorithms are typically much more efficient for solving DE compared to general-purpose B&B, they have not been shown to scale linearly with the number of scenarios.

1.3 Challenges of Existing Algorithms

Recently Robertson, Cheng, and Scott, 2020 observed that all three algorithms, addressing general nonconvex instances of TSP (Kannan, 2018; Cao and Zavala, 2019; Li and Grossmann, 2019) fall into the category of *projection-based decomposition algorithms* (PBDAs). Algorithms in this category directly solve $\text{TSP}^{\mathcal{X},\mathcal{Y}}$ (which can be considered a projection of $\text{DE}^{\mathcal{X},\mathcal{Y}}$ onto the \mathcal{X} space) by considering only the first-stage variables via second-stage optimal value functions $f_{\text{II},s}^{\mathcal{Y}_s}$. Robertson, Cheng, and Scott, 2020 argue that this approach likely suffers from the cluster effect, a phenomenon of some spatial B&B algorithms, where a large number of nodes may need to be visited near approximate global minimizers (Kearfott and Du, 1993; Du and Kearfott, 1994; Wechsung, Schaber, and Barton, 2014). To avoid this effect, the relaxations of both objective and constraints need to have a sufficiently high convergence order (Kannan and Barton, 2017b). Note that throughout the article we refer to convergence order in the sense of Hausdorff, unless stated otherwise. The convergence order of relaxations typically used in algorithms for (mixed-integer) nonlinear programs has been analyzed in a series of articles (cf. Bompadre and Mitsos, 2011; Najman and Mitsos, 2016; Kannan and Barton, 2017b; Cao, Song, and Khan, 2019). Robertson, Cheng, and Scott, 2020 show that as a result of performing search in the \mathcal{X} domain only, PBDAs need to construct relaxations of the so-called *scenario value functions*:

$$f_s^{\mathcal{X},\mathcal{Y}_s}(\mathbf{x}) := \begin{cases} f_{\text{I}}(\mathbf{x}) + f_{\text{II},s}^{\mathcal{Y}_s}(\mathbf{x}), & \mathbf{x} \in \mathcal{F}_s^{\mathcal{X},\mathcal{Y}_s} \\ +\infty, & \text{otherwise} \end{cases},$$

where $\mathcal{F}_s^{\mathcal{X},\mathcal{Y}_s}$ are the feasible subsets of \mathcal{X} in scenario s :

$$\mathcal{F}_s^{\mathcal{X},\mathcal{Y}_s} := \{\mathbf{x} \in \mathcal{X} \mid \mathbf{g}_{\text{I}}(\mathbf{x}) \leq \mathbf{0}, \exists \mathbf{y}_s \in \mathcal{Y}_s : \mathbf{g}_{\text{II},s}(\mathbf{x}, \mathbf{y}_s) \leq \mathbf{0}\}.$$

Adopting the convention for the minimum of an infeasible problem to be infinite, the weighted sum over the scenario value functions is equivalent to the objective of TSP. Robertson, Cheng, and Scott, 2020 demonstrate that only branching on \mathbf{x} generally causes $f_s^{\mathcal{X},\mathcal{Y}_s}$ to be nonsmooth, which in turn limits the achievable convergence order. In particular, even the ideal PBDA, which uses the tightest-possible relaxation for each $f_s^{\mathcal{X},\mathcal{Y}_s}$, i.e., the convex envelope, generally has a convergence order below 1, and only achieves first-order convergence if all $f_s^{\mathcal{X},\mathcal{Y}_s}$ are Lipschitz. On the other hand, they show that this ideal relaxation has second-order convergence if $f_s^{\mathcal{X},\mathcal{Y}_s}$ are twice continuously differentiable, and furthermore, that the algorithm of Li and Grossmann, 2019 is equivalent to using this ideal relaxation, if optimal dual multipliers λ_s^* are used. Note that in general, generating convex envelopes of arbitrary $f_s^{\mathcal{X},\mathcal{Y}_s}$ (via optimal dual multipliers or otherwise) is prohibitively expensive. Furthermore, even for convex f , \mathbf{g}_{I} and $\mathbf{g}_{\text{II},s}$, and even in the absence of discrete variables, the $f_s^{\mathcal{X},\mathcal{Y}_s}$ are not guaranteed to be smooth, but rather only lower semi-continuous (cf., e.g., Theorem 35, Chapter 3 of Birge and Louveaux, 2011). In summary, using PBDAs, i.e., branching on \mathbf{x} only, limits convergence order to below one in general. As a result Robertson, Cheng, and Scott, 2020 state that PBDAs are expected to suffer from clustering, and suggest to search for alternative decomposition approaches, rather than for better relaxations in PBDAs. While a higher convergence order can certainly be advantageous, we point out that this conclusion might be overly pessimistic, as the occurrence of clustering is determined by the interplay of both convergence order, and growth order of the objective and constraint functions (also see Kannan and Barton, 2017b).

Nevertheless, the three aforementioned PBDAs (Kannan, 2018; Cao and Zavala, 2019; Li and Grossmann, 2019) may potentially have further issues. First, for each node n with domain $\mathcal{X}^n \in \mathbb{X}$, visited by the outer B&B algorithm searching on \mathcal{X} , an inner algorithm searches on $\mathcal{X}^n \times \mathcal{Y}_s$ during the solution of the subproblems. The consideration of \mathbf{x} in both levels will therefore result in repeated consideration of the same domain, constituting a duplication of work. Second, in the general case, where there are nonconvexities in the second stage (through nonconvex objectives or constraints, or integer variables), the lower bounding subproblems must at least occasionally be solved globally to guarantee convergence. In addition, Kannan, 2018 and Cao and Zavala, 2019 also solve their upper bounding problems globally, while Li and Grossmann, 2019 do not explicitly state whether their solutions are local or global. Finally, the nesting of these expensive bounding routines in an outer B&B algorithm, bears resemblance to early ideas for solving general mixed-integer nonlinear programming problems, which considered branching on the integer variables and globally solving a continuous nonconvex problem in each node. However, such ideas have been abandoned since nested exponential approaches are considered computationally unfavorable (Smith and Pantelides, 1997).

1.4 A new Decomposition Algorithm for TSP

To improve convergence orders of the relaxations, and to avoid duplication of work and the nesting of expensive search routines, we propose an alternative decomposition algorithm for TSP. Similar to solving DE via a classical B&B algorithm, we explicitly branch on first- and second-stage variables, however, we still make use of the structure inherent to TSP to obtain decomposable bounding subproblems for each scenario. We call our proposed algorithm *MUSE-BB*, as it combines classical scenario decomposition with **multisection** (Karmakar, Mahato, and Bhunia, 2009) in a **B&B** algorithm. Efficient branching on multiple instances of a particular second-stage variable is made possible by the fact that bounding subproblems for each scenario are independent of second-stage variable instances from other scenarios: While branching a node on N_s second-stage variables results in 2^{N_s} child nodes, only $2 N_s$ independent subproblems need to be solved to update their lower bounds. Each child node can then be generated by combining bounds and variable domains from N_s out of the $2 N_s$ independent subproblems. To limit memory requirements as well as the number of generated child nodes with poor lower bounds, we filter the N_s candidate variables based on strong-branching scores, and additionally impose an upper limit on the number of partitions, used for creating child nodes.

Like classical B&B algorithms, MUSE-BB searches the full variable space. Thus in the worst-case, its runtime is expected to be exponential in N_s . However, the combination of decomposition with multisection allows for a more efficient exploration of the search space than with classical algorithms. Moreover, we analyze the convergence order of the lower bounding scheme used in MUSE-BB. We show that while this convergence order is generally lower than in classical B&B algorithms, it is at least as high as in PBDAs, and can be strictly larger when the scenario value functions $f_s^{\mathcal{X}, \mathcal{Y}_s}$ are not Lipschitz. In particular we show that the lower bounding scheme of MUSE-BB is (at least) first-order convergent if all functions and convex relaxations are Lipschitz. While our lower bounding scheme is generally not second-order convergent, we discuss a possible extension of MUSE-BB, whose lower bounding scheme achieves second-order convergence at unconstrained minimizers by dualizing nonanticipativity constraints instead of dropping them. Overall, the results indicate that MUSE-BB and its extension at least partially avoid issues with the cluster effect.

The remainder of the article is structured as follows: Section 2 gives a brief review of the decomposable bounding subproblems used in scenario decomposition algorithms for TSP. In Section 3 we motivate the use of multisection branching of second-stage variables to efficiently incorporate such decomposable bounding problems in a B&B algorithm, branching on both \mathbf{x} and \mathbf{y} . Section 4 presents the MUSE-BB algorithm, incorporating this multisection branching. It includes implementation details followed by a formal statement of the MUSE-BB algorithm and subroutines. In Section 5 we present convergence results for both our lower bounding problems, and the overall algorithm. We show that under mild conditions MUSE-BB converges to an ε_f -optimal solution in finite time for any $\varepsilon_f > 0$. Section 6 presents the results of computational experiments on a small test problem, highlighting the effect of different parameters on MUSE-BB, and Section 7 summarizes the results and gives an outlook on future work.

2 Decomposable Bounding Subproblems for TSP

In this section we review how bounds on TSP can be obtained from separate subproblems for each scenario. Since this approach trivially enables both parallelization and linear scaling of the computational work for bounding with N_s , its variants are the basis of many existing decomposition algorithms, as well as for MUSE-BB. The principal idea for decomposable bounding routines is that first-stage variables are complicating, because they appear in the objectives and constraints of all scenarios. Therefore, the problem can be decoupled by scenario, by either introducing independent copies of \mathbf{x} , or fixing its value. As shown in the following, these two cases result in subproblems which respectively provide lower and upper bounds on the optimal objective value $f^{\mathcal{X}, \mathcal{Y}}$ of $\text{TSP}^{\mathcal{X}, \mathcal{Y}}$.

An equivalent representation of $\text{DE}^{\mathcal{X}, \mathcal{Y}}$ and thus $\text{TSP}^{\mathcal{X}, \mathcal{Y}}$ is the lifting obtained by introducing a copy \mathbf{x}_s of \mathbf{x} for each scenario s and enforcing the equality of these copies, resulting in the following *nonanticipativity problem*.

$$\begin{aligned}
 f^{\mathcal{X}, \mathcal{Y}} &= \min_{\substack{\mathbf{x}_s \in \mathcal{X} \\ \mathbf{y} \in \mathcal{Y}}} \sum_{s \in \mathcal{S}} w_s f_s(\mathbf{x}_s, \mathbf{y}_s) \\
 \text{s. t. } & \sum_{s \in \mathcal{S}} \mathbf{H}_s \mathbf{x}_s = \mathbf{0} \\
 & \mathbf{g}_I(\mathbf{x}_s) \leq \mathbf{0} \quad \forall s \in \mathcal{S} \\
 & \mathbf{g}_{II,s}(\mathbf{x}_s, \mathbf{y}_s) \leq \mathbf{0} \quad \forall s \in \mathcal{S}.
 \end{aligned}
 \tag{DE}_{\text{NAC}}^{\mathcal{X}, \mathcal{Y}}$$

In DE_{NAC} , the first set of constraints enforces equality of all \mathbf{x}_s , thus, the coupling is moved to these so called

nonanticipativity constraints (NACs), where \mathbf{H}_s are appropriately shaped, sparse matrices. For simplicity, we assume the following, specific form of the NACs, also used, e.g., in Li and Grossmann, 2019:

$$\mathbf{x}_1 - \mathbf{x}_s = \mathbf{0} \quad \forall s \in \mathcal{S} \setminus \{1\}. \quad (\text{NACs})$$

Due to the linearity of the NACs, dualizing them with $N_s - 1$ multiplier vectors $\boldsymbol{\pi}_s \in \mathbb{R}^{N_x}$, $s \in \mathcal{S} \setminus \{1\}$ removes the coupling, as it allows to define the vector $\boldsymbol{\lambda} := (\boldsymbol{\lambda}_1, \dots, \boldsymbol{\lambda}_{N_s})$, consisting of scenario-specific multiplier subvectors

$$\begin{aligned} \boldsymbol{\lambda}_1 &:= - \sum_{s \in \mathcal{S} \setminus \{1\}} \boldsymbol{\pi}_s / w_s, \\ \boldsymbol{\lambda}_s &:= \boldsymbol{\pi}_s / w_s \quad s \in \mathcal{S} \setminus \{1\}. \end{aligned}$$

Note that inherently,

$$\sum_{s \in \mathcal{S}} w_s \boldsymbol{\lambda}_s = \mathbf{0}. \quad (1)$$

The resulting dualization gives rise to the *Lagrangian relaxation*

$$\begin{aligned} f_{\text{LR}}^{\mathcal{X}, \mathcal{Y}}(\boldsymbol{\lambda}) &:= \min_{\substack{\mathbf{x}_s \in \mathcal{X} \\ \mathbf{y}_s \in \mathcal{Y}}} \sum_{s \in \mathcal{S}} w_s [f_s(\mathbf{x}_s, \mathbf{y}_s) + \boldsymbol{\lambda}_s^\top \mathbf{x}_s] \\ \text{s. t. } &\mathbf{g}_I(\mathbf{x}_s) \leq \mathbf{0} \quad \forall s \in \mathcal{S} \\ &\mathbf{g}_{\text{II},s}(\mathbf{x}_s, \mathbf{y}_s) \leq \mathbf{0} \quad \forall s \in \mathcal{S}. \end{aligned} \quad \text{LR}^{\mathcal{X}, \mathcal{Y}}$$

By weak duality, the value $f_{\text{LR}}^{\mathcal{X}, \mathcal{Y}}(\boldsymbol{\lambda})$ provides a lower bound to $f^{\mathcal{X}, \mathcal{Y}}$ for any $\boldsymbol{\lambda}$ satisfying Eq. (1) (cf. e.g., Dür and Horst, 1997). Furthermore, this bound can be obtained by solving the N_s separate *Lagrangian subproblems*

$$\begin{aligned} f_{\text{LSP},s}^{\mathcal{X}, \mathcal{Y}_s}(\boldsymbol{\lambda}_s) &:= \min_{\substack{\mathbf{x}_s \in \mathcal{X} \\ \mathbf{y}_s \in \mathcal{Y}_s}} f_s(\mathbf{x}_s, \mathbf{y}_s) + \boldsymbol{\lambda}_s^\top \mathbf{x}_s \\ \text{s. t. } &\mathbf{g}_I(\mathbf{x}_s) \leq \mathbf{0} \\ &\mathbf{g}_{\text{II},s}(\mathbf{x}_s, \mathbf{y}_s) \leq \mathbf{0}, \end{aligned} \quad \text{LSP}_s^{\mathcal{X}, \mathcal{Y}_s}$$

and calculating the Lagrangian relaxation based lower bound as

$$f_{\text{LR}}^{\mathcal{X}, \mathcal{Y}}(\boldsymbol{\lambda}) := \sum_{s \in \mathcal{S}} w_s f_{\text{LSP},s}^{\mathcal{X}, \mathcal{Y}_s}(\boldsymbol{\lambda}_s) \leq f^{\mathcal{X}, \mathcal{Y}}. \quad (\text{LRLB})$$

The best such bound is obtained by solving the Lagrangian dual, which can be written as

$$f_{\text{LR}}^{\mathcal{X}, \mathcal{Y}}(\boldsymbol{\lambda}^*) := \max_{\substack{\boldsymbol{\lambda} \in \mathbb{R}^{N_s N_x} \\ \sum_{s \in \mathcal{S}} \boldsymbol{\lambda}_s = \mathbf{0}}} f_{\text{LSP},s}^{\mathcal{X}, \mathcal{Y}_s}(\boldsymbol{\lambda}_s). \quad \text{L}^{\mathcal{X}, \mathcal{Y}}$$

It can be shown that if the sets $\mathcal{F}_s^{\mathcal{X}, \mathcal{Y}_s}$ have a nonempty intersection, the resulting bound corresponds to the minimum of the weighted sum of convex envelopes of scenario value functions, (Robertson, Cheng, and Scott, 2020), i.e:

$$f_{\text{LR}}^{\mathcal{X}, \mathcal{Y}}(\boldsymbol{\lambda}^*) = \min_{\mathbf{x} \in \mathcal{X}} \sum_{s \in \mathcal{S}} w_s \text{conv} f_s^{\mathcal{X}, \mathcal{Y}_s}(\mathbf{x}).$$

In that sense $f_{\text{LR}}^{\mathcal{X}, \mathcal{Y}}(\boldsymbol{\lambda}^*)$ constitutes the best bound obtainable via convex relaxation in the framework of scenario decomposition. Unfortunately, obtaining optimal dual multipliers $\boldsymbol{\lambda}^*$ is both computationally expensive and numerically challenging (Oliveira et al., 2013). We therefore only consider the implications of updating the dual multipliers in Section 5, whereas in the remainder of this work, we focus on the simpler case, also considered by Cao and Zavala, 2019, where all multipliers are fixed to zero. In that case, the scenario relaxation of $\text{DE}^{\mathcal{X}, \mathcal{Y}}$ consists of N_s *scenario problems* of the form

$$\begin{aligned} f_{\text{SP},s}^{\mathcal{X}, \mathcal{Y}_s} &:= \min_{\substack{\mathbf{x}_s \in \mathcal{X} \\ \mathbf{y}_s \in \mathcal{Y}_s}} f_s(\mathbf{x}_s, \mathbf{y}_s) \\ \text{s. t. } &\mathbf{g}_I(\mathbf{x}_s) \leq \mathbf{0} \\ &\mathbf{g}_{\text{II},s}(\mathbf{x}_s, \mathbf{y}_s) \leq \mathbf{0}. \end{aligned} \quad \text{SP}_s^{\mathcal{X}, \mathcal{Y}_s}$$

In Section 4.1 we will introduce further subproblems, obtained from additional relaxations of SP_s . To distinguish the different optimal objective values, we use corresponding subscripts. The globally optimal objective values $f_{\text{SP},s}^{\mathcal{X},\mathcal{Y}_s}$ of problems $\text{SP}_s^{\mathcal{X},\mathcal{Y}_s}$ can be used to obtain a lower bound $f_{\text{SP}}^{\mathcal{X},\mathcal{Y}}$ on the optimal objective value $f^{\mathcal{X},\mathcal{Y}}$ of $\text{DE}^{\mathcal{X},\mathcal{Y}}$, i.e.,

$$f_{\text{SP}}^{\mathcal{X},\mathcal{Y}} := \sum_{s \in \mathcal{S}} w_s f_{\text{SP},s}^{\mathcal{X},\mathcal{Y}_s} \leq f^{\mathcal{X},\mathcal{Y}}. \quad (\text{SPLB})$$

While the resulting first-stage solutions obtained for each scenario will generally differ from each other, the bound can be made arbitrarily tight by exhaustive branching on \mathbf{x} . PBDAs like Kannan, 2018; Cao and Zavala, 2019; Li and Grossmann, 2019 use this fact: while they branch on \mathbf{x}_s and \mathbf{y}_s during the global solution of the subproblems SP_s , the outer B&B search only requires branching on \mathbf{x} to ensure convergence. As shown by Robertson, Cheng, and Scott, 2020, however, the convergence order of such lower bounding schemes is inherently limited due to the nonsmoothness of $f_{\text{II},s}^{\mathcal{Y}_s}(\mathbf{x})$, incurred by projection, also cf. TSP and Section 1.

Upper bounds on $f^{\mathcal{X},\mathcal{Y}}$ can generally be obtained by evaluating any feasible point. Fixing \mathbf{x} to an arbitrary point $\tilde{\mathbf{x}} \in \mathcal{X}$ that is feasible with respect to \mathbf{g}_I , gives rise to N_s instances of RP_s . If each of these problems has at least one feasible point $\tilde{\mathbf{y}}_s$, the function values $f_{\text{II},s}(\tilde{\mathbf{x}}, \tilde{\mathbf{y}}_s)$ provide an upper bound on $f_{\text{II},s}^{\mathcal{Y}_s}(\tilde{\mathbf{x}})$, and thus the upper bounding function \bar{f} , defined as

$$\bar{f}(\tilde{\mathbf{x}}, \tilde{\mathbf{y}}) := f_I(\tilde{\mathbf{x}}) + \sum_{s \in \mathcal{S}} w_s f_{\text{II},s}(\tilde{\mathbf{x}}, \tilde{\mathbf{y}}_s) \geq f^{\mathcal{X},\mathcal{Y}} \quad (\text{UB})$$

provides an upper bound on the optimal objective value $f^{\mathcal{X},\mathcal{Y}}$. Thus, given a candidate for $\tilde{\mathbf{x}}$, values for $\tilde{\mathbf{y}}_s$ can be obtained by local or global solutions of $\text{RP}_s^{\mathcal{Y}_s}(\tilde{\mathbf{x}})$. Candidates proposed in the literature are commonly based on the individual solutions \mathbf{x}_s^* from the lower bounding subproblems. A common candidate is the (w_s -weighted) average $\tilde{\mathbf{x}} = \mathbf{x}^{\text{avg}} = \sum_{s \in \mathcal{S}} w_s \mathbf{x}_s^*$ (Kannan, 2018; Cao and Zavala, 2019; Li and Grossmann, 2019). However, since the feasible set of $\text{TSP}^{\mathcal{X},\mathcal{Y}}$ is generally nonconvex, this point may be infeasible. An alternative candidate that is at least guaranteed to be feasible with respect to \mathbf{g}_I , and $\mathbf{g}_{\text{II},s^{\text{rep}}}$, is $\tilde{\mathbf{x}} = \mathbf{x}_{s^{\text{rep}}}^*$, such that s^{rep} is a *representative* scenario for which $\mathbf{x}_{s^{\text{rep}}}^*$ is closest to \mathbf{x}^{avg} with respect to the relative Euclidean distance, i.e.,

$$s^{\text{rep}} \in \arg \min_{s \in \mathcal{S}} \sum_{i=1}^{N_x} \left(\frac{x_i^{\text{avg}} - x_{s,i}^*}{\bar{x}_i - \underline{x}_i} \right)^2, \quad (s^{\text{rep}})$$

where \bar{x}_i , and \underline{x}_i denote the original lower and upper bounds of x_i (Li and Grossmann, 2019). Note that while $\mathbf{x}_{s^{\text{rep}}}^*$ is trivially feasible in s^{rep} , it is generally not in other scenarios. Furthermore, if a candidate $\mathbf{x}_{s^{\text{rep}}}^*$ does happen to be feasible, there is no guarantee that local solutions to the corresponding instances of RP_s are found.

As with any spatial B&B method, in the general nonconvex case, a guarantee to find a feasible point allowing for termination is only given if the feasible set of $\text{DE}^{\mathcal{X},\mathcal{Y}}$ has a nonempty interior at a global minimizer, also compare with the analysis for single-stage programs in Kirst, Stein, and Steuermann, 2015. Even in the case of a nonempty interior, problems can be constructed such that a particular combination of branching and node selection never results in the discovery of a feasible lower bounding solution, see Example 3.1 in Kirst, Stein, and Steuermann, 2015. In such cases, an adaption of the tested candidates, such as the approach proposed by Kirst, Stein, and Steuermann, 2015 may be necessary. Unfortunately such approaches may not address the more general situation of an empty interior, e.g., due to the presence of equality constraints, although there are approaches that produce upper bounds without guaranteeing to find feasible points (Füllner, Kirst, and Stein, 2020). On the other hand, feasible, and even (approximately) globally optimal solutions can often be produced relatively easily for many applications. Because of this, we neither implement the methods presented in Kirst, Stein, and Steuermann, 2015 in MUSE-BB, nor analyze this issue further. Instead we follow the common approach to perform upper bounding via local solutions from candidate points, and concentrate this work on the issues pertaining to lower bounding.

In summary, by solving instances of the separable subproblems $\text{SP}_s^{\mathcal{X},\mathcal{Y}_s}$ and $\text{RP}_s^{\mathcal{Y}_s}(\tilde{\mathbf{x}})$, we can bound the desired optimal solution value of the original problem $\text{DE}^{\mathcal{X},\mathcal{Y}}$ from below and above:

$$f_{\text{SP}}^{\mathcal{X},\mathcal{Y}} \leq f^{\mathcal{X},\mathcal{Y}} \leq \bar{f}(\tilde{\mathbf{x}}, \tilde{\mathbf{y}}).$$

Assuming that arbitrarily good feasible points are found during the successive partitioning of the variable domains, the bounds can be tightened until some satisfactory accuracy $\varepsilon_f > 0$ is reached. The upper bound \bar{f} then serves as an ε_f -optimal solution to problem $\text{DE}^{\mathcal{X},\mathcal{Y}}$. In the following section we present a special branching scheme that efficiently combines the decomposable subproblems with partitioning of both \mathcal{X} and \mathcal{Y} .

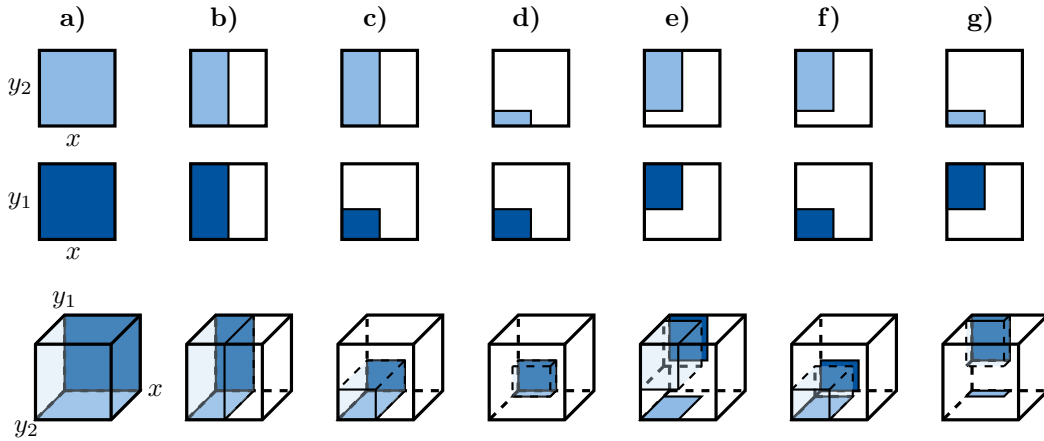


Fig. 1. Implications of branching in scenario decomposition. We consider nodes from solving an instance of DE with $N_x = N_y = 1$, and $N_s = 2$. In this case, each node corresponds to a 3D domain (bottom) and updating the lower bounds requires solving two bounding subproblems on a 2D domain (top). These subproblems can be considered projections on the $\mathcal{X} \times \mathcal{Y}_1$ and $\mathcal{X} \times \mathcal{Y}_2$ faces of the node domain (dark and light blue colors, respectively). **b)**: Branching the node from **a)** on x affects both subproblem domains. **c)**: Branching the node from **b)** on a single instance of y , here y_1 , only affects the associated subproblem domain, while the subproblem for the second scenario remains unchanged. **d)** through **g)**: Alternatively to **c)**, branching on all instances of y simultaneously results in four nodes instead of two. However, out of the eight subproblems associated with these nodes only four are distinct. When processing two complementary nodes, e.g., node **d)** (where both y_1 and y_2 are branched down), and node **e)** (where both y_1 and y_2 are branched up), all distinct subproblems are solved. Thus, explicitly processing the remaining nodes, i.e., **f)** and **g)** in our example, is unnecessary. Instead, bounds for these nodes can be generated by combining the results from the subproblems solved for **d)** and **e)**.

3 Multisection Branching for Decomposable Bounding Schemes

To avoid several issues associated with the nested branching of PBDAs (cf. Section 1), we propose to combine decomposable bounding schemes with explicit branching of both first- and second-stage variables. As argued below, standard branching of individual variables would eliminate some of the benefits of decomposable bounding schemes. We therefore propose a special branching scheme that either partitions a single first-stage variable or multiple second-stage variable instances in each iteration. To refer to the partition elements containing the lower/upper part of a branched variable domain, we say the respective variable was *branched down/up*.

In a B&B algorithm for TSP using separable lower and upper bounding problems, branching on elements of \mathbf{x} and \mathbf{y} has different implications for the resulting nodes: each node n is characterized by the domains $\mathcal{X}^n \subset \mathcal{X}$ and $\mathcal{Y}^n \subset \mathcal{Y}$, where $\mathcal{Y}^n := \times_{s \in \mathcal{S}} \mathcal{Y}_s^n$; $\mathcal{Y}_s^n \subset \mathcal{Y}_s$. To obtain a lower bound on n , variants of the N_s subproblems $\text{SP}_s^{\mathcal{X}^n, \mathcal{Y}_s^n}$ are solved. While branching on an element of \mathbf{x} results in partition of \mathcal{X}^n into two subdomains, e.g., \mathcal{X}^d and \mathcal{X}^u , and thus generally in changed bound contributions from all subproblems (compare cases **a)** and **b)** in Fig. 1), branching on an element of \mathbf{y} , e.g., $y_{s,i}$, only partitions the second-stage variable domain \mathcal{Y}_s^n of the associated scenario s (compare cases **b)** and **c)** in Fig. 1). Thus, if we were to only branch on $y_{s,i}$, each of the two resulting child nodes would have $N_s - 1$ unchanged subproblems with respect to n . An example for this situation is given by the case **c)** of Fig. 1. In the parallel setting, where at least two subproblems can be solved simultaneously, this implies that standard branching on second-stage variables leaves some processing capacity unused. In other words, we could only exploit the parallelizable solution of subproblems when processing nodes obtained from branching on first-stage variables.

To enable parallelism when processing nodes produced from second-stage branching, we can branch on all N_s instances of a particular second-stage variable, instead of a single one. Note that such a multisection is equivalent to N_s sequential bisections, i.e., it splits the original node into 2^{N_s} child nodes instead of two, also see the cases **d)** through **g)** of Fig. 1. Multisection has previously been used in different B&B algorithms for general nonlinear problems. Mostly this was in the form of branching the domain of a single variable at multiple points (also called ‘multisplitting’) (Csallner, Csendes, and Markót, 2000; Markót, Csendes, and Csallner, 2000; Kazazakis, 2017), but there are also examples of using multisection in the present sense, i.e., branching once on multiple variables (Karmakar, Mahato, and Bhunia, 2009). While these works showed that multisplitting and multisection can result

in better computational performance than bisection, the considered B&B algorithms used standard bounding procedures and thus needed to process all of the resulting nodes individually. In contrast, when solving TSP, the use of separable bounding subproblems such as SP_s^n allows us to generate bounds for the exponential number of nodes resulting from multisection without explicitly processing each one individually: for each scenario s , branching on the associated second-stage variable instance partitions the domain \mathcal{Y}_s^n into two subdomains, \mathcal{Y}_s^d , and \mathcal{Y}_s^u . Combining these new domains with the unchanged domain \mathcal{X}^n therefore results in two different subproblems (i.e., $\text{SP}_s^{\mathcal{X}^n, \mathcal{Y}_s^d}$, and $\text{SP}_s^{\mathcal{X}^n, \mathcal{Y}_s^u}$) per scenario, i.e., multisection of second-stage variables only results in $2N_s$ distinct subproblems. The subproblems for each of 2^{N_s} child nodes simply correspond to one of the possible combinations of selecting one of the two subproblems for each scenario. This means that to update lower bounds on all 2^{N_s} child nodes, only the $2N_s$ distinct subproblems need to be solved. Note that this can be achieved by processing any two of the 2^{N_s} nodes that contain complementary subproblems. One such choice consists of the pair of nodes resulting from branching all instances of the selected second-stage variable down, or up. In the following we respectively call these two nodes the *lower and upper sibling nodes*.

In summary, if a first-stage variable is selected for branching, we perform standard bisection resulting in two child nodes, whereas if a second-stage variable is selected, we instead perform multisection branching of all associated variable instances for different scenarios, resulting in 2^{N_s} nodes. In both cases, only two nodes need to be processed after branching a given node n : after first-stage branching, these two nodes are simply the child nodes with domains $(\mathcal{X}^d, \mathcal{Y}^n)$ and $(\mathcal{X}^u, \mathcal{Y}^n)$. After second-stage branching, we process the sibling nodes, with domains $(\mathcal{X}^n, \mathcal{Y}^d)$ and $(\mathcal{X}^n, \mathcal{Y}^u)$, where $\mathcal{Y}^d := \times_{s \in \mathcal{S}} \mathcal{Y}_s^d$ and $\mathcal{Y}^u := \times_{s \in \mathcal{S}} \mathcal{Y}_s^u$. While theoretically one could generate 2^{N_s} nodes after each second-stage branching, this poses several issues in an actual implementation. To address this, it is possible to filter the partitions of each multisection, i.e., to keep only a “promising” subset and thus produce a small number of high quality nodes. The process we use for this will be presented in Section 4.4.

4 Proposed Algorithm

We now present the spatial multisection B&B algorithm MUSE-BB for the solution of $\text{TSP}^{\mathcal{X}, \mathcal{Y}}$. Algorithm 1 presents a formal statement of MUSE-BB; the relevant subroutines will be presented in the following. For conciseness, we assume throughout this section that given a node n , we have access to its domains \mathcal{X}^n and \mathcal{Y}^n , and lower bound \underline{f}^n , as well as the domains \mathcal{X}_s^n and \mathcal{Y}_s^n , and lower bounds \underline{f}_s^n of the corresponding subproblems. Under this assumption, it suffices to provide nodes to the subroutines instead of all associated data. If a node n can be fathomed, we set its lower bound to ∞ .

On a high level, MUSE-BB only differs from a standard B&B algorithm in the use of different processing subroutines for nodes obtained from branching on first- and second-stage variables. In each iteration we select a node n from a list of nodes \mathcal{N} (Line 4 in Algorithm 1). If n corresponds to the root node or any node obtained from branching on first-stage variables, it is processed and either fathomed ($\underline{f}^n = \infty$) or branched (Lines 16–17). If on the other hand n corresponds to a node that was multisectioned in a previous iteration, i.e., branched on N_s second-stage variables as presented in Section 3, it has a corresponding entry in the sibling map \mathcal{M}_{sib} . When we detect this (Line 5), we perform a special “sibling iteration” (Lines 6–14). For this we recover the two sibling nodes d and u from \mathcal{M}_{sib} , and process them together (Lines 6 and 7). If this does not result in the fathoming of the parent node (Line 8), we can use the results to generate processed child nodes whose number is exponential in the number of branched variables. However, instead of using all N_s partitions of the original multisection, we filter the partitions and only branch on a subset of variable instances (Line 8, also see Section 4.4). We only consider branching via the partition of the original domain by hyperplanes, orthogonal to the branched variable dimensions. Because of this and the related concept of an orthant, i.e., the intersection of k mutually orthogonal half-spaces in k -dimensional Euclidean space, we refer to the nodes resulting from the filtered multisection as “orthant nodes” in the following. The list \mathcal{L} , and the map \mathcal{M} , returned from the filtered multisection, determine the subproblem data (from p, d , or u) to be used for a particular orthant node o (Lines 9 and 11). The number k of orthant nodes to be generated is determined by the length of \mathcal{L} (Line 10). As the orthant nodes are already in a processed state, we can immediately branch them, provided they are not fathomed (Line 12).

In the course of the algorithm, each selected node is either fathomed or branched, until the lower and upper bounds converge to ε_f optimality. On termination, MUSE-BB provides an incumbent $(\mathbf{x}^\dagger, \mathbf{y}^\dagger)$, with an associated objective value $\bar{f} = f(\mathbf{x}^\dagger, \mathbf{y}^\dagger)$ that is at most ε_f larger than the global lower bound \underline{f} .

We implement MUSE-BB as an extension of our deterministic global optimization solver and open-source project MAiNGO (Bongartz et al., 2018). In Sections 4.1–4.2 we detail how lower bounding and range reduction schemes available in MAiNGO are adapted to subproblems from Section 2 to obtain the decomposable bounding schemes

Algorithm 1: MUSE-BB

```

Input : Instance of  $\text{TSP}^{\mathcal{X}, \mathcal{Y}}$ , tolerance  $\varepsilon_f$ , effective partition limit  $k_{\max}$ , strong-branching threshold  $\eta$ 
Output: Incumbent point  $(\mathbf{x}^\dagger, \mathbf{y}^\dagger)$ , incumbent objective value  $\bar{f}$ , certificate  $\underline{f}$ 
1  $n \leftarrow \mathcal{X} \times \mathcal{Y}; \underline{f}^n \leftarrow -\infty; \mathcal{N} \leftarrow \{n\}; \bar{f} \leftarrow \infty;$ 
2  $\mathcal{M}_{\text{sib}} \leftarrow$  empty Map;
3 while  $\mathcal{N} \neq \emptyset$  do // there are nodes to be processed
4    $n \leftarrow$  select a node and remove from  $\mathcal{N}$ 
5   if  $n \in \mathcal{M}_{\text{sib}}$  then // do a ‘‘sibling iteration’’
6      $p \leftarrow n; (d, u) \leftarrow \mathcal{M}_{\text{sib}}[p];$ 
7      $(\underline{f}^n, \bar{f}^n, \mathbf{x}^n, \mathbf{y}^n) \leftarrow$  processSiblings( $p, d, u$ ); // see Subroutine 3 in Section 4.3
8     if  $\bar{f}^p < \infty$  then
9        $(\mathcal{M}, \mathcal{L}) \leftarrow$  filteredMultiSection( $p, d, u$ ); // see Subroutine 4 in Section 4.4
10      foreach  $i \in \{0, \dots, 2^{|\mathcal{L}|-1}\}$  do
11         $o \leftarrow$  generateOrthantNode( $i, p, d, u, \mathcal{M}, \mathcal{L}$ ); // see Subroutine 5 in Section 4.4
12        if  $\bar{f}^o < \infty$  then branchNode( $o$ ); // see Subroutine 1 in Section 4.3
13      end
14    end
15  else // do a ‘‘normal iteration’’
16     $(\underline{f}^n, \bar{f}^n, \mathbf{x}^n, \mathbf{y}^n) \leftarrow$  processNode( $n$ ); // see Subroutine 2 in Section 4.3
17    if  $\bar{f}^n < \infty$  then branchNode( $n$ ); // see Subroutine 1 in Section 4.3
18  end
19   $\underline{f} \leftarrow \min_{n \in \mathcal{N}} \underline{f}^n;$ 
20  if  $\bar{f}^n < \bar{f}$  then  $(\mathbf{x}^\dagger, \mathbf{y}^\dagger, \bar{f}) \leftarrow (\mathbf{x}^n, \mathbf{y}^n, \bar{f}^n);$ 
21  if  $\underline{f} + \varepsilon_f > \bar{f}$  then return  $(\mathbf{x}^\dagger, \mathbf{y}^\dagger, \bar{f}, \underline{f});$ 
22 end
23 return  $(\mathbf{x}^\dagger, \mathbf{y}^\dagger, \bar{f}, \underline{f});$ 

```

used in the processing subroutines. Since node processing in Subroutines 2 and 3 comprises the main computational work, these routines are parallelized in our implementation. The main theoretical results we present in Section 5 do not depend on the presented bounding schemes, i.e., alternative ones may be employed analogously. Next, we discuss the branching of first- and second-stage variables (Subroutine 1) and detail how the resulting nodes are processed in ‘‘normal’’ and ‘‘sibling iterations’’ (Subroutines 2 and 3) in Section 4.3. Finally, we present the subroutines for the filtered multisection and orthant node generation in Section 4.4.

4.1 Lower and Upper Bounding

Our deterministic global solver MAiNGO (Bongartz et al., 2018) employs a general-purpose B&B algorithm with lower bounding problems obtained via McCormick-based relaxation techniques (McCormick, 1976; Tsoukalas and Mitsos, 2014; Villanueva, 2015; Chachuat et al., 2015; Najman and Mitsos, 2016; Najman, Bongartz, and Mitsos, 2021). When solving TSP via equivalence to DE, we generate and solve such relaxations based on $\text{DE}^{\mathcal{X}^n, \mathcal{Y}^n}$ for each node n . In the following, we abbreviate $\text{DE}^{\mathcal{X}^n, \mathcal{Y}^n}$ as DE^n .

PBDAs like Cao and Zavala, 2019, on the other hand, only branch on the first-stage variables and solve N_s subproblems $\text{SP}_s^{\mathcal{X}^n, \mathcal{Y}_s}$ (or variants thereof) in each node. To ensure convergence, the three reviewed algorithms (Kannan, 2018; Cao and Zavala, 2019; Li and Grossmann, 2019) at least occasionally solve these subproblems to global optimality. This generally also requires branching on \mathbf{x}_s and \mathbf{y}_s , albeit not the outer algorithm.

In MUSE-BB we also generate lower bounds based on SP_s , however, we partition both the \mathcal{X} and \mathcal{Y} domains in the same B&B tree and thus consider subproblems based on $\text{SP}_s^{\mathcal{X}^n, \mathcal{Y}_s^n}$ (abbreviated as SP_s^n in the following) instead of $\text{SP}_s^{\mathcal{X}^n, \mathcal{Y}_s}$. In contrast to PBDAs, the explicit partitioning of the \mathcal{Y} domain, renders global solution of subproblems unnecessary for convergence. We therefore further relax the subproblems SP_s^n , resulting in cheaper lower bounding problems. In particular, we make use of the available relaxation techniques in MAiNGO to construct the following

McCormick based convex relaxations of SP_s^n :

$$\begin{aligned} f_{\text{MC},s}^n &:= \min_{\substack{\mathbf{x}_s \in \mathcal{X}_s^n \\ \mathbf{y}_s \in \mathcal{Y}_s^n}} f_s^{\text{cv},n}(\mathbf{x}_s, \mathbf{y}_s) \\ &\text{s. t. } \mathbf{g}_I^{\text{cv},n}(\mathbf{x}_s) \leq \mathbf{0} \\ &\quad \mathbf{g}_{\text{II},s}^{\text{cv},n}(\mathbf{x}_s, \mathbf{y}_s) \leq \mathbf{0}, \end{aligned} \quad \text{MC}_s^n$$

where $f_s^{\text{cv},n}$, $\mathbf{g}_I^{\text{cv},n}$, and $\mathbf{g}_{\text{II},s}^{\text{cv},n}$ are the McCormick based convex relaxations of the functions f_s , \mathbf{g}_I , and $\mathbf{g}_{\text{II},s}$, on $\mathcal{X}^n \times \mathcal{Y}_s^n$, respectively (McCormick, 1976; Tsoukalas and Mitsos, 2014; Najman, Bongartz, and Mitsos, 2021). These problems are further linearized based on subtangents at one or more linearization points (cf. Najman and Mitsos, 2019). By default (and in all experiments in Section 6) we only linearize at the midpoint of the node domain. The resulting lower bounding problems take the form:

$$\begin{aligned} f_{\text{LP},s}^n &:= \min_{\substack{\mathbf{x}_s \in \mathcal{X}_s^n \\ \mathbf{y}_s \in \mathcal{Y}_s^n \\ v \in \mathbb{R}}} v \\ &\text{s. t. } \text{sub}_{f_s}^n(\mathbf{x}_s, \mathbf{y}_s) \leq v \\ &\quad \text{sub}_{\mathbf{g}_I}^n(\mathbf{x}_s) \leq \mathbf{0} \\ &\quad \text{sub}_{\mathbf{g}_{\text{II},s}}^n(\mathbf{x}_s, \mathbf{y}_s) \leq \mathbf{0} \end{aligned} \quad \text{LP}_s^n$$

Here, sub_ϕ^n are subtangents of the convex relaxation of the function ϕ at the center of the domain of node n , i.e.,

$$\text{sub}_\phi^n(\bullet) := \phi^{\text{cv},n}(\mathbf{m}_\bullet) + \check{\nabla} \phi^{\text{cv},n}(\mathbf{m}_\bullet)^\top (\bullet - \mathbf{m}_\bullet) \quad (\text{subtangent})$$

where the superscript ‘cv,n’ denotes the corresponding convex relaxation, \mathbf{m}_\bullet denotes the midpoint of either \mathcal{X}^n or $\mathcal{X}^n \times \mathcal{Y}_s^n$ (depending on the passed variables), and $\check{\nabla}$ denotes a subgradient, i.e., $\check{\nabla} \phi^{\text{cv},n}(\mathbf{m}_\bullet) \in \partial \phi^{\text{cv},n}(\mathbf{m}_\bullet)$, where $\partial \phi^{\text{cv},n}(\mathbf{m}_\bullet)$ is the subdifferential of $\phi^{\text{cv},n}$ at \mathbf{m}_\bullet . Since $f_{\text{LP},s}^n$ are valid lower bounds on the globally optimal objective values $f_{\text{SP},s}^{\mathcal{X}^n, \mathcal{Y}_s^n}$ of SP_s^n , they provide a valid lower bound for node n , i.e:

$$f_{\text{LP}}^n := \sum_{s \in S} w_s f_{\text{LP},s}^n \leq f_{\text{SP}}^n \leq f^{\mathcal{X}^n, \mathcal{Y}^n}. \quad (\text{LPLB}^n)$$

Evidently this bound is generally weaker than the one obtained via global solution (see SPLB), but it is also much cheaper to compute.

For upper bounding, we solve instances of the form $\text{RP}_s^{\mathcal{Y}_s^n}(\tilde{\mathbf{x}}^n)$ (abbreviated as RP_s^n in the following), instead of $\text{RP}_s^{\mathcal{Y}_s^n}(\tilde{\mathbf{x}}^n)$ as in PBDAs. Furthermore, in contrast to Kannan, 2018 and Cao and Zavala, 2019 who solve their upper bounding problems globally, we again aim to reduce computational cost by solving RP_s^n locally. We obtain $\tilde{\mathbf{x}}^n$ from the lower bounding solution corresponding to s^{rep} (see Section 2). If the corresponding local solutions of RP_s^n result in a feasible $\tilde{\mathbf{y}}^n = (\tilde{\mathbf{y}}_1, \dots, \tilde{\mathbf{y}}_{N_s})$, the corresponding objective values $f_{\text{II},s}(\tilde{\mathbf{x}}^n, \tilde{\mathbf{y}}_s^n) \geq f_{\text{II},s}^{\mathcal{Y}_s^n}(\tilde{\mathbf{x}}^n)$ can be aggregated to a globally valid upper bound \bar{f}^n , via the upper bounding function (UB), i.e:

$$\bar{f}^n := \bar{f}(\tilde{\mathbf{x}}^n, \tilde{\mathbf{y}}^n) \geq f^{\mathcal{X}, \mathcal{Y}} \quad (\text{UB}^n)$$

If \bar{f}^n is smaller than the previously best upper bound \bar{f} , the incumbent $(\mathbf{x}^\dagger, \mathbf{y}^\dagger)$ and \bar{f} are updated with $(\tilde{\mathbf{x}}^n, \tilde{\mathbf{y}}^n)$ and \bar{f}^n , respectively.

4.2 Range Reduction

In this section we discuss decomposable range reduction routines for tightening variable bounds in B&B algorithms for TSP. We first consider two general points, namely, how the NACs can enable fathoming by infeasibility after application of these routines, and how dominance rules give rise to scenario-specific objective cuts. We then present the specific routines employed in MUSE-BB. While range reduction is not necessary from a theoretical standpoint, it can improve the efficiency of the algorithm by reducing the search domain.

Based on decomposable bounding problems such as SP_s^n or LP_s^n , one can obtain decomposable range reduction routines by applying standard techniques to the subproblems instead of the full problem DE^n , allowing for parallel updates of the bounds for the variables $(\mathbf{x}_s, \mathbf{y}_s)$ of each scenario s . After each round of range reduction, the NACs

can be used to tighten the first-stage variable bounds. More explicitly, if \mathcal{X}_s^n denotes the tightened first-stage variable domain for node n and scenario s after any of the presented decomposable range reduction routines, a valid reduction of the overall domain \mathcal{X}^n is evidently given by the intersection $\mathcal{X}^{n'}$:

$$\mathcal{X}^{n'} := \bigcap_{s \in \mathcal{S}} \mathcal{X}_s^n \quad (\mathcal{X}_s^n \text{ aggregation})$$

In particular, if $\mathcal{X}^{n'}$ is empty, node n can be fathomed by infeasibility.

If an upper bound \bar{f} is known, dominance rules can be used to derive objective cuts for range reduction routines. Since in a decomposable bounding scheme objective values obtainable in any particular node n are limited from below by the local lower bound $f_{\text{SP},s}^n$, all nodes for which $f_{\text{SP},s}^n > \bar{f}$ holds can be *fathomed by dominance*. To derive a scenario-specific cutoff based on a given value of \bar{f} , we rewrite the dominance condition in terms of scenario-specific lower bounds. Using (SPLB), a node is dominated if

$$\sum_{s \in \mathcal{S}} w_s f_{\text{SP},s}^{\mathcal{X}^n, \mathcal{Y}_s^n} > \bar{f}.$$

Note that replacing any $f_{\text{SP},s}^{\mathcal{X}^n, \mathcal{Y}_s^n}$ by a smaller value (say $\underline{f}_{\text{SP},s}^n$) results in an even stronger condition, that implies the above. Thus for any particular scenario s , the node is dominated if

$$\underline{f}_{\text{SP},s}^n > \frac{\bar{f} - \sum_{s' \in \mathcal{S} \setminus \{s\}} w_{s'} \underline{f}_{\text{SP},s'}^n}{w_s} =: \bar{f}_s^n \quad (s\text{-domination})$$

The above approach is a slight generalization to the scenario-specific upper bounds proposed by Li and Li, 2015 for the ‘primal problems’ in their decomposition method. In particular, any valid lower bounds $\underline{f}_{\text{SP},s}^n$ can be used. In MUSE-BB we use the maximum of $f_{\text{LP},s}^n$ and an interval arithmetic based lower bound based on the objective of SP_s^n .

MAiNGO implements three range reduction techniques: constraint propagation (CP, cf. e.g. Schichl and Neumaier, 2005), optimization-based bounds tightening (OBBT, cf. e.g. Gleixner et al., 2016), duality-based bounds tightening and probing (both referred to as DBBT in the following, cf. e.g. Ryoo and Sahinidis, 1995).

CP essentially refers to the inverse propagation of feasible intervals of the constraint values, i.e., $(-\infty, 0]$ in our case, to the variables (Schichl and Neumaier, 2005). This allows to determine conservative variable ranges for which the constraints can be fulfilled and thus enables domain reduction by intersecting the variable domains with these valid ranges. Thus, applying CP to the subproblems SP_s^n instead of DE^n directly gives a decomposable routine.

The OBBT procedure consists of minimizing or maximizing a selected variable v subject to the (relaxed) constraints of the original problem (Gleixner et al., 2016). In our case, we consider scenario-specific OBBT-problems, based on the lower bounding subproblems LP_s^n , i.e., they take the form:

$$\begin{aligned} \underline{v} \setminus \bar{v} = \min \setminus \max v \\ \mathbf{x}_s \in \mathcal{X}_s^n \\ \mathbf{y}_s \in \mathcal{Y}_s^n \\ \text{s. t.} \quad \text{sub}_{f_s}^n(\mathbf{x}_s, \mathbf{y}_s) \leq \bar{f}_s^n \\ \text{sub}_{g_1}^n(\mathbf{x}_s) \leq \mathbf{0} \\ \text{sub}_{g_{1,s}}^n(\mathbf{x}_s, \mathbf{y}_s) \leq \mathbf{0} \end{aligned} \quad \text{OBBT}_{s,v}^n$$

While no finite upper bound \bar{f} is known, the first constraint is dropped. For each iteration, we initially consider all variables for OBBT, and apply a variant of the *trivial filtering heuristic* from Gleixner et al., 2016 after each pass. Similar OBBT based problems have been proposed, e.g., by Li and Li, 2016; Kannan, 2018; Cao and Zavala, 2019 for their respective algorithms.

DBBT uses objective bounds and duality information from the node subproblems that are typically solved in spatial B&B algorithms (Ryoo and Sahinidis, 1995) to tighten variable domains. In our case, if all subproblems LP_s^n are feasible, the solutions $(\tilde{\mathbf{x}}_s, \tilde{\mathbf{y}}_s)$, associated reduced cost multipliers $(\mathbf{r}_{x,s}, \mathbf{r}_{y,s})$, and lower bounds $f_{\text{LP},s}^n$ are available. If in addition a finite upper bound \bar{f} is known, we can compute scenario-specific \bar{f}_s^n values from *s-dominance* and perform DBBT. For variables v for which the solution value v^* corresponds to the respective

Subroutine 1: branchNode(n)

```

1  $v \leftarrow$  select a variable from  $(\mathbf{x}, \mathbf{y})$  maximizing largest relative domain width  $\times$  branching priority;
2 if  $v \in \{x_i, | i \in \{1, \dots, N_x\}\}$  then //  $v$  corresponds to some  $x_i$ 
3   |  $(d, u) \leftarrow$  bisect  $n$  along the domain of  $v$ ;
4   |  $\mathcal{N} \leftarrow \mathcal{N} \cup \{d, u\}$ ;
5 else //  $v$  corresponds to  $y_{s',i}$  for some  $s'$ 
6   |  $i \leftarrow$  index for which  $v = y_{s',i}$ ;
7   |  $d \leftarrow n; u \leftarrow n$ ; // Initialize  $d$  and  $u$  as copies of  $n$ 
8   | foreach  $s \in \mathcal{S}$  do // branch  $d/u$  down/up on all instances of  $v$ 
9     |  $v \leftarrow y_{s,i}$ ;
10    |  $d \leftarrow$  lower half of bisecting  $d$  along the domain of  $v$ ;
11    |  $u \leftarrow$  upper half of bisecting  $u$  along the domain of  $v$ ;
12  | end
13  |  $\mathcal{N} \leftarrow \mathcal{N} \cup \{n\}$ ;
14  |  $\mathcal{M}_{\text{sib}}[n] \leftarrow (d, u)$ ;
15 end

```

lower or upper bound, the complementary bound may be tightened:

$$\begin{aligned}
& \text{if } v^* = \underline{v}, \text{ set } \bar{v} = \min\left(\bar{v}, \underline{v} + \frac{\bar{f}_s^n - f_{\text{LP},s}^n}{r}\right) \\
& \text{if } v^* = \bar{v}, \text{ set } \underline{v} = \max\left(\underline{v}, \bar{v} + \frac{\bar{f}_s^n - f_{\text{LP},s}^n}{r}\right)
\end{aligned} \tag{DBBT}$$

where r is the corresponding entry in $\mathbf{r}_{x,s}$ or $\mathbf{r}_{y,s}$, which must be positive in the first case and negative in the second one. For variables for which the solution lies between the bounds, two probing variants of LP_s^n can be solved: in these probing LPs, the variable is temporarily fixed to one of its bounds and DBBT is applied based on the new reduced cost multipliers and optimal objective values. As probing is relatively expensive, it is deactivated by default (and in all experiments of Section 6).

Since each subproblem contains only part of the information of DE^n , the presented range-reduction routines will generally be less effective than their full space counterparts. Thus, the use of parallelized range reduction needs to result in sufficiently large reductions of wall time to warrant the looser variable bounds. In comparison to the solution time of a lower bounding problem, CP is computationally very cheap, which makes its decomposable variant less appealing. Nevertheless it must be used when processing sibling nodes obtained from multisection branching (cf. Section 3), as the resulting domains are needed for the generation of orthant nodes, also see Subroutine 5 in Section 4. OBBT on the other hand is a relatively expensive procedure. This typically causes OBBT to dominate the computational work done per iteration and thus makes a decomposable OBBT variant more appealing. Finally, the use of decomposable lower bounding problems inherently requires the use of decomposable DBBT, as duality information necessary for a full space variant is not available.

4.3 Branching and Node Processing

In this section, we present the branching and processing routines of Algorithm 1. In Subroutine 1, we first present how processed nodes are branched, as this determines the kind of iteration that will be performed for the child nodes. Following this, we present the processing of nodes obtained from first- and second-stage branching in Subroutines 2 and 3.

Any processed node n that is not fathomed is branched on either a first-stage variable or on multiple second-stage variable instances, as outlined in Subroutine 1. For this, we select some first- or second-stage variable v , maximizing the product of *relative domain width* (i.e., current over original interval width) and branching priority (assumed to be nonzero), to ensure exhaustive partitioning. If v is an element of \mathbf{x} , i.e., $v = x_i$, we bisect the associated domain $\mathcal{X}_i^n = [\underline{x}_i, \bar{x}_i]$ at some branching point x_i^b , and add the two resulting nodes with the lower and upper part of the original domain (i.e., $[\underline{x}_i, x_i^b]$ and $[x_i^b, \bar{x}_i]$) to the list of open nodes (Lines 3 and 4 in Subroutine 1). In MUSE-BB, x_i^b always corresponds to the center of the interval, i.e., $0.5(\underline{x}_i + \bar{x}_i)$.

Subroutine 2: processNode(n)

- 1 do CP based on DE^n ; fathom by dominance or infeasibility;
 - 2 do OBBT based on LP_s^n ; fathom by dominance; apply \mathcal{X}_s^n aggregation, fathom by infeasibility ;
 - 3 solve LP_s^n and set $\underline{f}_s^n \leftarrow f_{LP,s}^n \forall s \in \mathcal{S}$, use $LPLB^n$, set $\underline{f}^n \leftarrow f_{LP}^n$, fathom by dominance or infeasibility ;
 - 4 $\tilde{\mathbf{x}}^n \leftarrow$ solution of LP_s^n with $s = s^{\text{rep}}$;
 - 5 $(\tilde{\mathbf{y}}_s^n, \bar{f}_s^n) \leftarrow$ solution and objective value of $RP_s^n \forall s \in \mathcal{S}$, update $(\tilde{\mathbf{y}}^n, \bar{f}^n)$ via UB^n , fathom by dominance ;
 - 6 do DBBT based on LP_s^n , fathom by dominance;
 - 7 **return** $(\underline{f}^n, \bar{f}^n, \tilde{\mathbf{x}}^n, \tilde{\mathbf{y}}^n)$
-

If instead, v is an element of \mathbf{y} , i.e., $v = y_{s',i}$, for some s' , we perform the proposed multisection branching. As pointed out in Section 3, the child nodes of this multisection can subsequently be generated from the results of two complementary nodes. Therefore we only need to generate the lower and upper sibling node at this point. Taking the example from Fig. 1: multisectioning a parent node p , corresponding to node **b**) in Fig. 1, results in sibling nodes d , and u , corresponding to nodes **d**), and **e**), respectively, which we create by branching all N_s instances of the selected second-stage variable $y_{s,i}$ down / up (Lines 6–12).

For a practical algorithm, we need to limit the number of nodes that will be generated in the sibling iterations, as will be outlined in Section 4.4. This is done via a filtered multisection which requires domain and bound data from the parent node n as well as the sibling nodes. We therefore return the parent node to the list of open nodes and create the mapping $n \mapsto (d, u)$ in \mathcal{M}_{sib} (Lines 13 and 14). When the node n is selected a second time in Algorithm 1, this is detected via a lookup in \mathcal{M}_{sib} and we perform a sibling iteration instead.

For the root node and all nodes resulting from first-stage branching, we do a “normal iteration”, i.e., the respective node is processed as specified in Subroutine 2, and either fathomed, or branched as specified in Subroutine 1. The only difference of Subroutine 2 with respect to a standard B&B algorithm is the possible use of decomposable bounding and range reduction routines from Section 4.1 and Section 4.2. In our implementation, we solve scenario subproblems for OBBT (Line 2 of Subroutine 2), lower and upper bounding (Lines 3 and 5), and DBBT (Line 6) in parallel, while the computationally cheap CP (Line 1) is done using the full problem, DE^n . To generate a candidate solution $\tilde{\mathbf{x}}^n$ for upper bounding (Line 4), we use a representative scenario s^{rep} as outlined in Section 2.

With sibling nodes, obtained from second-stage branching, we do a “sibling iteration”. Before we give the formal statement of the combined processing of siblings in Subroutine 3, we recall that child nodes from multisection can be generated by combining the results from different subproblems of both siblings (cf. Section 3). In contrast to Subroutine 2, the use of decomposable range reduction and bounding routines is thus mandatory in Subroutine 3. Moreover, we cannot perform \mathcal{X}_s^n aggregation after doing range reduction routines on $n \in \{d, u\}$, because the resulting tightening would only be valid for the respective sibling node. However, we can first propagate results from range reduction of both siblings to the parent node p , whose multi section resulted in d and u , and then back to the siblings: let $\mathcal{X}_s^d, \mathcal{X}_s^u$ and $\mathcal{Y}_s^d, \mathcal{Y}_s^u$ denote the tightened variable domains obtained after applying some range reduction to the subproblems of d and u for scenario s . Then the unions of the first- and second-stage domains are a valid tightening of the corresponding domains from the parent node p , i.e:

$$\begin{aligned} \mathcal{X}_s^p &\leftarrow \text{conv}(\mathcal{X}_s^d \cup \mathcal{X}_s^u) \\ \mathcal{Y}_s^p &\leftarrow \text{conv}(\mathcal{Y}_s^d \cup \mathcal{Y}_s^u) \end{aligned} \quad (\text{parent } s\text{-domain tightening})$$

Here, the use of the convex hull of the unions is purely for ease of implementation, as it ensures the resulting domains are representable as hyperrectangles. Once we have applied parent s -domain tightening for all scenarios, we can use the resulting \mathcal{X}_s^p for \mathcal{X}_s^p aggregation. Intersecting the resulting $\mathcal{X}^{p'}$ with \mathcal{X}_s^d and \mathcal{X}_s^u results in a valid tightening of the sibling domains:

$$\begin{aligned} \mathcal{X}_s^{d'} &\leftarrow \mathcal{X}_s^d \cap \mathcal{X}^{p'} \\ \mathcal{X}_s^{u'} &\leftarrow \mathcal{X}_s^u \cap \mathcal{X}^{p'} \end{aligned} \quad (\text{sibling } s\text{-domain tightening})$$

With this in place we can now review Subroutine 3. For each scenario, we execute the range reduction and lower bounding routines for the corresponding subproblem of both siblings. Any of these routines may indicate that either d or u can be fathomed because the subproblem for some scenario s is dominated or infeasible. However, the results from the remaining subproblems of the fathomable sibling can still be combined with the results of the subproblem for s from the other sibling to generate child nodes. Thus we continue the sibling iteration as long as

Subroutine 3: processSiblings(p, d, u)

```

1 foreach  $s \in \mathcal{S}$  do
2   | foreach  $n \in \{d, u\}$  do CP based on  $\text{SP}_s^n$ ; fathom by dominance or infeasibility;
3   | apply parent  $s$ -domain tightening; fathom by infeasibility;
4 end
5 apply  $\mathcal{X}_s^p$  aggregation, apply sibling  $s$ -domain tightening  $\forall s \in \mathcal{S}$ , fathom by infeasibility;
6 foreach  $s \in \mathcal{S}$  do
7   | foreach  $n \in \{d, u\}$  do OBBT based on  $\text{LP}_s^n$ ; fathom by dominance;
8   | apply parent  $s$ -domain tightening; fathom by infeasibility;
9 end
10 apply  $\mathcal{X}_s^p$  aggregation, apply sibling  $s$ -domain tightening  $\forall s \in \mathcal{S}$ , fathom by infeasibility;
11 foreach  $s \in \mathcal{S}$  do
12   | foreach  $n \in \{d, u\}$  do solve  $\text{LP}_s^n$ , set  $\underline{f}_s^n \leftarrow f_{\text{LP},s}^n$ , and fathom by infeasibility;
13   | check for  $s$ -domination; fathom by dominance;
14 end
15 foreach  $s \in \mathcal{S}$  do
16   | foreach  $n \in \{d, u\}$  do do DBBT based on  $\text{LP}_s^n$ ; fathom by dominance;
17   | apply parent  $s$ -domain tightening; fathom by infeasibility;
18 end
19 apply  $\mathcal{X}_s^p$  aggregation, apply sibling  $s$ -domain tightening  $\forall s \in \mathcal{S}$ , fathom by infeasibility;
20  $\tilde{\mathbf{x}}^p \leftarrow$  solution of  $\text{LP}_s^n$  with  $s$  from a variant of  $s^{\text{rep}}$  that considers all feasible scenarios for  $n \in \{d, u\}$ ;
21 foreach  $s \in \mathcal{S}$  do
22   |  $(\tilde{\mathbf{y}}_s^p, \bar{f}_s^p) \leftarrow$  solution and objective value of  $\text{RP}_s^p$ , check for  $s$ -domination; fathom by dominance;
23 end
24 update  $(\tilde{\mathbf{y}}^p, \bar{f}^p)$  via  $\text{UB}^p$ ;
25 return  $(\underline{f}^p, \bar{f}^p, \tilde{\mathbf{x}}^p, \tilde{\mathbf{y}}^p)$ 

```

for each scenario there is at least one feasible, undominated subproblem from either sibling. For lower bounding (Lines 11–14 in Subroutine 3) we solve the subproblems LP_s^n , using the associated domains after CP (Lines 1–4) and OBBT (Lines 6–9). Following this, we perform DBBT (Lines 15–18). We perform all range reduction (Lines 1–4, Lines 6–9, and Lines 15–18), as well as bounding (Lines 11–14, and Lines 21–23) in parallel. Based on the final variable domains and objective bounds, we can generate processed orthant nodes as detailed in Section 4.4. In analogy to Subroutine 2, we could solve one upper bounding problem for each such orthant node, however, this would result in an exponential number of upper bounding problems. Instead, we choose to solve only a single set of upper bounding problems $\text{RP}_s^p(\tilde{\mathbf{x}}^p)$ (Lines 21–23 in Subroutine 3), using the \mathcal{Y}_s^p domains, resulting from parent s -domain tightening after DBBT. We select $\tilde{\mathbf{x}}^n$ to be one of the first-stage solutions of the feasible subproblems of both siblings, based on a representative scenario s^{rep} , that takes into account the subproblems of both siblings.

4.4 Filtered Multisection

In this section we present a filtered multisection that addresses issues pertaining to the inherently exponential number of child nodes resulting from multisection branching, as presented in Section 3. After motivating this filtered multisection we give a formal statement in Subroutine 4. Following this, we comment on the possibility of adapting a related approach used in Cao and Zavala, 2019, for branching on first-stage variables. Finally we present the generation of orthant nodes in Subroutine 5.

The ability to generate 2^{N_s} bounded child nodes by processing and recombining the results from just two sibling nodes may seem attractive, however, handling an exponential number of nodes for arbitrary N_s can quickly become an issue in practice. Consider for instance a simple problem with $N_x = N_y = 1$; simply storing the variable bounds of child nodes from a single second-stage branching as 8 byte double values requires $16(1 + N_s)2^{N_s}$ bytes, e.g., more than two terabytes of memory for $N_s = 32$. At least in principle, we could avoid this memory issue by generating the nodes on demand in later iterations, however, doing this in an appropriate order, e.g., by increasing lower bound would require additional computations. More importantly, it is possible that for some of the partitions neither of the two subproblems improves the lower bound of the parent node significantly. This can result in a large number

Subroutine 4: filteredMultiSection(p, d, u)

```

1  $\mathcal{M} \leftarrow$  empty map; // mapping  $s$  with single feasible subproblem to the corresponding sibling
2  $\mathcal{L} \leftarrow$  empty list; // containing  $s$  for which both sibling subproblems are feasible
3 foreach  $s \in \mathcal{S}$  do
4   if  $f_s^d = \infty$  then // variable corresponding to  $s$  will be branched
5      $\mathcal{M}[s] = u$ ;
6   else if  $f_s^u = \infty$  then // variable corresponding to  $s$  will be branched
7      $\mathcal{M}[s] = d$ ;
8   else // variable corresponding to  $s$  might be branched (see Lines 14-15)
9     append  $s$  to  $\mathcal{L}$ ;
10  end
11 end
12  $\sigma_{\max} = \max_{s \in \mathcal{L}} \sigma_s$ ;
13 if  $\sigma_{\max} \leq \varepsilon_\sigma^2$  then replace  $\sigma_s$  and  $\sigma_{\max}$  with scores based on relative widths of variable domains;
14 delete all  $s$  for which  $\sigma_s \leq \eta \sigma_{\max}$  from  $\mathcal{L}$ ;
15 delete all but the  $k_{\max}$  best entries from  $\mathcal{L}$ ;
16 return  $(\mathcal{M}, \mathcal{L})$ ;

```

of nodes with weak objective bounds that all need to be processed separately, slowing down the algorithm.

To address this issue, we can select a subset of the N_s partitions that allows for a significant increase of the lower bound or reduction of the overall domain size, compared to the parent node. We then revert the original multisection in favor of a second, filtered multisection, comprising only the variable instances corresponding to the selected partitions. For this, we use Subroutine 4, which will be presented in the following. Note that each partition corresponds to a particular scenario s , a branched variable instance $y_{s,i}$, and two associated sibling subproblems with complementary domains for $y_{s,i}$. For each partition we get one of three results:

- Case 1) Both subproblems are infeasible, this immediately implies infeasibility of the parent node p .
- Case 2) Exactly one subproblem is infeasible, only the domain of the feasible subproblem can contribute to the generation of feasible orthant nodes, i.e., selecting this partition does not increase their number.
- Case 3) Both subproblems are feasible, selecting this partition doubles the resulting number of orthant nodes.

Since Case 1) is already addressed by the fathoming rules in Subroutine 3, Subroutine 4 only needs to address Cases 2) and 3). We select all partitions from Case 2) (Lines 4–7 in Subroutine 4), as they effectively result in a domain reduction, without affecting the number of generated nodes. The feasible subproblems associated with these partitions are stored in the map \mathcal{M} . The remaining partitions, corresponding to Case 3), are collected in \mathcal{L} (Line 9).

As the number $k \leq N_s$ of partitions selected from Case 3) determines the resulting number of child nodes, we call k the “effective number of partitions”. To determine which partitions should be selected, we use a heuristic based on strong-branching scores (Applegate et al., 1995; Achterberg, Koch, and Martin, 2005): given sibling nodes d and u obtained from the parent node p , each partition, i.e., each scenario s , is assigned a strong-branching score σ_s . For this, we employ the default scoring function of SCIP, proposed in Achterberg, 2007, which is calculated as

$$\sigma_s := \max(\underline{f}_s^d - \underline{f}_s^p, \varepsilon_\sigma) \max(\underline{f}_s^u - \underline{f}_s^p, \varepsilon_\sigma) \quad (\sigma_s)$$

Here the constant ε_σ ensures a nonnegative score for cases where only one sibling improves upon the parent bound.

We select only those partitions in \mathcal{L} with a score of at least $\eta \sigma_{\max}$, where $\eta \in (0, 1]$ and σ_{\max} is the largest of the scores Lines 12 and 13. Additionally, a maximum number of effective partitions k_{\max} can be imposed to ensure that the filtered multisection produces at most $2^{k_{\max}}$ child nodes (Line 15). If all scores are smaller than ε_σ^2 , we instead rank and select partitions based on relative widths (Lines 12 and 13). This ensures exhaustive partitioning in the limit, necessary for the convergence of MUSE-BB, also see Lemma 1 and Corollary 3 in Section 5. A visualization of the proposed multisection branching procedure is given in Fig. 2.

The use of strong-branching scores in Subroutine 4 suggests a relation between filtered multisection and standard strong-branching, where *alternative* bisections of a set of N_v variables are considered. While standard strong-branching requires processing $2 N_v$ full nodes to select a single bisection, i.e., generate 2 child nodes, we only process

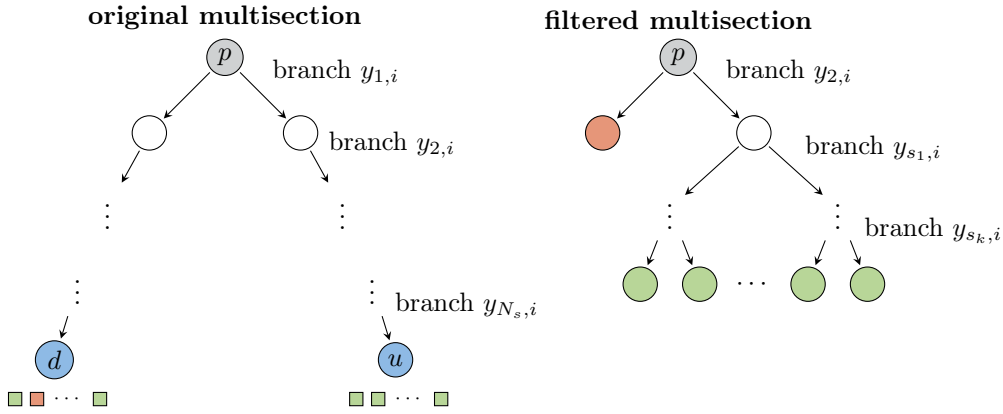


Fig. 2. Example for multisection branching and filtered multisection. In the original multisection (left) the parent node p is branched on all second stage variable instances $y_{s,i}$ for a given variable index i . Instead of generating all 2^{N_s} nodes, we only generate the leftmost and rightmost node, corresponding to branching all variable instances down (d) or up (u), respectively. We process these sibling nodes (blue) by solving the resulting subproblems (squares). In the example, the subproblem for $s = 2$ of d is infeasible (red) while all other subproblems are feasible (green). Right: based on the subproblem results, we perform a second, filtered multisection of p , involving a subset k of the original N_s partitions (right). This can be interpreted as generating a tree of k sequential bisections: all partitions producing exactly one feasible subproblem (here only the partition of $y_{2,i}$) are kept, as they do not increase the total number of child nodes. For the partitions resulting in two feasible subproblems, we consider the bound improvement w.r.t. the corresponding subproblems of p to compute the associated strong-branching scores σ_s . The partitions are filtered based on the values of σ_s and the algorithm parameters η and k_{\max} . We reject partitions for which improvement is considered insufficient, i.e., those with $\sigma_s < \eta\sigma_{\max}$, for a threshold $\eta \in (0, 1]$. The remaining ones are sorted by descending strong-branching score, resulting in an ordering of the associated scenarios (i.e., s_1, \dots, s_k). We keep at most the k_{\max} best partitions, and generate the resulting 2^k orthant nodes (green) using appropriate combinations of domains and bounds from the feasible sibling subproblems.

$2N_s$ subproblems (equivalent to 2 full nodes) and may generate an exponential number of nodes in each filtered multisection. Nevertheless, standard strong-branching might also be useful in MUSE-BB, as indicated by its use in the related algorithm of Cao and Zavala, 2019 for the selection of first-stage variables: in each iteration, the authors consider all elements of x via strong-branching, solving LP relaxations of the associated instances of DE^n for the $2N_x$ child nodes. For the two nodes of the selected bisection, they then perform the global solution of the subproblems SP_s , required for the convergence of their algorithm. While a similar approach could also be adopted in MUSE-BB, we do not require expensive global bounding routines for convergence; hence solving full-space LP relaxations based on DE^n is relatively expensive in our case. Alternatively we could solve the decomposable LP relaxations LP_s^n , and aggregate the strong-branching scores σ_s , e.g., via a w_s -weighted sum. As pointed out above, this would require to process $2N_x$ nodes instead of just 2. Due to the importance of first-stage branching for TSP (also see Section 6), this effort may in fact be warranted, however, we do not consider this idea further here, and instead branch only on individual first-stage variables as indicated in Subroutine 1.

The map \mathcal{M} , and list \mathcal{L} , returned by Subroutine 4 are used within Subroutine 5 for the generation of individual orthant nodes. For this, we collect the appropriate variable domains and subproblem objective values for each orthant from one of the siblings or the parent node (Lines 16–18 in Subroutine 5). For each scenario, the respective node is determined, based on whether the associated partition was selected ($s \in \mathcal{M}$ or $s \in \mathcal{L}$) or not (Lines 4–15). If s is in the map \mathcal{M} , we only use the data from the feasible subproblem of the associated sibling node (Lines 4 and 5). If instead, the scenario is in \mathcal{L} , appropriate subproblem data is taken based on the orthant index i (cf. Lines 10 and 11 of Algorithm 1) to determine the sibling node from which to use data (Lines 6–12 in Subroutine 5). Otherwise the partition is rejected, i.e., we use the data from the parent (Line 14). Note that the latter case does not imply that the solution of the associated subproblems was in vain, as it may still result in tightened variable bounds due to parent s -domain tightening (Lines 3, 8 and 17 in Subroutine 3). Once data for all scenarios has been collected, we aggregate the overall second-stage domain and scenario-weighted lower bound (Lines 20 and 21). Finally we test whether the orthant node is infeasible or dominated and return it (Line 22).

Subroutine 5: generateOrthantNode($i, p, d, u, \mathcal{M}, \mathcal{L}$)

```

1  $\mathbf{b} \leftarrow$  vector of  $|\mathcal{L}|$  bits, representing  $i$ ;
2  $\mathcal{X}^o \leftarrow \mathcal{X}^p$ ;
3 foreach  $s \in \mathcal{S}$  do
4   if  $s \in \mathcal{M}$  then // use data from the feasible subproblem of partition  $s$ 
5      $n \leftarrow \mathcal{M}[s]$ ;
6   else if  $s \in \mathcal{L}$  then // use data from the sibling subproblem corresponding to orthant id  $i$ 
7      $j \leftarrow$  position of  $s$  in  $\mathcal{L}$ ;
8     if  $b_j = 0$  then
9        $n \leftarrow d$ ;
10    else
11       $n \leftarrow u$ 
12    end
13  else // use parent data (partition  $s$  was filtered in Lines 14-15 of Subroutine 4)
14     $n \leftarrow p$ ;
15  end
16   $\mathcal{X}^o \leftarrow \mathcal{X}^o \cap \mathcal{X}_s^n$ ;
17   $\mathcal{Y}_s^o \leftarrow \mathcal{Y}_s^n$ ;
18   $\underline{f}_s^o \leftarrow \underline{f}_s^n$ ;
19 end
20  $\mathcal{Y}^o \leftarrow \bigtimes_{s \in \mathcal{S}} \mathcal{Y}_s^o$ ;
21  $\underline{f}^o \leftarrow \sum_{s \in \mathcal{S}} w_s \underline{f}_s^o$ ;
22 if  $\mathcal{X}^o = \emptyset$  or  $\underline{f}^o > \bar{f}$  then  $\underline{f}^o = \infty$ ;
23 return  $o$ ;
```

5 Theoretical Results

In this section we present convergence results for the lower bounding schemes used in MUSE-BB, and highlight the connection to the convergence of the algorithm itself. When applied to the domains of individual B&B nodes, the lower bounding problems presented in Section 4.1 give rise to different *lower bounding schemes* (LBSs). Their quality is determined by their underestimation of the true optimal value, and their capacity to quickly detect infeasible subdomains. In the following we analyze the asymptotic behavior of these two qualities for LBSs relevant to MUSE-BB, as the size of B&B nodes diminishes. In particular, we consider the LBSs based on: (i) dropping or dualizing the NACs, corresponding to the subproblems SP_s^n , or LSP_s^n , respectively, (ii) the McCormick relaxations of subproblems from (i), and (iii) the linear programming relaxations, resulting from subtangent relaxation of subproblems from (ii). Formally, the asymptotic behavior of a LBS for a sequence of descendant nodes is quantified by the convergence order (Kannan and Barton, 2017a). We first introduce additional notation and definitions related to this convergence order in Section 5.1, and then present conditions under which different LBSs achieve first- and second-order convergence, respectively in Sections 5.2 and 5.3. As a result of the first-order convergence, we show that MUSE-BB guarantees finite termination with an ε_f -optimal solution in Section 5.2. In Section 5.3 we analyze an extension of MUSE-BB in which the NACs are dualized instead of dropped. We show that employing this dualization within MUSE-BB is equivalent to adding the terms $\lambda_s^* \mathbf{x}_s$, to the objective function relaxations in the subproblems LP_s^n , and performing dual iterations to update the multipliers λ_s . Provided optimal multipliers λ_s^* are obtained, we show that this results in stronger convergence properties, with implications for the so-called cluster effect (Kearfott and Du, 1993; Du and Kearfott, 1994). In particular, while theoretical results of Kannan and Barton, 2017b indicate that the current implementation of MUSE-BB may mitigate clustering around typical constrained minimizers, mitigating clustering around typical unconstrained minimizers may require an extension such as the one presented in Section 5.3.

Before we give the formal definition of a LBS and the associated convergence order, we highlight the impact of the quality of lower bounds via two examples. For this we define the width of an interval.

Definition 1 (width of a multidimensional interval). A measure for the width of a multidimensional interval

$\mathcal{V} = \times_{i \in \{1, \dots, m\}} [\underline{v}_i, \bar{v}_i] \subset \mathbb{R}^m$ is given by:

$$W(\mathcal{V}) := \max_{i \in \{1, \dots, m\}} (\bar{v}_i - \underline{v}_i)$$

As shown by Kannan and Barton, 2017b, the occurrence of clustering is related to the convergence order of the LBS, which in turn is defined in terms of the ‘size of B&B nodes’, i.e., the width of the domain of branched variables, measured by Definition 1 (also see Kannan and Barton, 2017a). In algorithms like PBDAs, this node size is given by $W(\mathcal{X}^n)$, whereas in algorithms like MUSE-BB it is given by the width of the overall variable domain, i.e., $W(\mathcal{Z}^n)$. While MUSE-BB will of course require more frequent branching than PBDAs to reach a given node size, the LBSs used in MUSE-BB may achieve a higher convergence order than the scheme $\text{SP}_s^{\mathcal{X}^n, \mathcal{Y}_s}$, used in PBDAs.

The following example illustrates this situation for LBSs based on SP_s , i.e., the simplest scenario relaxation, corresponding to dropping the NACs from $\text{DE}_{\text{NAC}}^{\mathcal{X}, \mathcal{Y}}$: while the scheme $\text{SP}_s^{\mathcal{X}^n, \mathcal{Y}_s}$, where only \mathcal{X} is partitioned, results in an absolute optimality gap that diminishes with $\sqrt{W(\mathcal{X}^n)}$, the gap produced by the scheme $\text{SP}_s^{\mathcal{X}^n, \mathcal{Y}_s^n}$, which additionally partitions \mathcal{Y} , diminishes with $W(\mathcal{Z}^n)$.

Example 1. Consider the following instance of $\text{DE}^{\mathcal{X}, \mathcal{Y}}$ with $N_x = N_y = 1, N_s = 2$ and an original domain with $\mathcal{X} = \mathcal{Y}_1 = \mathcal{Y}_2 = [0, 2]$. Take

$$\begin{aligned} w_1 f_1(x_1, y_1) &= -y_1; & \mathbf{g}_{\text{II},1}(x_1, y_1) &= -x_1 + y_1^2 \\ w_2 f_2(x_1, y_2) &= 2y_2; & \mathbf{g}_{\text{II},2}(x_2, y_2) &= x_2 - y_2^2 \end{aligned}$$

The objectives imply that at the optimum $\mathbf{z}^{\text{DE}^n} = (x_1^{\text{DE}^n}, y_1^{\text{DE}^n}, y_2^{\text{DE}^n})$ of DE^n , $y_1^{\text{DE}^n}$ is maximized and $y_2^{\text{DE}^n}$ is minimized. For any feasible node n with $\mathcal{Z}^n = [\underline{x}^n, \bar{x}^n] \times [\underline{y}_1^n, \bar{y}_1^n] \times [\underline{y}_2^n, \bar{y}_2^n]$, the bounds and constraints imply $y_1^{\text{DE}^n} \leq \min\{\sqrt{x^{\text{DE}^n}}, \bar{y}_1^n\}$ and $y_2^{\text{DE}^n} \geq \max\{\sqrt{x^{\text{DE}^n}}, \underline{y}_2^n\}$. We have $y_1^{\text{DE}} = y_2^{\text{DE}} = \sqrt{x^{\text{DE}}}$ on the original domain, and thus $f(x^{\text{DE}}, y_1^{\text{DE}}, y_2^{\text{DE}}) = \sqrt{x^{\text{DE}}}$, which is minimized at $\mathbf{z}^{\text{DE}} = (x^{\text{DE}}, y_1^{\text{DE}}, y_2^{\text{DE}}) = (0, 0, 0)$, with objective value 0.

Now consider the lower bounds generated by lower bounding schemes based on SP_s on any nested sequence of nodes converging to the optimum \mathbf{z}^{DE} . Since all nodes in such sequences satisfy $\underline{x}^n = \underline{y}_s^n = 0$, the optimal solutions of the associated instance of SP_s satisfy $y_1^{\text{SP}^n} = \min\{\sqrt{\bar{x}^n}, \bar{y}_1^n\}$ and $y_2^{\text{SP}^n} = \max\{\sqrt{\bar{x}^n}, \underline{y}_2^n\} = 0$, and thus from the constraint $\mathbf{g}_{\text{II},2}$, we have $x_2^{\text{SP}^n} = y_2^{\text{SP}^n} = 0$.

In $\text{SP}_s^{\mathcal{X}^n, \mathcal{Y}_s}$, only x is branched, and the width of a node n corresponds to $W^n = W(\mathcal{X}^n) = \bar{x}^n$, while $W(\mathcal{Y}_s^n) = \bar{y}_s^n = 2$ remains constant. Since $\bar{x}^n < 2$, we have: $y_1^{\text{SP}^n} = \sqrt{W^n}$, and thus $f_{\text{DE}}^n - f_{\text{SP}}^n = \sqrt{W^n}$.

In $\text{SP}_s^{\mathcal{X}^n, \mathcal{Y}_s^n}$, both x and y_s are branched, and the width of a node n corresponds to $W^n = W(\mathcal{Z}^n)$. For a given width W^n , the largest value for $f_{\text{DE}}^n - f_{\text{SP}}^n$ over all nodes n' with $W(\mathcal{Z}^{n'}) = W^n$ will be produced by the node n with $\bar{x}^n = \bar{y}_s^n = W^n$. Once $W^n < 1$, we have that $\sqrt{W^n} > W^n$, and thus $y_1^{\text{SP}^n} = W^n$, and $f_{\text{DE}}^n - f_{\text{SP}}^n = W^n$.

While Example 1 shows that for certain problems the scheme $\text{SP}_s^{\mathcal{X}^n, \mathcal{Y}_s}$ will produce weaker bounds than $\text{SP}_s^{\mathcal{X}^n, \mathcal{Y}_s^n}$ for a given node width, the following example demonstrates that this is not always the case, i.e., both LBSs may produce absolute optimality gaps that diminish linearly (and not better) with the node width.

Example 2. Take Example 1, but change the constraints to

$$\mathbf{g}_{\text{II},1}(x_1, y_1) = -x_1 + y_1; \quad \mathbf{g}_{\text{II},2}(x_2, y_2) = x_2 - y_2.$$

which implies that $y_1^{\text{DE}} = y_2^{\text{DE}} = x^{\text{DE}}$ on the original domain, and thus $f(x^{\text{DE}}, y_1^{\text{DE}}, y_2^{\text{DE}}) = x^{\text{DE}}$. This is again minimized at $\mathbf{z}^{\text{DE}} = (x^{\text{DE}}, y_1^{\text{DE}}, y_2^{\text{DE}}) = (0, 0, 0)$, with objective value 0. Now for both $\text{SP}_s^{\mathcal{X}^n, \mathcal{Y}_s}$, and $\text{SP}_s^{\mathcal{X}^n, \mathcal{Y}_s^n}$, it is easy to see that $x_2^{\text{SP}^n} = y_2^{\text{SP}^n} = 0$, and $x_1^{\text{SP}^n} = y_1^{\text{SP}^n} = W^n$, resulting in $f_{\text{DE}}^n - f_{\text{SP}}^n = W^n$, i.e., an optimality gap that decreases exactly linearly with the node width.

As we shall see in Section 5.1, β -order convergence of a LBS requires that the optimality gap decreases proportionally to $(W^n)^\beta$, with $\beta > 0$, i.e., a higher value of β is associated with a better quality of the LBS. Robertson, Cheng, and Scott, 2020 showed that the convergence orders below one of LBSs used in PBDAs are inherent to the projection resulting from running a B&B in the \mathcal{X} space only. In particular, even LBSs based on the ideal relaxation, i.e., on convex envelopes of the scenario value functions $f_s^{\mathcal{X}^n, \mathcal{Y}_s}$ may have less than first-order convergence, unless $f_s^{\mathcal{X}^n, \mathcal{Y}_s}$ is Lipschitz, which is not guaranteed in general. In contrast, we show in Section 5.2 that the scheme $\text{SP}_s^n = \text{SP}_s^{\mathcal{X}^n, \mathcal{Y}_s^n}$, obtained by simply dropping the NACs, has at least first-order convergence under

the much milder assumption that the objective and constraint functions of DE are Lipschitz. If additionally, the used convex relaxations are Lipschitz, subsequent convex and linear relaxations used in MUSE-BB preserve this first-order convergence.

As demonstrated by Examples 1 and 2, the convergence order may still be as low as one, despite branching on second-stage variables. In Section 5.3 we show that this limitation is inherent to dropping the NACs, and that dualizing them instead results in a LBS that is as least as strong as the presented one, but additionally guarantees second-order convergence at unconstrained minimizers.

Despite this promising outlook for MUSE-BB, we need to point out that the seemingly superior convergence order of LBSs for MUSE-BB compared to that of PBDAs may be relativized by the fact that the occurrence of clustering is not exclusively determined by convergence order, but also by the local growth order of objective and constraint functions, see Kannan and Barton, 2017b. Even if for a given problem, a LBS for MUSE-BB has a higher convergence order than a comparable scheme for a PBDA, the lower order might still be sufficient to mitigate clustering in PBDAs. This is because by operating in the projected space, the relevant growth order for PBDAs is that of the scenario value functions $f_s^{\mathcal{X}, \mathcal{Y}_s}$, which may also be reduced compared that of the original objective functions f_s . In Example 1, e.g., we have $f_1^{\mathcal{X}, \mathcal{Y}_1}(x) = \sqrt{x}$, and thus a growth order of 1/2, matching the convergence order of the scheme $SP_s^{\mathcal{X}^n, \mathcal{Y}_s}$, indicating that clustering might still be avoided, despite the reduced convergence order. Conditions for which PBDAs or algorithms like MUSE-BB will show superior performance are thus not immediately clear from the present analysis.

5.1 Preliminaries

To avoid the so-called cluster effect (Kearfott and Du, 1993; Du and Kearfott, 1994; Wechsung, Schaber, and Barton, 2014) where a B&B algorithm visits a large number of nodes near approximate global minimizers, LBSs need to exhibit a sufficiently large convergence order. Early works on clustering (Kearfott and Du, 1993; Du and Kearfott, 1994; Wechsung, Schaber, and Barton, 2014) focused on clustering around unconstrained minimizers, where the convergence order of LBSs is equivalent to the convergence order of the relaxations used for the objective function. Around constrained minimizers, on the other hand, one additionally needs to consider the effect of relaxing the feasible set, leading to an extended notion of convergence order (Kannan and Barton, 2017b; Kannan and Barton, 2017a), which additionally depends on the convergence orders of the relaxations used for the constraint functions. In B&B for general nonlinear programming problems, relaxations of objective and constraints are typically generated by convex relaxation methods. In Bompadre and Mitsos, 2011 we therefore analyzed the convergence order of McCormick (McCormick, 1976), α -BB (Adjiman and Floudas, 2008), and convex hull relaxations. Convergence orders for (further) relaxation through polyhedral outer approximation were investigated by Rote, 1992; Tawarmalani and Sahinidis, 2004; Khan, 2018. While Kannan and Barton, 2017b consider a classical LBS for general nonlinear programming problems based on convex relaxation, their conclusions are not dependent on this type of LBS. Kannan and Barton, 2017a present a more general definition of a LBS, and give conditions under which convex and Lagrangian relaxations with appropriate convergence orders result in first- and second-order convergent LBS.

In preparation for Definition 4, where we use an extended notion of convergence order of a LBS in the sense of Kannan and Barton, 2017a, we introduce additional nomenclature and definitions. For each B&B node n and the corresponding *subproblem domains* $\mathcal{Z}_s^n := \mathcal{X}^n \times \mathcal{Y}_s^n$, we introduce the *scenario-specific feasible sets*

$$\mathcal{F}_s^n := \{(\mathbf{x}, \mathbf{y}_s) \in \mathcal{Z}_s^n : \mathbf{g}_I(\mathbf{x}) \leq \mathbf{0}, \mathbf{g}_{II,s}(\mathbf{x}, \mathbf{y}_s) \leq \mathbf{0}\}.$$

Similarly, for the *overall domains* $\mathcal{Z}^n := \mathcal{X}^n \times \mathcal{Y}^n$, associated with each node n , we express the *feasible set* of $DE^n = DE^{\mathcal{X}^n, \mathcal{Y}^n}$ as

$$\mathcal{F}^n := \{(\mathbf{x}, \mathbf{y}) \in \mathcal{Z}^n : (\mathbf{x}, \mathbf{y}_s) \in \mathcal{F}_s^n \forall s \in \mathcal{S}\}.$$

Furthermore, since we branch on both \mathbf{x} and \mathbf{y} , the distinction between them becomes irrelevant in many parts of the following analysis. For conciseness, we therefore aggregate the first- and second-stage variables, i.e., we introduce the notation $(\mathbf{x}, \mathbf{y}) = (\mathbf{x}, \mathbf{y}_1, \dots, \mathbf{y}_{N_s}) =: \mathbf{z} \in \mathcal{Z}^n \subset \mathbb{R}^{N_z}$, and $(\mathbf{x}, \mathbf{y}_s) =: \mathbf{z}_s \in \mathcal{Z}_s^n \subset \mathbb{R}^{N_{z,s}}$, where, $N_z := N_x + N_s N_y$ and $N_{z,s} := N_x + N_y$.

Definition 2 (distance between two sets). A measure for the distance of two sets $\mathcal{Z}_1, \mathcal{Z}_2 \subset \mathbb{R}^m$ is given by:

$$d(\mathcal{Z}_1, \mathcal{Z}_2) := \inf_{\substack{\mathbf{z}_1 \in \mathcal{Z}_1 \\ \mathbf{z}_2 \in \mathcal{Z}_2}} \|\mathbf{z}_1 - \mathbf{z}_2\|$$

Throughout this text, $\|\bullet\|$ denotes the Euclidian norm.

Definition 3 (violation measure). A measure for the minimum constraint violation of some optimization problem $\widetilde{\text{DE}}(\mathcal{V})$ with variable domain $\mathcal{V} \subset \mathbb{R}^{N_v}$ and constraints $\mathbf{g}_{\widetilde{\text{DE}}} : \mathbb{R}^{N_v} \rightarrow \mathbb{R}^{N_g^{\widetilde{\text{DE}}}}$, on some subdomain $\mathcal{V}^n \subset \mathcal{V}$ is given by:

$$\begin{aligned} \text{vio}_{\widetilde{\text{P}}}^n &:= d\left(\{\mathbf{g}_{\widetilde{\text{DE}}}(\mathbf{v}) : \mathbf{v} \in \mathcal{V}^n\}, \mathbb{R}_-^{N_g^{\widetilde{\text{DE}}}}\right) \\ &= \min_{\mathbf{v} \in \mathcal{V}^n} \left(\sum_{j=1}^{N_g^{\widetilde{\text{DE}}}} \max\{g_{\widetilde{\text{DE}},j}(\mathbf{v}), 0\}^2 \right)^{1/2}, \end{aligned}$$

where \mathbb{R}_- denotes the nonpositive orthant.

Alternative to [Definition 3](#), one may also define the violation in terms of, e.g., the ∞ -norm, which would yield $\min_{\mathbf{v} \in \mathcal{V}^n} \max_{j \in \{1, \dots, N_g^{\widetilde{\text{DE}}}\}} \max\{0; g_{\widetilde{\text{DE}},j}(\mathbf{v})\}$. We chose [Definition 3](#), following [Kannan and Barton, 2017b](#); [Kannan and Barton, 2017a](#), who use it, within their definitions of convergence order of LBSs ([Definition 8](#) and [14](#), respectively). For clarity, we separate the definition of violation from that of convergence order.

We adapt [Definition 14](#) of [Kannan and Barton, 2017a](#) to scenario-based LBSs of $\text{TSP}^{\mathcal{X},\mathcal{Y}}$. All such schemes effectively lift the deterministic equivalent formulation DE^n to the equivalent nonanticipativity formulation $\text{DE}_{\text{NAC}}^{\mathcal{X},\mathcal{Y}}$, which introduces separate first-stage variables and constraints for each scenario and couples them via the NACs. Following this, scenario-based LBSs obtain relaxations of $\text{TSP}^{\mathcal{X},\mathcal{Y}}$, by dropping or dualizing the NACs from $\text{DE}_{\text{NAC}}^{\mathcal{X},\mathcal{Y}}$, potentially followed by further relaxations of the objective and constraints.

Definition 4 (Hausdorff convergence order of scenario-based LBSs). Denote the optimal objective value of DE^n as f_{DE}^n , and let R^n be any relaxation of DE^n that decomposes into the N_s scenario relaxations of the form:

$$f_{\text{R},s}^n := \min_{\mathbf{z}_s \in \mathcal{F}_{\text{R},s}^n} f_{\text{R},s}(\mathbf{z}_s) \quad \text{R}_s^n$$

where $f_{\text{R},s}$ and $\mathcal{F}_{\text{R},s}^n$ are respective relaxations of f_s and \mathcal{F}_s^n . Therefore, the weighted sum of the optimal objective values $f_{\text{R},s}^n$ underestimates f_{DE}^n , i.e.,

$$f_{\text{R}}^n := \sum_{s \in \mathcal{S}} w_s f_{\text{R},s}^n \leq f_{\text{DE}}^n.$$

We say that (the LBS based on) R_s^n has:

1. β_f -order (Hausdorff) convergence at a feasible point $\mathbf{z} \in \mathcal{Z}$ if there exists $C_f > 0$ such that for every $\mathcal{Z}^n \subset \mathcal{Z}$ with $\mathbf{z} \in \mathcal{Z}^n$,

$$f_{\text{DE}}^n - f_{\text{R}}^n \leq C_f W(\mathcal{Z}^n)^{\beta_f}$$

2. β_g -order (Hausdorff) convergence at an infeasible point $\mathbf{z} \in \mathcal{Z}$ if there exists $C_g > 0$ such that for every $\mathcal{Z}^n \subset \mathcal{Z}$ with $\mathbf{z} \in \mathcal{Z}^n$,

$$\text{vio}_{\text{DE}}^n - \text{vio}_{\text{R}}^n \leq C_g W(\mathcal{Z}^n)^{\beta_g}$$

We say that (the LBS based on) R_s^n has (Hausdorff) convergence of order β on \mathcal{Z} if it has β -order (Hausdorff) convergence at each $\mathbf{z} \in \mathcal{Z}$.

The generic scenario-based relaxation R_s^n encompasses all LBSs we consider: LSP_s^n ; SP_s^n ; the additional relaxation of these problems, resulting from replacing all functions by their McCormick relaxations on \mathcal{Z}^n (i.e., MC_s^n in the case of SP_s^n); and the linear outer approximation of MC_s^n through subtangents, LP_s^n . In all cases, the convergence order is with respect to DE^n , i.e., feasibility and infeasibility are always to be understood with respect to the original variables and constraints. As in [Definition 14](#) of [Kannan and Barton, 2017a](#), the convergence order at feasible [infeasible] points establishes an upper bound on the underestimation of the optimal objective value [minimal constraint violation] in terms of the node width. Thus, the theoretical results of [Kannan and Barton, 2017b](#) are directly applicable. In particular, assuming sufficiently small prefactors C_f and C_g , and that all minimizers are strict, the previous analyses indicate that second-order convergence at feasible points mitigates clustering around unconstrained minimizers located at points of differentiability ([Wechsung, Schaber, and Barton, 2014](#); [Kannan and](#)

Barton, 2017b), while first-order convergence suffices for unconstrained minimizers if they are located at points of nondifferentiability (Wechsung, 2014; Kannan and Barton, 2017b). At constrained minimizers, on the other hand, first-order convergence may mitigate clustering if the objective and active constraints grow linearly around the minimizer Kannan and Barton, 2017b.

Note that according to Definition 3, the constraint violations vio_{DE}^n and vio_{R}^n are defined relative to the overall constraints of the respective problems. In contrast to DE^n , all scenario relaxations R_s^n by definition have separate copies of the first-stage variables \mathbf{x} and the first-stage constraints \mathbf{g}_{I} (or their relaxations) for each scenario s . Hence, the total number of variables and constraints of the N_s subproblems R_s^n are $N_\xi := N_s(N_x + N_y)$, and $N_g^{\text{R}} := N_s(N_{\text{I}} + N_{\text{II}})$, respectively. Similarly to \mathbf{g}_{DE} , we define \mathbf{g}_{R} by aggregating the constraint functions of R_s^n for all s ; i.e., \mathbf{g}_{R} is the vector-valued function $\mathbf{g}_{\text{R}} : \times_{s \in \mathcal{S}}(\mathcal{Z}_s) \mapsto \mathbb{R}^{N_g^{\text{R}}}$, such that for $\boldsymbol{\xi} = (\mathbf{x}_1, \mathbf{y}_1, \dots, \mathbf{x}_{N_s}, \mathbf{y}_{N_s, N_y}) \in \times_{s \in \mathcal{S}}(\mathcal{Z}_s) \subset \mathbb{R}^{N_\xi}$ we have:

$$\mathbf{g}_{\text{R}}(\boldsymbol{\xi}) := \begin{pmatrix} g_{\text{R},1}(\boldsymbol{\xi}) \\ \vdots \\ g_{\text{R},N_g^{\text{R}}}(\boldsymbol{\xi}) \end{pmatrix},$$

e.g., when using LSP_s^n or SP_s^n for R_s^n , we define these entries as

$$\mathbf{g}_{\text{LSP}}(\boldsymbol{\xi}) = \mathbf{g}_{\text{SP}}(\boldsymbol{\xi}) = \begin{pmatrix} g_{\text{I},1}(\mathbf{x}_1) \\ \vdots \\ g_{\text{I},N_{\text{I}}}(\mathbf{x}_{N_s}) \\ g_{\text{II},1,1}(\mathbf{x}_1, \mathbf{y}_1) \\ \vdots \\ g_{\text{II},N_s,N_{\text{II}}}(\mathbf{x}_{N_s}, \mathbf{y}_{N_s}) \end{pmatrix}.$$

Since the bounds in Definition 4 are relative to the width of the overall variable domain \mathcal{Z}^n , it is only meaningful for B&B algorithms for which this width diminishes to 0. MUSE-BB clearly satisfies this condition, as shown for completeness in the following result.

Lemma 1 (Exhaustive Subdivision). *The branching scheme used in MUSE-BB is exhaustive, i.e., in the limit all infinite sequences of descendant nodes converge to some accumulation point.*

Proof. In Line 1 of Subroutine 1 we eventually select the variable corresponding to the dimension of \mathcal{Z}^n with largest relative domain width (since the effect of different branching priorities is canceled after a finite number of iterations). While the partition of the selected variable can still be rejected during variable filtering (Lines 14 and 15 in Subroutine 4), this can only happen a finite number of times, as the strong-branching scores are based on lower bound *improvements* which inherently tend to zero. Thus, the width of all variable domains tends to zero. \square

Note that since PBDAs only partition \mathcal{X} , $W(\mathcal{Z}^n)$ would need to be substituted with $W(\mathcal{X}^n)$ in the bounds of Definition 4 to obtain an appropriate alternative definition for PBDAs, also see the related Definition 14 and Section 5 of Kannan and Barton, 2017a.

5.2 First-Order Convergence

As we shall see in Lemma 2, branching on second-stage variables \mathbf{y} in addition to first-stage variables \mathbf{x} , resolves the possibility of convergence orders below one, i.e., SP_s^n can be guaranteed to have (at least) first-order convergence under the weak assumption of Lipschitz continuity of the objective and constraint functions. Furthermore, Corollaries 1 and 2 show that the additional relaxations used in MUSE-BB preserve first-order convergence.

Assumption 1 (Lipschitz, factorable functions with second order pointwise convergent relaxations). All constraint and objective functions are Lipschitz, i.e., there exist constants $L_{g,\text{I},i} > 0$; $i = 1, \dots, N_{\text{I}}$, and for all $s \in \mathcal{S}$ there exist constants $L_{g,\text{II},s,j} > 0$, $j = 1, \dots, N_{\text{II}}$; $L_{f,s} > 0$, such that:

$$\begin{aligned} |g_{\text{I},i}(\mathbf{x}) - g_{\text{I},i}(\mathbf{x}')| &\leq L_{g,\text{I},i} \|\mathbf{x} - \mathbf{x}'\| \quad \forall \mathbf{x}, \mathbf{x}' \in \mathcal{X}, i = 1, \dots, N_{\text{I}}, \\ |g_{\text{II},s,j}(\mathbf{z}_s) - g_{\text{II},s,j}(\mathbf{z}'_s)| &\leq L_{g,\text{II},s,j} \|\mathbf{z}_s - \mathbf{z}'_s\| \quad \forall \mathbf{z}_s, \mathbf{z}'_s \in \mathcal{Z}_s, j = 1, \dots, N_{\text{II}}, \\ |f_s(\mathbf{z}_s) - f_s(\mathbf{z}'_s)| &\leq L_{f,s} \|\mathbf{z}_s - \mathbf{z}'_s\| \quad \forall \mathbf{z}_s, \mathbf{z}'_s \in \mathcal{Z}_s. \end{aligned}$$

The following Lemma shows first-order convergence of the LBS based on SP_s^n . Its proof relies on the fact that in any given node n , points from the domains $\mathcal{Z}_s^n = \mathcal{X}^n \times \mathcal{Y}_s^n$ of scenario subproblems are at most $\sqrt{N_x + N_y} W(\mathcal{Z}_s^n)$ apart. Furthermore, the overall node domain is $\mathcal{Z}^n = \mathcal{X}^n \times \mathcal{Y}^n$ and thus $W(\mathcal{Z}_s^n) \leq W(\mathcal{Z}^n)$. We point out that all of the algebraic steps in the following proof would also hold when replacing SP_s^n with the LBS $\text{SP}_s^{\mathcal{X}^n, \mathcal{Y}_s^n}$ used in PBDA. Thus in fact, both LBS have first-order convergence in the \mathcal{Z} space. However, while for MUSE-BB $W(\mathcal{Z}^n)$ tends to zero by Lemma 1, it does not for PBDAs, where $\mathcal{Y}^n = \mathcal{Y}$ for all nodes n , and hence only $W(\mathcal{X}^n)$ tends to zero. A meaningful convergence order for $\text{SP}_s^{\mathcal{X}^n, \mathcal{Y}_s^n}$ would therefore require bounds in terms of $W(\mathcal{X}^n)$ instead of $W(\mathcal{Z}^n)$, also see the note before Lemma 1 and the related Definition 14 and Section 5 of Kannan and Barton, 2017a.

Lemma 2 (first-order convergence of SP_s^n). *Under Assumption 1, SP_s^n has a convergence order of $\beta \geq 1$.*

Proof. Recall that Definition 4 considers convergence orders at feasible and infeasible points with respect to DE^n , leading to a natural proof outline.

Convergence Order at Feasible Points: First consider some nested sequence of nodes converging to a point \tilde{z} that is *feasible* in DE . Since \tilde{z} is contained in all nodes n of such sequences, DE^n (and thus SP_s^n) have optimal solutions for each n . Let $z^{\text{DE}^n} = (\mathbf{x}^{\text{DE}^n}, \mathbf{y}^{\text{DE}^n}) = (\mathbf{x}^{\text{DE}^n}, \mathbf{y}_1^{\text{DE}^n}, \dots, \mathbf{y}_{N_s}^{\text{DE}^n}) \in \mathcal{Z}^n$ be an optimal solution to DE^n , and define $z_s^{\text{DE}^n} = (\mathbf{x}^{\text{DE}^n}, \mathbf{y}_s^{\text{DE}^n}) \in \mathcal{Z}_s^n$. Similarly, let $z_s^{\text{SP}^n} = (\mathbf{x}_s^{\text{SP}^n}, \mathbf{y}_s^{\text{SP}^n}) \in \mathcal{Z}_s^n$ be an optimal solution to SP_s^n . Using the Lipschitz property of f_s , we can immediately express the difference in optimal objective values as:

$$\begin{aligned} f_{\text{DE}}^n - f_{\text{SP}}^n &= \sum_{s \in \mathcal{S}} w_s \left(f_s(z_s^{\text{DE}^n}) - f_s(z_s^{\text{SP}^n}) \right) \\ &\leq \sum_{s \in \mathcal{S}} w_s C_{f,s}^{\text{SP}} W(\mathcal{Z}^n) \end{aligned}$$

where $C_{f,s}^{\text{SP}} := L_{f,s} \sqrt{N_x + N_y}$. Thus SP_s^n has at least first-order convergence at all feasible points with $C_f = \sum_{s \in \mathcal{S}} w_s C_{f,s}^{\text{SP}}$.

Convergence Order at Infeasible Points: Now consider some nested sequence of nodes converging to a point \tilde{z} that is *infeasible* in DE , i.e., $\tilde{z} \notin \mathcal{F}$. By compactness of \mathcal{F} , all such sequences eventually reach a node n that does not contain any feasible point, i.e., $\text{vio}_{\text{DE}}^n > 0$. Let $\tilde{z}^{\text{DE}^n} = (\tilde{\mathbf{x}}^{\text{DE}^n}, \tilde{\mathbf{y}}^{\text{DE}^n}) = (\tilde{\mathbf{x}}^{\text{DE}^n}, \tilde{\mathbf{y}}_1^{\text{DE}^n}, \dots, \tilde{\mathbf{y}}_{N_s}^{\text{DE}^n}) \in \mathcal{Z}^n$ and $\zeta^{\text{DE}^n} \in \mathbb{R}_-^{N_g}$ be points at which the minimum constraint violation vio_{DE}^n is attained, i.e., $\text{vio}_{\text{DE}}^n = \|\mathbf{g}(\tilde{z}^{\text{DE}^n}) - \zeta^{\text{DE}^n}\|$. Similarly, let $\tilde{\xi}^{\text{SP}^n} = (\tilde{\mathbf{x}}_1^{\text{SP}^n}, \tilde{\mathbf{y}}_1^{\text{SP}^n}, \dots, \tilde{\mathbf{x}}_{N_s}^{\text{SP}^n}, \tilde{\mathbf{y}}_{N_s}^{\text{SP}^n}) \in \times_{s \in \mathcal{S}}(\mathcal{Z}_s^n)$ and $\tilde{\zeta}^{\text{SP}^n} \in \mathbb{R}_-^{N_g}$ be points at which the minimum constraint violation vio_{SP}^n is attained, i.e., $\text{vio}_{\text{SP}}^n = \|\mathbf{g}_{\text{SP}}(\tilde{\xi}^{\text{SP}^n}) - \tilde{\zeta}^{\text{SP}^n}\|$. Furthermore, define $\tilde{z}_s^{\text{DE}^n} = (\tilde{\mathbf{x}}_s^{\text{DE}^n}, \tilde{\mathbf{y}}_s^{\text{DE}^n}) \in \mathcal{Z}_s^n$ and $\tilde{z}_s^{\text{SP}^n} = (\tilde{\mathbf{x}}_s^{\text{SP}^n}, \tilde{\mathbf{y}}_s^{\text{SP}^n}) \in \mathcal{Z}_s^n$.

To derive an upper bound on $\text{vio}_{\text{DE}}^n - \text{vio}_{\text{SP}}^n$, we first give a lower bound on the minimum constraint violation vio_{SP}^n . For this we drop positive terms in the definition of vio_{SP}^n , corresponding to the first-stage constraints of all but the first scenario:

$$\begin{aligned} \text{vio}_{\text{SP}}^n &= \left\| \mathbf{g}_{\text{SP}}(\tilde{\xi}^{\text{SP}^n}) - \tilde{\zeta}^{\text{SP}^n} \right\| \\ &= \left(\sum_j^{N_g^{\text{SP}}} \left| g_{\text{SP},j}(\tilde{\xi}^{\text{SP}^n}) - \tilde{\zeta}_j^{\text{SP}^n} \right|^2 \right)^{1/2} \\ &= \left(\left| g_{\text{I},1}(\tilde{\mathbf{x}}_1^{\text{SP}^n}) - \tilde{\zeta}_1^{\text{SP}^n} \right|^2 + \dots + \left| g_{\text{I},N_{\text{I}}}(\tilde{\mathbf{x}}_1^{\text{SP}^n}) - \tilde{\zeta}_{N_{\text{I}}}^{\text{SP}^n} \right|^2 + \dots + \left| g_{\text{I},N_{\text{I}}}(\tilde{\mathbf{x}}_{N_s}^{\text{SP}^n}) - \tilde{\zeta}_{N_s N_{\text{I}}}^{\text{SP}^n} \right|^2 \right. \\ &\quad \left. + \left| g_{\text{II},1,1}(\tilde{\mathbf{z}}_1^{\text{SP}^n}) - \tilde{\zeta}_{N_s N_{\text{I}}+1}^{\text{SP}^n} \right|^2 + \dots + \left| g_{\text{II},N_s,N_{\text{II}}}(\tilde{\mathbf{z}}_{N_s}^{\text{SP}^n}) - \tilde{\zeta}_{N_s^{\text{SP}}}^{\text{SP}^n} \right|^2 \right)^{1/2} \\ &\geq \left(\left| g_{\text{I},1}(\tilde{\mathbf{x}}_1^{\text{SP}^n}) - \tilde{\zeta}_1^{\text{SP}^n} \right|^2 + \dots + \left| g_{\text{I},N_{\text{I}}}(\tilde{\mathbf{x}}_1^{\text{SP}^n}) - \tilde{\zeta}_{N_{\text{I}}}^{\text{SP}^n} \right|^2 \right. \\ &\quad \left. + \left| g_{\text{II},1,1}(\tilde{\mathbf{z}}_1^{\text{SP}^n}) - \tilde{\zeta}_{N_s N_{\text{I}}+1}^{\text{SP}^n} \right|^2 + \dots + \left| g_{\text{II},N_s,N_{\text{II}}}(\tilde{\mathbf{z}}_{N_s}^{\text{SP}^n}) - \tilde{\zeta}_{N_s^{\text{SP}}}^{\text{SP}^n} \right|^2 \right)^{1/2} \\ &=: \left\| \tilde{\mathbf{g}}^{\text{SP}^n} - \zeta^{\text{SP}^n} \right\| \end{aligned} \tag{2}$$

Note that this corresponds to a projection of the associated points from $\mathbb{R}_-^{N_g^{\text{SP}}}$ onto $\mathbb{R}_-^{N_g^{\text{DE}}}$, i.e., $\tilde{\mathbf{g}}^{\text{SP}^n}, \zeta^{\text{SP}^n} \in \mathbb{R}_-^{N_g^{\text{DE}}}$.

We can now derive the desired upper bound on $\text{vio}_{\text{DE}}^n - \text{vio}_{\text{SP}}^n$. By [Definition 3](#), we have

$$\text{vio}_{\text{DE}}^n - \text{vio}_{\text{SP}}^n = \left\| \mathbf{g}(\tilde{\mathbf{z}}^{\text{DE}^n}) - \boldsymbol{\zeta}^{\text{DE}^n} \right\| - \left\| \mathbf{g}_{\text{SP}}(\tilde{\boldsymbol{\xi}}^{\text{SP}^n}) - \boldsymbol{\zeta}^{\text{SP}^n} \right\|,$$

and underestimation of the subtracted part by the projection from [Eq. \(2\)](#) gives

$$\text{vio}_{\text{DE}}^n - \text{vio}_{\text{SP}}^n \leq \left\| \mathbf{g}(\tilde{\mathbf{z}}^{\text{DE}^n}) - \boldsymbol{\zeta}^{\text{DE}^n} \right\| - \left\| \tilde{\mathbf{g}}^{\text{SP}^n} - \boldsymbol{\zeta}^{\text{SP}^n} \right\|,$$

By definition of the infimum in vio_{DE}^n , we have $\left\| \mathbf{g}(\tilde{\mathbf{z}}^{\text{DE}^n}) - \boldsymbol{\zeta}^{\text{DE}^n} \right\| \leq \left\| \mathbf{g}(\tilde{\mathbf{z}}^{\text{DE}^n}) - \boldsymbol{\zeta} \right\|$ for all $\boldsymbol{\zeta} \in \mathbb{R}_-^{N_{\text{DE}}}$, in particular, choosing $\boldsymbol{\zeta}^{\text{SP}^n}$ results in

$$\text{vio}_{\text{DE}}^n - \text{vio}_{\text{SP}}^n \leq \left\| \mathbf{g}(\tilde{\mathbf{z}}^{\text{DE}^n}) - \boldsymbol{\zeta}^{\text{SP}^n} \right\| - \left\| \tilde{\mathbf{g}}^{\text{SP}^n} - \boldsymbol{\zeta}^{\text{SP}^n} \right\|.$$

Applying the reverse triangle inequality gives

$$\text{vio}_{\text{DE}}^n - \text{vio}_{\text{SP}}^n \leq \left\| \mathbf{g}(\tilde{\mathbf{z}}^{\text{DE}^n}) - \tilde{\mathbf{g}}^{\text{SP}^n} \right\|,$$

and thus by definition of the Euclidian norm and $\tilde{\mathbf{g}}^{\text{SP}^n}$:

$$\begin{aligned} \text{vio}_{\text{DE}}^n - \text{vio}_{\text{SP}}^n &\leq \left(\left| g_{\text{I},1}(\tilde{\mathbf{x}}^{\text{DE}^n}) - g_{\text{I},1}(\tilde{\mathbf{x}}_1^{\text{SP}^n}) \right|^2 + \cdots + \left| g_{\text{I},N_{\text{I}}}(\tilde{\mathbf{x}}^{\text{DE}^n}) - g_{\text{I},N_{\text{I}}}(\tilde{\mathbf{x}}_1^{\text{SP}^n}) \right|^2 \right. \\ &\quad \left. + \left| g_{\text{II},1,1}(\tilde{\mathbf{z}}_1^{\text{DE}^n}) - g_{\text{II},1,1}(\tilde{\mathbf{z}}_1^{\text{SP}^n}) \right|^2 + \cdots + \left| g_{\text{II},N_s,N_{\text{II}}}(\tilde{\mathbf{z}}_{N_s}^{\text{DE}^n}) - g_{\text{II},N_s,N_{\text{II}}}(\tilde{\mathbf{z}}_{N_s}^{\text{SP}^n}) \right|^2 \right)^{1/2}. \end{aligned}$$

By Lipschitz continuity of each individual constraint function, all differences can be bounded by the respective Lipschitz constants

$$\begin{aligned} \text{vio}_{\text{DE}}^n - \text{vio}_{\text{SP}}^n &\leq \left(\left(L_{g_{\text{I},1}} \left\| \tilde{\mathbf{x}}^{\text{DE}^n} - \tilde{\mathbf{x}}_1^{\text{SP}^n} \right\| \right)^2 + \cdots + \left(L_{g_{\text{I},N_{\text{I}}}} \left\| \tilde{\mathbf{x}}^{\text{DE}^n} - \tilde{\mathbf{x}}_1^{\text{SP}^n} \right\| \right)^2 \right. \\ &\quad \left. + \left(L_{g_{\text{II},1,1}} \left\| \tilde{\mathbf{z}}_1^{\text{DE}^n} - \tilde{\mathbf{z}}_1^{\text{SP}^n} \right\| \right)^2 + \cdots + \left(L_{g_{\text{II},N_s,N_{\text{II}}}} \left\| \tilde{\mathbf{z}}_{N_s}^{\text{DE}^n} - \tilde{\mathbf{z}}_{N_s}^{\text{SP}^n} \right\| \right)^2 \right)^{1/2}. \end{aligned}$$

Finally, since the maximum distances of points in \mathcal{X}^n and \mathcal{Z}^n are $\sqrt{N_x} \mathbf{W}(\mathcal{X}^n)$ and $\sqrt{N_x + N_y} \mathbf{W}(\mathcal{Z}_s^n)$, respectively, and since both $\mathbf{W}(\mathcal{X}^n)$ and $\mathbf{W}(\mathcal{Z}_s^n)$ can be overestimated by $\mathbf{W}(\mathcal{Z}^n)$ we have:

$$\begin{aligned} \text{vio}_{\text{DE}}^n - \text{vio}_{\text{SP}}^n &\leq \left(\left(L_{g_{\text{I},1}} \sqrt{N_x} \mathbf{W}(\mathcal{X}^n) \right)^2 + \cdots + \left(L_{g_{\text{I},N_{\text{I}}}} \sqrt{N_x} \mathbf{W}(\mathcal{X}^n) \right)^2 \right. \\ &\quad \left. + \left(L_{g_{\text{II},1,1}} \sqrt{N_x + N_y} \mathbf{W}(\mathcal{Z}_s^n) \right)^2 + \cdots + \left(L_{g_{\text{II},N_s,N_{\text{II}}}} \sqrt{N_x + N_y} \mathbf{W}(\mathcal{Z}_s^n) \right)^2 \right)^{1/2} \\ &\leq C_g \mathbf{W}(\mathcal{Z}^n) \end{aligned}$$

Thus SP_s^n has at least first-order convergence at all infeasible points with

$$C_g = \sqrt{N_x \sum_{i=1}^{N_{\text{I}}} L_{g_{\text{I},i}}^2 + (N_x + N_y) \sum_{s \in \mathcal{S}} \sum_{j=1}^{N_{\text{II}}} L_{g_{\text{II},s,j}}^2}.$$

Conclusion: As the LBS based on SP_s^n has convergence orders of $\beta \geq 1$ at both feasible and infeasible points, it has convergence order of $\beta \geq 1$. \square

Unsurprisingly, when the [Assumption 1](#) is not satisfied, the convergence order of MUSE-BB can also be below 1. For instance, take [Example 1](#) but use $w_1 f_1 = -\sqrt{y_1}$; this gives a convergence order of 0.5.

Next we show that both the McCormick based LBS, MC_s^n , as well as its linearization via subtangents, LP_s^n , inherit the first-order convergence of SP_s^n under mild additional assumptions. For both of these convergence results, we require the following assumption:

Assumption 2 (first-order pointwise convergent relaxations). The objective function f_s and all elements of the constraint functions \mathbf{g}_I and $\mathbf{g}_{II,s}$ have first-order *pointwise convergent* relaxations, i.e., there exist constants $C_{f,s}^{\text{MC}} > 0, s \in \mathcal{S}, C_{g,I,i}^{\text{MC}} > 0, i = 1, \dots, N_I$, and $C_{g,II,s,j}^{\text{MC}} > 0, s \in \mathcal{S}, j = 1, \dots, N_{II}$, such that for all $\mathcal{Z}^n \subset \mathcal{Z}$ and any s , the convex relaxations $f_s^{\text{cv},n}, \mathbf{g}_I^{\text{cv},n}$ and $\mathbf{g}_{II,s}^{\text{cv},n}$ in MC_s^n satisfy

$$\begin{aligned} f_s(\mathbf{z}_s) - f_s^{\text{cv},n}(\mathbf{z}_s) &\leq C_{f,s}^{\text{MC}} W(\mathcal{Z}_s^n), \quad \forall \mathbf{z}_s \in \mathcal{Z}_s^n, \\ \mathbf{g}_{I,i}(\mathbf{x}) - \mathbf{g}_{I,i}^{\text{cv},n}(\mathbf{x}) &\leq C_{g,I,i}^{\text{MC}} W(\mathcal{X}^n), \quad \forall \mathbf{x} \in \mathcal{X}^n, \quad i = 1, \dots, N_I, \\ \mathbf{g}_{II,s,j}(\mathbf{z}_s) - \mathbf{g}_{II,s,j}^{\text{cv},n}(\mathbf{z}_s) &\leq C_{g,II,s,j}^{\text{MC}} W(\mathcal{Z}_s^n), \quad \forall \mathbf{z}_s \in \mathcal{Z}_s^n, \quad j = 1, \dots, N_{II}. \end{aligned}$$

In fact, for many functions McCormick relaxations satisfying an even stronger variant of [Assumption 2](#), with second- instead of just first-order pointwise convergence are known (also see Bompadre and Mitsos, 2011). For our purposes, however, [Assumption 2](#) is sufficient.

Corollary 1 (first-order convergence of MC_s^n). *Under Assumptions 1 and 2, MC_s^n has a convergence order of $\beta \geq 1$.*

Proof. By [Lemma 2](#), the scheme SP_s^n has first-order convergence with respect to the original problem DE^n . Furthermore, under [Assumption 2](#), the LBS MC_s^n has at least first-order convergence with respect to SP_s^n by [Theorem 1](#) of Kannan and Barton, 2017a. Combining these results implies first-order convergence of MC_s^n with respect to DE^n . \square

For the first-order convergence of LP_s^n , we additionally require the following assumption:

Assumption 3 (Lipschitz convex relaxations). For any node n the convex relaxations $f_s^{\text{cv},n}, \mathbf{g}_I^{\text{cv},n}$, and $\mathbf{g}_{II,s}^{\text{cv},n}$ in MC_s^n are Lipschitz, i.e., there exist constants $L_{f,s}^{\text{MC}} > 0, L_{g,I,i}^{\text{MC}} > 0; i = 1, \dots, N_I$, and $L_{g,II,s,j}^{\text{MC}}, j = 1, \dots, N_{II}$, that constitute upper bounds on the norm of the respective subgradients. In particular, this implies:

$$\begin{aligned} \|\check{\nabla} f_s^{\text{cv},n}(\mathbf{z}_s)^\top (\mathbf{z}'_s - \mathbf{z}_s)\| &\leq L_{f,s}^{\text{MC}} \sqrt{N_x + N_y} W(\mathcal{Z}_s^n), \quad \forall \mathbf{z}_s, \mathbf{z}'_s \in \mathcal{Z}_s^n \\ \|\check{\nabla} \mathbf{g}_{I,i}^{\text{cv},n}(\mathbf{x})^\top (\mathbf{x}' - \mathbf{x})\| &\leq L_{g,I,i}^{\text{MC}} \sqrt{N_x} W(\mathcal{X}^n), \quad \forall \mathbf{x}, \mathbf{x}' \in \mathcal{X}^n, \quad i = 1, \dots, N_I, \\ \|\check{\nabla} \mathbf{g}_{II,s,j}^{\text{cv},n}(\mathbf{z}_s)^\top (\mathbf{z}'_s - \mathbf{z}_s)\| &\leq L_{g,II,s,j}^{\text{MC}} \sqrt{N_x + N_y} W(\mathcal{Z}_s^n), \quad \forall \mathbf{z}_s, \mathbf{z}'_s \in \mathcal{Z}_s^n, \quad j = 1, \dots, N_{II}. \end{aligned}$$

[Assumption 3](#) is satisfied if the relaxations used for all intrinsic functions are Lipschitz (cf. Scott, Stuber, and Barton, 2011). This in turn is the case for standard relaxations of a wide class of functions, provided they are Lipschitz themselves.

Corollary 2 (first-order convergence of LP_s^n). *Under Assumptions 1–3, LP_s^n has a convergence order of $\beta \geq 1$.*

Proof. We structure the proof as in [Lemma 2](#).

Convergence Order at Feasible Points: First consider some nested sequence of nodes converging to a point $\tilde{\mathbf{z}}$ that is feasible in DE . For all nodes n of such sequences let $\mathbf{z}_s^{\text{DE}^n}$ and $\mathbf{z}_s^{\text{LP}^n}$ be solutions of DE^n , and LP_s^n , respectively, and note that

$$f_{\text{LP},s}^n = \text{sub}_{f_s}^n(\mathbf{z}_s^{\text{LP}^n}) = f_s^{\text{cv},n}(\mathbf{m}_{\mathbf{z}_s}^n) + \check{\nabla} f_s^{\text{cv},n}(\mathbf{m}_{\mathbf{z}_s}^n)^\top (\mathbf{z}_s^{\text{LP}^n} - \mathbf{m}_{\mathbf{z}_s}^n),$$

where $\mathbf{m}_{\mathbf{z}_s}^n$ is the midpoint of \mathcal{Z}_s^n , see [subtangent](#). We can bound the difference of optimal values of DE^n , and LP_s^n by subtracting and adding the terms $f_s(\mathbf{m}_{\mathbf{z}_s}^n)$ and applying [Assumptions 1–3](#):

$$\begin{aligned} f_{\text{DE}}^n - f_{\text{LP}}^n &= \sum_{s \in \mathcal{S}} w_s (f_{\text{DE},s}^n - f_{\text{LP},s}^n) = \sum_{s \in \mathcal{S}} w_s \left(f_s(\mathbf{z}_s^{\text{DE}^n}) - \text{sub}_{f_s}^n(\mathbf{z}_s^{\text{LP}^n}) \right) \\ &= \sum_{s \in \mathcal{S}} w_s \left(f_s(\mathbf{z}_s^{\text{DE}^n}) - f_s(\mathbf{m}_{\mathbf{z}_s}^n) + f_s(\mathbf{m}_{\mathbf{z}_s}^n) - f_s^{\text{cv},n}(\mathbf{m}_{\mathbf{z}_s}^n) - \check{\nabla} f_s^{\text{cv},n}(\mathbf{m}_{\mathbf{z}_s}^n)^\top (\mathbf{z}_s^{\text{LP}^n} - \mathbf{m}_{\mathbf{z}_s}^n) \right) \\ &\leq \sum_{s \in \mathcal{S}} w_s C_{f,s}^{\text{LP}} W(\mathcal{Z}^n) \end{aligned}$$

where $C_{f,s}^{\text{LP}} := \left((L_{f,s} + L_{f,s}^{\text{MC}}) \sqrt{N_x + N_y} + C_{f,s}^{\text{MC}} \right)$. Thus LP_s^n has first-order convergence at feasible points with $C_f = \sum_{s \in \mathcal{S}} w_s C_{f,s}^{\text{LP}}$.

Convergence Order at Infeasible Points: Now consider some sequence of nodes converging to an infeasible point. As in the proof of Lemma 2, let $\tilde{\mathbf{z}}^{\text{DE}^n} = (\tilde{\mathbf{x}}^{\text{DE}^n}, \tilde{\mathbf{y}}^{\text{DE}^n}) = (\tilde{\mathbf{x}}^{\text{DE}^n}, \tilde{\mathbf{y}}_1^{\text{DE}^n}, \dots, \tilde{\mathbf{y}}_{N_s}^{\text{DE}^n}) \in \mathcal{Z}^n$, and $\zeta^{\text{DE}^n} \in \mathbb{R}_-^{N_g^{\text{DE}}}$ be points at which the minimum constraint violation vio_{DE}^n is attained, i.e., $\text{vio}_{\text{DE}}^n = \|\mathbf{g}(\tilde{\mathbf{z}}^{\text{DE}^n}) - \zeta^{\text{DE}^n}\|$, and, let $\tilde{\boldsymbol{\xi}}^{\text{LP}^n} = (\tilde{\mathbf{x}}_1^{\text{LP}^n}, \tilde{\mathbf{y}}_1^{\text{LP}^n}, \dots, \tilde{\mathbf{x}}_{N_s}^{\text{LP}^n}, \tilde{\mathbf{y}}_{N_s}^{\text{LP}^n}) \in \times_{s \in \mathcal{S}}(\mathcal{Z}_s^n)$ and $\tilde{\boldsymbol{\zeta}}^{\text{LP}^n} \in \mathbb{R}_-^{N_g^{\text{LP}}}$ be points at which the minimum constraint violation vio_{LP}^n is attained, i.e., $\text{vio}_{\text{LP}}^n = \|\mathbf{g}_{\text{LP}}(\tilde{\boldsymbol{\xi}}^{\text{LP}^n}) - \tilde{\boldsymbol{\zeta}}^{\text{LP}^n}\|$, where \mathbf{g}_{LP} is the vector-valued function containing the constraints of all LP_s^n , i.e., the subtangents of the entries in \mathbf{g}_{SP} , see [subtangent](#).

Using the same arguments as in the proof of Lemma 2 with $\mathbf{g}_{\text{LP}}(\tilde{\boldsymbol{\xi}}^{\text{LP}^n})$ instead of $\mathbf{g}_{\text{SP}}(\tilde{\boldsymbol{\xi}}^{\text{SP}^n})$ we can bound the difference in violation measures of DE^n and LP_s^n , resulting in:

$$\begin{aligned} \text{vio}_{\text{DE}}^n - \text{vio}_{\text{LP}}^n &\leq \left(\left| g_{\text{I},1}(\tilde{\mathbf{x}}^{\text{DE}^n}) - \text{sub}_{g_{\text{I},1}}^n(\tilde{\mathbf{x}}_1^{\text{LP}^n}) \right|^2 + \dots + \left| g_{\text{I},N_{\text{I}}}(\tilde{\mathbf{x}}^{\text{DE}^n}) - \text{sub}_{g_{\text{I},N_{\text{I}}}}^n(\tilde{\mathbf{x}}_1^{\text{SP}^n}) \right|^2 \right. \\ &\quad \left. + \left| g_{\text{II},1,1}(\tilde{\mathbf{z}}_1^{\text{DE}^n}) - \text{sub}_{g_{\text{II},1,1}}^n(\tilde{\mathbf{z}}_1^{\text{SP}^n}) \right|^2 + \dots + \left| g_{\text{II},N_s,N_{\text{II}}}(\tilde{\mathbf{z}}_{N_s}^{\text{DE}^n}) - \text{sub}_{g_{\text{II},N_s,N_{\text{II}}}}^n(\tilde{\mathbf{z}}_{N_s}^{\text{SP}^n}) \right|^2 \right)^{1/2} \end{aligned}$$

as with the objective function, we can bound the differences between each constraint function and the respective subgradient, using [Assumptions 1–3](#), which results in

$$\text{vio}_{\text{DE}}^n - \text{vio}_{\text{LP}}^n \leq C_g^{\text{LP}} W(\mathcal{Z}^n),$$

where

$$C_g^{\text{LP}} := \sqrt{\sum_{i=1}^{N_{\text{I}}} \left((L_{g,\text{I},i} + L_{g,\text{I},i}^{\text{MC}}) \sqrt{N_x} + C_{g,\text{I},i}^{\text{MC}} \right)^2 + \sum_{s \in \mathcal{S}} \sum_{j=1}^{N_{\text{II}}} \left((L_{g,\text{II},s,j} + L_{g,\text{II},s,j}^{\text{MC}}) \sqrt{N_x + N_y} + C_{g,\text{II},s,j}^{\text{MC}} \right)^2}.$$

Thus LP_s^n has first-order convergence at any infeasible point with $C_g = C_g^{\text{LP}}$.

Conclusion: As the LBS based on LP_s^n has convergence orders of $\beta \geq 1$ at both feasible and infeasible points, it has convergence order of $\beta \geq 1$. \square

We are now in the position to prove finite ε_f -convergence of MUSE-BB.

Corollary 3 (finite termination of MUSE-BB). *Under [Assumptions 1–3](#), MUSE-BB terminates finitely for any optimality tolerance $\varepsilon_f > 0$, either providing an ε_f -optimal solution or a certificate that the problem is infeasible.*

Proof. By Lemma 1, each sequence of descendant nodes converges to some accumulation point $\tilde{\mathbf{z}}$. We show that the use of any LBS R_s^n with convergence order of $\beta > 0$ implies that all such sequences finitely reach a node that can be fathomed by value dominance or infeasibility.

Convergence at Feasible Points: First consider sequences for which $\tilde{\mathbf{z}}$ is feasible. After a finite number of iterations, any such sequence will produce a node n , for which $W(\mathcal{Z}^n) \leq \left(\frac{\varepsilon_f}{C_f} \right)^{1/\beta}$, which implies that $f_{\text{DE}}^n - f_{\text{R}}^n \leq \varepsilon_f$, i.e., that n is fathomed by value dominance.

Convergence at Infeasible Points: Next consider sequences for which $\tilde{\mathbf{z}}$ is infeasible, and which are not terminated finitely because some descendant node can be fathomed by value dominance. By compactness of the feasible set, any such sequence will eventually produce a node \tilde{n} that contains no feasible point, and thus has a positive violation measure $\text{vio}_{\text{DE}}^{\tilde{n}}$. Since the violation measure increases monotonically for descendants of node \tilde{n} , the sequence is terminated when or before the descendant node n is produced, for which $W(\mathcal{Z}^n) \leq \left(\frac{\text{vio}_{\text{DE}}^{\tilde{n}}}{C_g} \right)^{1/\beta}$, as this implies $0 \leq \text{vio}_{\text{DE}}^n - \text{vio}_{\text{DE}}^{\tilde{n}} \leq \text{vio}_{\text{R}}^n$, i.e., infeasibility is detected by the scheme R_s^n , and node n is fathomed by infeasibility.

Conclusion: In summary, each node sequence terminates finitely and since the original domain is compact, the total number of sequences must be finite. By Corollary 2, the assumptions imply that the LBS $\text{R}_s^n = \text{LP}_s^n$, used in MUSE-BB has a convergence order of $\beta > 1$, thus MUSE-BB terminates finitely, once all sequences of descendant nodes are terminated. \square

After demonstrating first-order convergence of the LBS employed by MUSE-BB and the resulting ε_f -convergence, we now consider in which cases these convergence properties may be sufficient to mitigate clustering. As indicated by Kannan and Barton, 2017b, clustering may be mitigated around individual minimizers of DE, if the convergence order of the LBS is larger or equal to the order at which objective and constraint functions grow around this

minimizer. While [Example 2](#) demonstrates that SP_s^n (and by extension, also LP_s^n) may have a convergence order as low as one at *constrained minimizers*, objective and constraint functions typically grow at a linear rate around such points ([Kannan and Barton, 2017b](#)). Therefore LP_s^n may mitigate clustering around typical constrained minimizers, provided the respective coefficients C_f and C_g are sufficiently small ([Kannan and Barton, 2017b](#)). On the other hand, at *unconstrained minimizers*, where f is differentiable, f grows quadratically or faster. As a result, a LBS needs to have at least second-order convergence at unconstrained minimizers to mitigate clustering ([Du and Kearfott, 1994](#); [Wechsung, Schaber, and Barton, 2014](#); [Kannan and Barton, 2017b](#)). Unfortunately, the convergence order of SP_s^n may also be as low as one at unconstrained minimizers, as shown by the following example.

Example 3. Consider an instance of [DE](#) with $N_x = 1, N_y = 0, N_s = 2$ and an original domain $\mathcal{X} = [-1, 1]$. Take

$$w_1 f_1(x_1) = 0.5(x_1 - 1)^2; \quad w_2 f_2(x_2) = 0.5(x_2 + 1)^2$$

such that $f(x) = x^2 + 1$, and thus the optimal solution and objective value are $x^{\text{DE}} = 0$, and $f(x^{\text{DE}}) = 1$, respectively. For any nested sequence of nodes converging to this optimum, the solutions x^{DE^n} of the node problem DE^n lie in $\mathcal{X}^n = [\underline{x}^n, \bar{x}^n]$, and thus $\underline{x}^n \leq 0, \bar{x}^n \geq 0$. For such nodes, the solutions of SP_s^n are $x_1^{\text{SP}^n} = \bar{x}^n$, and $x_2^{\text{SP}^n} = \underline{x}^n$, respectively. Hence the difference in objective values is:

$$\begin{aligned} f_{\text{DE}}^n - f_{\text{SP}}^n &= 1 - 0.5\left((\bar{x}^n - 1)^2 + (\underline{x}^n + 1)^2\right) \\ &= -0.5(\bar{x}^n)^2 + \bar{x}^n - \underline{x}^n - 0.5(\underline{x}^n)^2 \end{aligned}$$

Now consider a sequence for which $\bar{x}^n = W^n, \underline{x}^n = 0$; for this sequence the above expression simplifies to

$$f_{\text{DE}}^n - f_{\text{SP}}^n = W^n - 0.5(W^n)^2.$$

Now for any $C_f > 0$ this expression becomes larger than $C_f(W^n)^2$ for the node n_0 , for which

$$W^{n_0} < \frac{1}{C_f + 0.5},$$

i.e., SP_s^n is at best first-order convergent at the unconstrained minimizer x^{DE^n} .

In summary, the present implementation of MUSE-BB may suffer from clustering around unconstrained minimizers. To address this, an alternative LBS with at least quadratic convergence order is required. In the following section we analyze an extension of MUSE-BB whose LBS has this property.

5.3 Second-Order Convergence

In this section we show that using LSP_s^n instead of SP_s^n , i.e., dualizing the NACs instead of dropping them, enables at least second-order convergence at unconstrained minimizers. Additionally, we consider the resulting effect on the implementation, i.e., how the LBS LP_s^n needs to be adapted when using LSP_s^n .

A necessary condition for a LBS to have β -order convergence is that the relaxations used for its construction have β -order convergence, also see [Kannan and Barton, 2017a](#). While this condition is generally not sufficient for β -order convergence of the resulting LBS, it is sufficient for β -order convergence around *Slater points*, i.e., *unconstrained feasible points* (Corollaries 2, 3 of [Kannan and Barton, 2017a](#)).

The analysis of [Robertson, Cheng, and Scott, 2020](#) for PBDA shows that the optimal objective value $f_{\text{LR}}^{\mathcal{X}^n, \mathcal{Y}}(\boldsymbol{\lambda}^*)$, obtained from the subproblems $\text{LSP}_s^{\mathcal{X}^n, \mathcal{Y}_s}$, where the NACs are dualized instead of dropped, is equivalent to minimizing the w_s -weighted sum of convex envelopes of $f_s^{\mathcal{X}^n, \mathcal{Y}}$. As a result, $f_{\text{LR}}^{\mathcal{X}^n, \mathcal{Y}}(\boldsymbol{\lambda}^*)$ constitutes a (constant valued) relaxation of the objective function f on the domain $\mathcal{X}^n \times \mathcal{Y}$. Furthermore, they show that this relaxation is at least second-order convergent with respect to $W(\mathcal{X}^n)$, i.e.,

$$\min_{\mathbf{x} \in \mathcal{X}^n} \sum_{s \in \mathcal{S}} f_s^{\mathcal{X}^n, \mathcal{Y}_s}(\mathbf{x}) - f_{\text{LR}}^{\mathcal{X}^n, \mathcal{Y}}(\boldsymbol{\lambda}^*) \leq \tau W(\mathcal{X}^n)^\beta$$

with $\beta \geq 2$, provided the scenario value functions $f_s^{\mathcal{X}^n, \mathcal{Y}_s}$ are \mathcal{C}^2 , i.e., twice continuously differentiable. We point out that in fact, the slightly weaker assumption that f merely has bounded second-order directional derivatives, i.e., that it is $\mathcal{C}^{1,1}$, is also sufficient for second-order convergence of $f_{\text{LR}}^{\mathcal{X}^n, \mathcal{Y}}(\boldsymbol{\lambda}^*)$, also see [Zlobec, 2005](#). In the special case where the $f_s^{\mathcal{X}^n, \mathcal{Y}_s}$ are convex, β above may take any positive value, i.e., the convergence is arbitrarily high.

Note that β -order convergence of $f_{\text{LR}}^{\mathcal{X}^n, \mathcal{Y}}(\boldsymbol{\lambda}^*)$ immediately implies β -order convergence of the LBS $\text{LSP}_s^{\mathcal{X}^n, \mathcal{Y}_s}$ at unconstrained feasible points (and in particular at unconstrained minimizers), because around such points f_{DE}^n , i.e., the optimal value of DE^n , is equivalent to $\min_{\mathbf{x} \in \mathcal{X}^n} \sum_{s \in \mathcal{S}} f_s^{\mathcal{X}^n, \mathcal{Y}_s}(\mathbf{x})$, also see Corollaries 2 and 3 of Kannan and Barton, 2017a. Furthermore, β -order convergence with respect to $W(\mathcal{X}^n)$ implies β -order convergence with respect to $W(\mathcal{Z}^n)$, since $W(\mathcal{X}^n) \leq W(\mathcal{Z}^n)$. As a result, the same line of argument naturally also holds for the scheme $\text{LSP}_s^n := \text{LSP}_s^{\mathcal{X}^n, \mathcal{Y}_s^n}$, which for any \mathcal{X}^n produces stronger bounds than $\text{LSP}_s^{\mathcal{X}^n, \mathcal{Y}_s}$. Hence, the relaxations $f_{\text{LR}}^{\mathcal{X}^n, \mathcal{Y}^n}(\boldsymbol{\lambda}^*)$ are at least second-order convergent, and Corollaries 2 and 3 of Kannan and Barton, 2017a ensure second-order convergence of LSP_s^n at unconstrained feasible points. The following example demonstrates the improvement of convergence order of LSP_s^n over SP_s^n .

Example 4. Take the problem from Example 3. The optimal dual values for this problem are $\boldsymbol{\lambda}_s^* = (2, -2)$, such that the objectives of LSP_s^n are $f_s(x_s) + \boldsymbol{\lambda}_s x_s = (x_s \mp 1)^2 \pm 2x_s = x_s^2 + 1$. Hence, both subproblems are solved at $x_1^{\text{LSP}^n} = x_2^{\text{LSP}^n} = x^{\text{DE}^n} = 0$, and the difference in objective values is:

$$f_{\text{DE}}^n - f_{\text{LSP}}^n = 1 - 0.5 \left((0+1)^2 + (0+1)^2 \right) = 0,$$

i.e., LSP_s^n is exact and as such has arbitrarily high convergence order at the unconstrained minimizer x^{DE^n} .

Note that the arbitrarily high convergence order in Example 4 results from the fact that the scenario value functions $f_s^{\mathcal{X}, \mathcal{Y}_s}$ are convex. If $f_s^{\mathcal{X}, \mathcal{Y}_s}$ are not convex, at least second-order convergence is guaranteed by the previous arguments.

Several results from nonlinear parametric programming provide different regularity conditions under which $f_s^{\mathcal{X}^n, \mathcal{Y}_s}$ are \mathcal{C}^2 . In particular, if we assume f is \mathcal{C}^2 , and that the second-order sufficient condition (SOSC):

$$\begin{aligned} \nabla f(\mathbf{z}^{\text{DE}}) &= \mathbf{0} \\ \nabla^2 f(\mathbf{z}^{\text{DE}}) &\succ 0 \end{aligned} \quad (\text{SOSC}(\mathbf{z}^{\text{DE}}))$$

holds at an unconstrained minimizer $\mathbf{z}^{\text{DE}} = (\mathbf{x}^{\text{DE}}, \mathbf{y}^{\text{DE}})$ of DE , the fact that $f_s^{\mathcal{X}^n, \mathcal{Y}_s}$ are \mathcal{C}^2 follows from the Implicit Function Theorem (Fiacco, 1983, cf., e.g., Corollary 3.2.3).

Other variants of the Implicit Function Theorem provide similar results for unconstrained minimizers that do not satisfy $\text{SOSC}(\mathbf{z}^{\text{DE}})$, e.g., Theorem 3.3 of Ginchev, Torre, and Rocca, 2009, or even for constrained minimizers, satisfying certain regularity conditions, related to the growth of the Lagrangian of f , e.g., Fiacco, 1983 and Stechliniski, Khan, and Barton, 2018.

We next show how the stronger convergence properties of the LBS LSP_s^n can be incorporated into MUSE-BB via an adaption of the lower bounding problems subproblems LP_s^n . Recall that LP_s^n result from three subsequent levels of relaxation: after dropping the NACs from $\text{DE}_{\text{NAC}}^{\mathcal{X}, \mathcal{Y}}$ (i), the resulting subproblems SP_s^n are further relaxing the via McCormick's method (ii) and outer approximation (iii), resulting in the linear lower bounding problems LP_s^n . In this context, dualizing the NACs, corresponds to replacing the subproblems SP_s^n with LSP_s^n , and performing the subsequent relaxations. Note that the only difference between SP_s^n and LSP_s^n are the additional terms $\boldsymbol{\lambda}_s^\top \mathbf{x}_s$. The McCormick relaxation of the sum of the original, nonlinear objective $f_s(\mathbf{x}_s, \mathbf{y}_s)$, and the linear term $\boldsymbol{\lambda}_s^\top \mathbf{x}_s$ is simply $f_s^{\text{cv}, n}(\mathbf{x}_s, \mathbf{y}_s) + \boldsymbol{\lambda}_s^\top \mathbf{x}_s$ (cf. Proposition 2 of Bompadre and Mitsos, 2011). Next we consider the subgradients of these terms: if $\tilde{\nabla} f_s^{\text{cv}, n}$ is the subgradient of $f_s^{\text{cv}, n}$, used in the original instance of LP_s^n , then $\tilde{\nabla} f_s^{\text{cv}, n} + \boldsymbol{\lambda}_s$ is a valid subgradient of $f_s^{\text{cv}, n}(\mathbf{x}_s, \mathbf{y}_s) + \boldsymbol{\lambda}_s^\top \mathbf{x}_s$ (cf. Proposition 2.3.3 of Clarke, 1990). As a result, replacing SP_s^n with LSP_s^n in MUSE-BB is equivalent to adding $\boldsymbol{\lambda}_s$ to the coefficients of \mathbf{x}_s in the first set of constraints, of the subproblems LP_s^n . Furthermore, the multipliers can be updated by performing dual iterations with these modified linear lower bounding subproblem.

Thus similar to PBDAs, the LBS used in MUSE-BB can be made second-order convergent at certain minimizers by dualizing the NACs instead of dropping them. However, the use of optimal dual multipliers $\boldsymbol{\lambda}^*$ appears to be a requirement for second-order convergence, and, as already pointed out in Section 4.1, obtaining such multipliers is generally very challenging. The fact that SP_s^n can be interpreted as an instance of LSP_s^n with the suboptimal multipliers $\boldsymbol{\lambda} = \mathbf{0}$, indicates that even suboptimal multipliers may result in a first-order convergent LBS, also see the related result on a Lagrangian dual-based LBS for general nonlinear programming problems in Theorem 6 of Kannan and Barton, 2017a. Therefore it may be sufficient to limit multiplier updates to small nodes suspected to contain the neighborhoods of critical minimizers. However, we leave the investigation of such approaches for future work.

6 Computational Results

We now present computational results obtained with the parallelized decomposition algorithm MUSE-BB, and outline how it compares against solving the deterministic equivalent formulation $DE^{x,y}$ with the standard version of MAiNGO. We do not compare with other deterministic global solvers as these generally employ different routines for management of the B&B tree, generating relaxations of individual functions, and solving individual lower and upper bounding problems, distorting the effect of the decomposition. MUSE-BB performs upper bounding based on the subproblems SP_s^n , and OBBT, lower bounding, and DBBT, based on the separable subproblems LP_s^n . All scenario subproblems are solved simultaneously, using one thread per scenario. MAiNGO performs upper bounding based on DE^n and all other routines based on a linearization of DE^n , using a single thread.

We consider variants of a simple test problem with $N_x = N_y = 1$ and $N_s = 4, 8, \text{ and } 16$, i.e., with different size based on the number of scenarios. The test problem is a simplified design and operation problem for a combined heat and power (CHP) system, based on stochastic heat and power demands. Scenarios for demand data are generated from a seeded pseudorandom sampling, ensuring identical instances upon repetition for a given N_s value. The problem involves nonlinearities related to economies of scale, thermal and electrical efficiencies, and the implementation of a minimal part-load constraint. A detailed description of the problem is given in Appendix A.

We focus on the performance difference of the lower bounding routines, hence all experiments are performed with initial points based on dense uniform sampling of 1000 values in each of the x and y_s domains, which always results in ε_f -optimal initial points, that are never improved during the course of the algorithm. We use the default settings of MAiNGO, including a relative optimality tolerance of 1%. All computational experiments are performed on the RWTH Compute Cluster ‘‘CLAIX-2018’’. Each compute node has 2 Intel Xeon Platinum 8160 Processors with 2.1 GHz, 24 cores each, i.e., there is a total of 48 cores per compute node, and 4 GB of main memory per core. In initial tests we observed significant variation of run times, both for MAiNGO and MUSE-BB. We attribute this variation to execution on particular – likely overloaded – compute nodes which consistently require longer solution times compared to other compute nodes. To reduce the effect of this variation, we repeat the solution of each considered instance 20 times and report median values of the resulting solution times and optimality gaps.

6.1 Importance of Branching Priority

Initially we will focus on the case $k_{\max} = 1$, i.e., we branch only on second-stage variable instances that either produce infeasible subproblems or produce the highest strong-branching score. This means each multisection of second stage variables results in at most 2 child nodes being created, i.e., as in a standard B&B algorithm like MAiNGO.

In problems like DE , exhibiting two-stage structure, the first-stage variables appear in all of the scenario subproblems, while the second-stage variable instances only appear in one, each. This suggests a higher importance of branching on first-stage vs. second-stage variables, especially with increasing N_s . In B&B algorithms, the priority with which variables are branched is typically controlled via branching priorities for individual variables, which are multiplied with the relative interval width before selecting a variable to branch on, also cf. the description of [Subroutine 1](#). As a result, it seems intuitive that B&B algorithms solving DE may generally benefit from relatively high branching priorities for the first-stage variables compared to the second-stage variables, independent of whether decomposition is used or not. For this reason, we compare how MAiNGO and MUSE-BB perform with different branching priority ratios

$$\rho = \frac{\text{first-stage branching priority}}{\text{second-stage branching priority}},$$

which in the present case ($N_x = N_y = 1$) correspond to the branching priority of x (the priority for y_s being 1).

[Fig. 3](#) shows the wall times spent in B&B when using MAiNGO and MUSE-BB on problem instances with $N_s \in \{4, 8, 16\}$. Both individual times (colored dots), as well as the median times (horizontal lines) are depicted. [Tab. 1](#) lists the median wall times and relative gaps for instances which do not terminate within the time-limit of one hour. In general, the ρ values minimizing average wall time for each scenario are much lower for MAiNGO than for MUSE-BB. However, low ρ values lead to significantly worse performance for MUSE-BB than for MAiNGO, e.g., all runs for $(N_s, \rho) = (8, 1)$ time out after one hour with a median remaining gap of 2.4%. For $N_s = 16$, all instances solved with MAiNGO time out, while for MUSE-BB almost all instances with ρ values above 4 terminate (with the exception of two outliers for $\rho = 16$). This indicates the importance of appropriate branching priorities when solving stochastic problems in general, and when using MUSE-BB in particular. When comparing the best ρ values for each scenario (bold in [Tab. 1](#)), MUSE-BB outperforms MAiNGO in terms of wall time by a factor of 3.5 and 15 for $N_s = 4$ and $N_s = 8$, respectively. For $N_s = 16$ the value is expected to be significantly larger than $3600/295.3 \approx 12$.

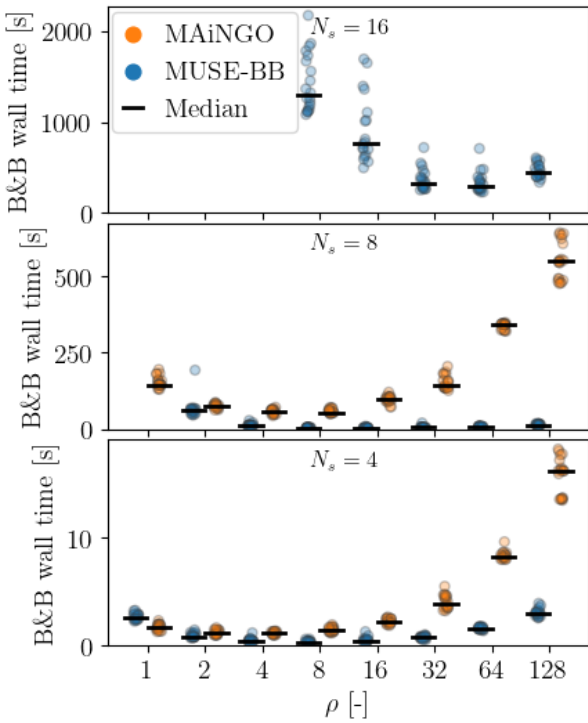


Fig. 3. Variation of solution time for deterministic equivalent (MAiNGO) and parallel decomposition (MUSE-BB) with ρ for $N_s \in \{4, 8, 16\}$ over 20 runs each. Parameter combinations without data points did not terminate within 3600s, also see Tab. 1.

Note that already for these relatively small problem sizes outperformance is close to or even larger than the number of scenarios and thus the number of used threads. This implies that MUSE-BB can be more favorable than more general parallelization approaches such as, e.g., the MPI parallelization of MAiNGO, where open nodes are processed by different CPUs (not used in this work). While such general parallelization approaches are more widely applicable, they do not exploit the special problem structure of DE. Consequently they may be used in conjunction with the parallel processing of individual B&B nodes presented in this work to optimally use computational infrastructure.

The results indicate that optimal branching priority ratios (i.e., ρ values resulting in minimal median wall time) may increase with the number of scenarios considered. Nevertheless, a projection-based approach, where only the first-stage variables are branched (corresponding to $\rho \rightarrow \infty$) appears unfavorable, as wall times increase significantly for large ρ -values.

6.2 Effect of Multisection

We next consider the effect of the multisection parameters k_{\max} , and η . Recall that every time a second-stage variable is selected for branching, we solve the $2N_s$ independent subproblems, resulting from the multisection involving the corresponding N_s variable instances for different scenarios. We then use the results to compute strong-branching scores σ_s for each partitioned variable, and create up to $2^{k_{\max}}$ child nodes, with the actual number being controlled by the value of the strong-branching threshold $\eta \in (0, 1]$, i.e., we reject partitions with a strong-branching score below $\eta\sigma_s$, see Section 4.4.

For each N_s value, we take the three ρ values for which MUSE-BB performed best at $k_{\max} = 1$, and perform further experiments for $k_{\max} \in \{2, 4, 8\}$, and $\eta \in \{0.1, 0.2, 0.5, 0.8, 1\}$. Increasing values of k_{\max} , and decreasing values of η allow a larger number of child nodes to be created from each multisection, i.e., the maximum is $2^8 = 256$ for $(k_{\max}, \eta) = (8, 1)$. We point out that multiple variables may achieve the maximum strong-branching score. Hence, even for $\eta = 1$, the settings $k_{\max} = 1$, and $k_{\max} > 1$, may produce different B&B trees (and thus wall times) for a given problem instance, as the latter setting allows multiple variables to be branched, while the former does not.

Tab. 1. Median B&B wall times in seconds over 20 runs, or remaining relative optimality gaps in % (computed as 1 - ratio of lower to upper bound) after 3600s for solving the CHP sizing model with different number of scenarios and branching priorities, using MAiNGO and MUSE-BB. Two out of the 20 runs for the instance $N_s = \rho = 16$, solved with MUSE-BB, timed out. The median is computed with respect to the remaining 18 runs. Minima for each column (highlighted in bold) indicate that the performance of MUSE-BB relatively to MAiNGO improves with an increase of scenarios, and thus problem size.

algor.	MAiNGO			MUSE-BB		
	$\rho \setminus N_s$	4	8	16	4	8
1	1.7	145	17%	2.6	2.4%	20%
2	1.1	77	8.8%	0.82	62	7.6%
4	1.1	59	4.6%	0.42	12	2.8%
8	1.4	55	3.7%	0.33	4.3	1292
16	2.2	98	3.8%	0.43	3.5	765
32	3.9	142	4.3%	0.75	5.2	329
64	8.2	342	5.0%	1.6	7.8	295
128	16	550	5.7%	3.0	14	436

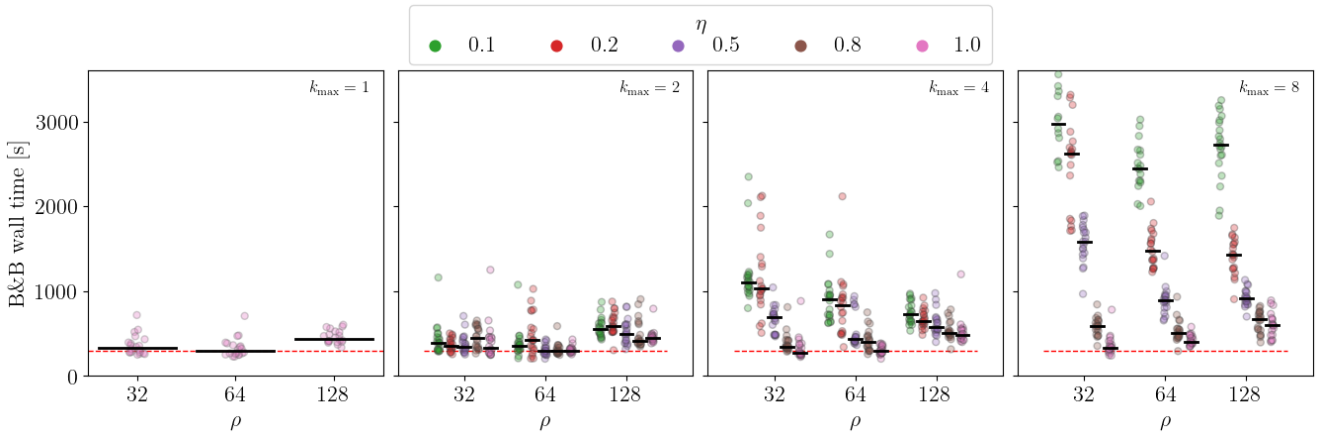


Fig. 4. Variation of solution times for solving the CHP sizing problem using MUSE-BB with $k_{\max} \in \{1, 2, 4, 8\}$, and $\eta \in \{0.1, 0.2, 0.5, 0.8, 1\}$ for the three ρ values resulting in the lowest median wall times for $(k_{\max}, N_s) = (1, 16)$. For each parameter combination, a set of 20 runs is performed. For $(k_{\max}, \rho, \eta) = (8, 32, 0.1)$, $(8, 32, 0.2)$, and $(8, 64, 0.1)$, 8, 2, and 3 runs timed out after 3600 s, respectively. Medians with respect to the remaining runs are depicted as horizontal black lines and the lowest median time for $k_{\max} = 1$ is depicted as a dashed red line for reference. Increasing k_{\max} generally results in larger wall times, and for $k_{\max} = 4$ and 8, increasing η results in smaller wall times.

As before, we repeat the solution for each parameter combination 20 times. Since combinations with $N_s = 4$, and $N_s = 8$, show no clear trend for the effect of k_{\max} , or η , we only focus on combinations with $N_s = 16$, the results of which are depicted in Fig. 4. The B&B wall times of all investigated combinations are visualized in Fig. 6 in Appendix B. Only a small set of parameter combinations results in improvements over the best median wall time for $k_{\max} = 1$, (i.e., 295 s for $\rho = 64$). However, these improvements are mostly insignificant, with the best median wall time of 272 s (achieved for $(k_{\max}, \rho, \eta) = (4, 32, 1)$) corresponding to an improvement of less than 8%. For the remaining parameter combinations median wall times remain the same or increase. While combinations with $(N_s, k_{\max}) = (16, 2)$ show no clear trend for the effect of η , for $(N_s, k_{\max}) = (16, 4)$, and $(16, 8)$, an increase of η results in reductions of wall time. In general, an increase of k_{\max} results in an increase of median wall times.

In summary, the results suggest that the setting $k_{\max} = 1$ is preferable for the majority of considered problem instances. Note that partitions which produce a single infeasible subproblem may always be used, as they effectively result in domain reduction, and do not increase the number of child nodes. Thus, for $k_{\max} = 1$, only a single pair of child nodes is generated, and the process of node generation is very similar to that of classical strong-branching in standard B&B. However, MUSE-BB solves smaller subproblems, which contain a subset of all problem variables and may reuse domain information from the rejected partitions to tighten the domain of the produced child nodes.

7 Summary and Outlook

We present MUSE-BB, a multisection B&B-based decomposition algorithm for the deterministic global optimization of general nonconvex nonlinear two-stage problems. We prove finite ε_f -convergence, show favorable convergence order of our lower bounding scheme, compared to existing algorithms, and provide initial computational results indicating good scalability of MUSE-BB with the number of scenarios.

Existing decomposition algorithms for two-stage nonconvex MINLP problems (Kannan, 2018; Cao and Zavala, 2019; Li and Grossmann, 2019) have been classified as PBDAs (Robertson, Cheng, and Scott, 2020), since they all employ spatial B&B in the first-stage variables. PBDAs achieve this by solving decomposable subproblems of both first- and second-stage variables in each node. To obtain good lower bounds, these subproblems are solved globally via a nested spatial B&B. Instead, we propose to branch on both first- and second-stage variables within a single B&B tree, and to further relax subproblems, avoiding duplicate branching on first-stage variables, and the nesting of spatial B&B procedures. We either branch normally on a single first-stage variable, or we simultaneously branch on multiple second-stage variables from different scenarios. While such multisection produces an exponential number of child nodes, the total number of distinct subproblems is only linear in the number of scenarios, by virtue of the decomposition. Thus, we only need to process the distinct subproblems and can generate child nodes by appropriately combining the subproblem results. To avoid an excessive number of child nodes with poor lower

bounds, we select a subset of variable partitions, using the associated strong-branching scores, which are readily available after processing. This allows to only generate child nodes corresponding to promising partitions with high strong-branching score.

Our theoretical results show that by branching on all variables, the lower bounding scheme of MUSE-BB generally has a convergence order of one, if all functions are Lipschitz. This is in contrast to lower bounding schemes of existing decomposition algorithms, which may have convergence orders below one, in general (Robertson, Cheng, and Scott, 2020). Whether or not this improved convergence order actually translates into an advantage with respect to the occurrence of clustering is however not clear at this point, and requires further investigation.

We perform initial computational experiments with a small test problem, which despite its size still incorporates relevant nonlinearities found in applications. Our results highlight the importance of choosing appropriate branching priorities for both general B&B and decomposition algorithms. Moreover, the results show that even for this small problem and small numbers of scenarios, MUSE-BB can significantly outperform the standard version of our open-source deterministic global solver MAiNGO, applied to the deterministic equivalent formulation. For the considered problem instances, the best wall times of MUSE-BB are achieved when limiting the number of child nodes resulting from multisection to two.

Future work includes theoretical and computational comparison of MUSE-BB with other decomposition algorithms; in particular, determining which method is preferable in different situations, e.g., depending on the number of first- and second-stage variables, and scenarios.

As with existing decomposition algorithms, the lower bounding scheme of MUSE-BB may be improved by dualizing the coupling (nonanticipativity) constraints instead of dropping them. The resulting lower bounding scheme can be shown to have second-order convergence at minimizers satisfying certain regularity conditions. However, this extension requires optimal dual multipliers, which are expensive to compute in general. The details of how such an extension can be implemented need to be clarified.

We aim to investigate the effect of combining the parallel bounding routines of MUSE-BB with more general B&B parallelization as implemented in MAiNGO, as this is expected to make MUSE-BB applicable to much larger, more realistic case studies. Furthermore, it may be interesting to generalize the presented implementation to problems with different numbers of second-stage variables and constraints. A related extension would allow branching on arbitrary combinations of second-stage variables from different scenarios, instead of limiting multisection to scenario instances of a particular second-stage variable. Finally, the decomposable bounding routines of MUSE-BB may enable efficient strong-branching in problems that do not fall into the category of two-stage programming problems, but still exhibit block structures, coupled by complicating constraints.

Acknowledgements

Simulations were performed with computing resources granted by RWTH Aachen University under project rwth1468. M. L., M. D., and A. M. acknowledge funding from the Helmholtz Association of German Research Centers. The authors are grateful to J. K. Scott for his instructive talk Robertson, Cheng, and Scott, 2020, providing a recording of this talk, and fruitful discussions.

Author Contribution

- A. M., D. B., M. L. contributed to the conceptual development of the algorithm.
- A. M., and M. L. developed the theoretical results (proofs and examples in 5).
- M. L. carried out the software implementation with guidance from D. B.
- M. L. designed and conducted the computational experiments and analyzed the results.

CRedit Authorship Contribution Statement

Conceptualization: A. M., D. B., M. L. Formal Analysis: A. M., M. L. Funding Acquisition: A. M., M. D. Methodology: A. M., M. L. Software: M. L. Supervision: A. M., M. D. Validation: M. L. Visualization: M. L. Writing – original draft: A. M., M. L. Writing – review & editing: All authors

A Test Problem

We consider the design of a combined heat and power (CHP) unit, i.e., an equipment sizing problem whose aim is to satisfy given heat and power demands at minimum cost, see Fig. 5. The size of the CHP is expressed as a

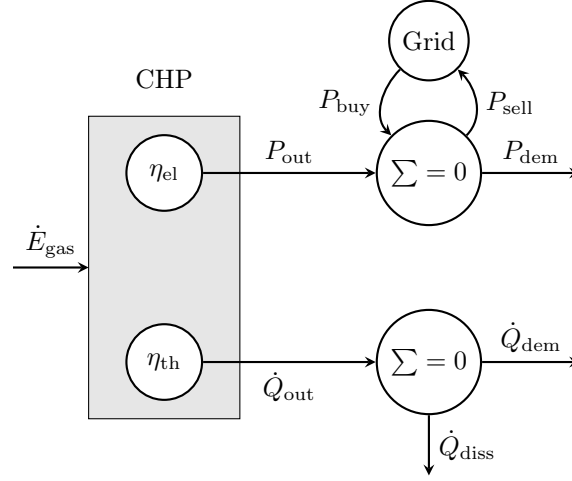


Fig. 5. Conceptual CHP operation

nominal heat output \dot{Q}_{nom} , which corresponds to the maximum thermal output \dot{Q}_{out} . The actual output at any given point is determined by a relative heat output \dot{Q}_{rel} :

$$\dot{Q}_{\text{out}} := \dot{Q}_{\text{nom}} \dot{Q}_{\text{rel}} \quad (3)$$

The energy input to the CHP in terms of lower heating value of natural gas, \dot{E}_{gas} , can be calculated via the thermal efficiency η_{th} , which is a function of \dot{Q}_{nom} and \dot{Q}_{rel} :

$$\dot{E}_{\text{gas}} := \frac{\dot{Q}_{\text{out}}}{\eta_{\text{th}}(\dot{Q}_{\text{nom}}, \dot{Q}_{\text{rel}})} \quad (4)$$

Following this the power output P_{out} can be computed via the electrical efficiency η_{el} , which is also a function of \dot{Q}_{nom} and \dot{Q}_{rel} :

$$P_{\text{out}} := \dot{E}_{\text{gas}} \eta_{\text{el}}(\dot{Q}_{\text{nom}}, \dot{Q}_{\text{rel}}) \quad (5)$$

The functional form of the efficiencies η_{th} and η_{el} is given by:

$$\eta_{\text{th}}(\dot{Q}_{\text{nom}}, \dot{Q}_{\text{rel}}) := \eta_{\text{th,nom}}(\dot{Q}_{\text{nom}}) \eta_{\text{th,rel}}(\dot{Q}_{\text{rel}}) \quad (6)$$

$$\eta_{\text{th,nom}}(\dot{Q}_{\text{nom}}) := 0.498 - \frac{\dot{Q}_{\text{nom}}}{21.17 \text{ MW}} \quad (7)$$

$$\eta_{\text{th,rel}}(\dot{Q}_{\text{rel}}) := 1.10 - 0.0768 (\dot{Q}_{\text{rel}} + 0.130)^2 \quad (8)$$

$$\eta_{\text{el}}(\dot{Q}_{\text{nom}}, \dot{Q}_{\text{rel}}) := \eta_{\text{el,nom}}(\dot{Q}_{\text{nom}}) \eta_{\text{el,rel}}(\dot{Q}_{\text{rel}}) \quad (9)$$

$$\eta_{\text{el,nom}}(\dot{Q}_{\text{nom}}) := 0.372 + \frac{\dot{Q}_{\text{nom}}}{21.17 \text{ MW}} \quad (10)$$

$$\eta_{\text{el,rel}}(\dot{Q}_{\text{rel}}) := 1.02 - 0.435 (0.774 \dot{Q}_{\text{rel}} - 1)^2 \quad (11)$$

A heat shortage, defined as

$$\dot{Q}_{\text{short}} := \dot{Q}_{\text{dem}} - \dot{Q}_{\text{out}} \quad (12)$$

must be avoided (i.e., \dot{Q}_{short} must be negative). Correspondingly, the power shortage can be defined as:

$$P_{\text{short}} := P_{\text{dem}} - P_{\text{out}} \quad (13)$$

A power shortage can be addressed by purchasing power from the grid, i.e.:

$$P_{\text{buy}} := \max(0, P_{\text{short}}) \quad (14)$$

If P_{short} or \dot{Q}_{short} are negative, the excess power can be sold to the grid at a reduced price, while the excess heat can be dissipated into the environment:

$$\dot{P}_{\text{sell}} := \max(0, -P_{\text{short}}) \quad (15)$$

$$\dot{Q}_{\text{diss}} := \max(0, -\dot{Q}_{\text{short}}). \quad (16)$$

With these definitions we can formulate a reduced-space problem that contains the nominal heat output as the only first-stage variable, i.e: $\mathbf{x} = (\dot{Q}_{\text{nom}}) \in [1.4 \text{ MW}, 2.3 \text{ MW}]$, and the part-load in each scenario as the only second-stage variable, i.e: $\mathbf{y}_s = (\dot{Q}_{\text{rel},s}) \in [0, 1]$.

We choose total annualized costs (TAC) in million € as the objective function. The first-stage objective function describes the annualized investment costs (according to an economy of scales approach) and the second-stage objectives correspond to the annual operating costs in each scenario:

$$f_{\text{I}}(\mathbf{x}) = 149\,567 \text{ €/a} \left(\frac{\dot{Q}_{\text{nom}}}{1 \text{ MW}} \right)^{0.9} \times 10^{-6} \quad (17)$$

$$\begin{aligned} f_{\text{II},s}(\mathbf{x}, \mathbf{y}_s) = T_{\text{op}} & \left(p_{\text{gas}} \dot{E}_{\text{gas},s} \right. \\ & + p_{\text{el,buy}} P_{\text{buy},s} \\ & \left. - p_{\text{el,sell}} P_{\text{sell},s} \right) \times 10^{-6} \end{aligned} \quad (18)$$

Where $T_{\text{op}} = 6000 \text{ h/a}$, $p_{\text{gas}} = 80 \text{ €/ (MW h)}$, $p_{\text{el,buy}} = 250 \text{ €/ (MW h)}$, $p_{\text{el,sell}} = 100 \text{ €/ (MW h)}$

We approximate the requirement that the CHP unit must either be inactive or operate above a minimal part-load threshold of 50% with quadratic second-stage constraints of the form

$$0.0619263 - (\dot{Q}_{\text{rel},s} - 0.25115)^2 \leq 0 \quad (19)$$

which restrict the relative outputs $\dot{Q}_{\text{rel},s}$ to less than 0.1%, or more than 50% part-load. An additional constraint is that

$$\dot{Q}_{\text{short},s} \leq 0, \quad (20)$$

also see Eq. (12). Note that Eq. (19) implies that heat demands corresponding to part-loads between 0.1% and 50% cannot be satisfied. To ensure the considered instances have a feasible solution, the randomly generated heat demands are set to 0 if they fall into this range. Similarly, the generated power and heat demands are capped to the highest possible production.

B Parameter Study for k_{\max} and η

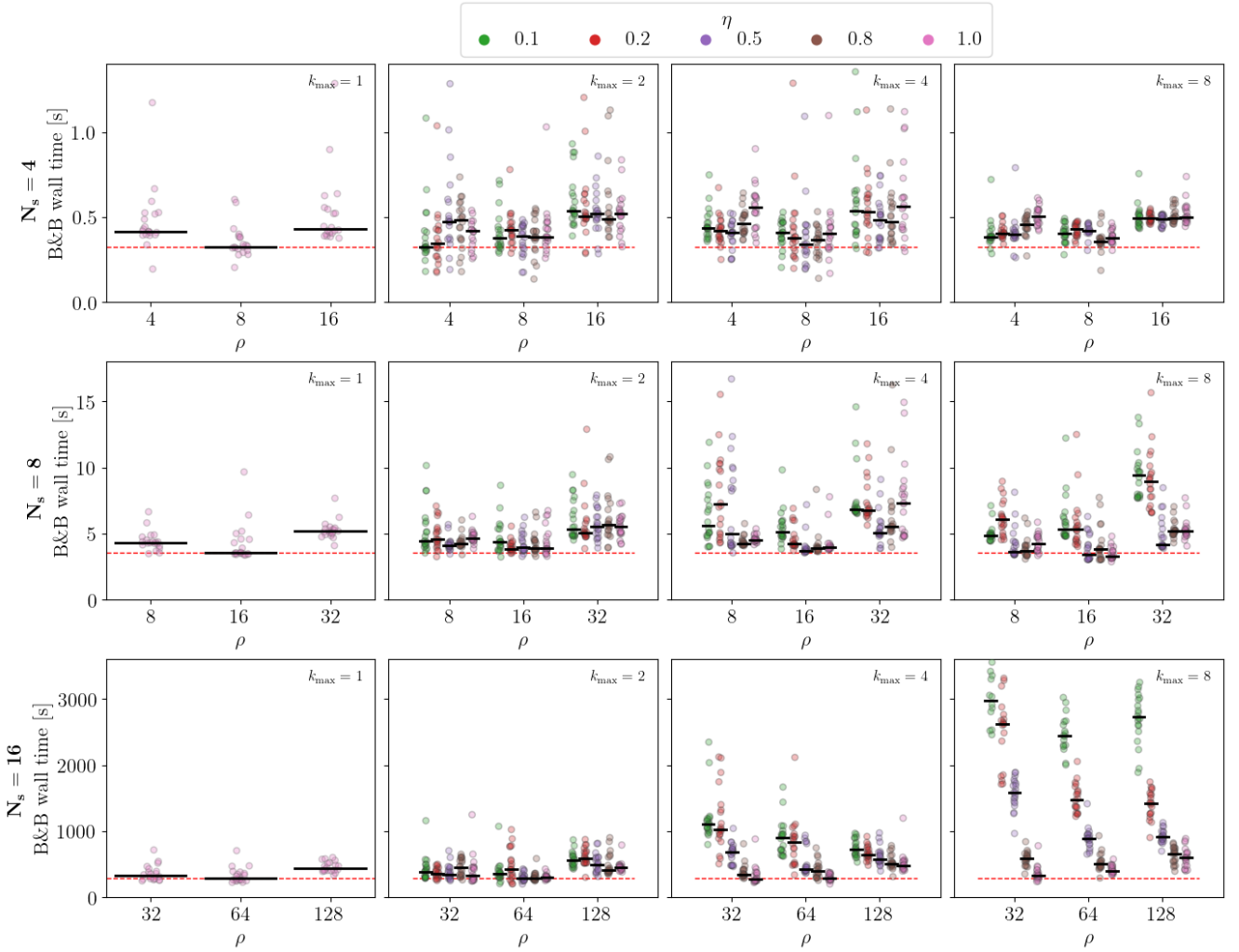


Fig. 6. Variation of solution times for solving the CHP sizing problem using MUSE-BB with $k_{\max} \in \{1, 2, 4, 8\}$, and $\eta \in \{0.1, 0.2, 0.5, 0.8, 1\}$ for the three ρ values resulting in the lowest median wall times for $N_s = 4, 8$, and 16 , with $k_{\max} = 1$. For each parameter combination, a set of 20 runs is performed. For $(k_{\max}, \rho, \eta) = (8, 32, 0.1)$, $(8, 32, 0.2)$, and $(8, 64, 0.1)$, 8, 2, and 3 runs timed out after 3600s, respectively. Medians with respect to the remaining runs are depicted as horizontal black lines and the lowest median time for $k_{\max} = 1$ is depicted as a dashed red line for reference. Whereas for $N_s = 4$, and 8, no clear trend is discernible, for $N_s = 16$, increasing k_{\max} generally results in larger wall times, and for $k_{\max} = 4$, and 8, increasing η results in smaller wall times.

C Overview of Functions and Optimization Problems

Function	explanation
f	overall objective function
f_I	first-stage objective function
$f_{II,s}$	second-stage objective function
$f_{II,s}^{\mathcal{Y}_s}$	second-stage optimal value function
f_s	scenario objective function
$f_s^{\mathcal{X}, \mathcal{Y}_s}$	scenario optimal value function

Problem	explanation
TSP	two-stage (stochastic programming) problem
DE (DE ⁿ)	deterministic equivalent form of TSP (restricted to the domain of node n)
DE _{NAC}	NAC formulation, equivalent to DE and TSP
RP _s ⁿ	recourse problems for a given value of \mathbf{x} for node n (providing upper bounds)
LSP _s ⁿ	relaxations of DE _{NAC} for node n by dualizing NACs with multipliers λ_s
SP _s ⁿ	relaxations of DE _{NAC} for node n by dropping NACs
MC _s ⁿ	McCormick relaxation of SP _s ⁿ for node n
LP _s ⁿ	linear relaxation of MC _s ⁿ for node n (providing lower bounds)
OBBT _{s,v} ⁿ	OBBT problems for variable v and node n
R _s ⁿ	generic scenario relaxation for node n

Nomenclature

Symbols

\mathcal{F}	feasible set of an optimization problem
f	objective function
\mathbf{g}	generic constraint function vector
\mathbf{h}	nonanticipativity constraints
\mathcal{L}	list of k scenarios for which both sibling subproblems are feasible, the associated second-stage variable instances will be branched, producing 2^k orthant nodes
\mathcal{M}	map from scenarios producing exactly one infeasible sibling subproblem to the sibling n with a feasible subproblem, the associated second-stage variable instances will be branched, but do not add to the number of orthant nodes generated
N	Number, e.g., of first-stage variables (subscript x) or second-stage constraints (subscript II)
n	node of the B&B tree
\mathcal{N}	Set of open nodes of the B&B tree
s	Scenario
$\check{\nabla}$	subgradient
\mathcal{X}	domain of \mathbf{x}
\mathbf{x}	first-stage variables
\mathcal{Y}	domain of \mathbf{y}
\mathbf{y}	second-stage variables

Subscripts

•	related to lower bound
I	related to first-stage
II	related to second-stage

Superscripts

•	related to upper bound
cv	convex relaxation
†	related to incumbent
*	related to optimal solution

References

- Achterberg (2007). “Constraint Integer Programming”. PhD thesis. TU Berlin.
- Achterberg, Koch, and Martin (2005). “Branching rules revisited”. In: *Oper. Res. Lett.* 33.1, pp. 42–54. DOI: [10.1016/j.orl.2004.04.002](https://doi.org/10.1016/j.orl.2004.04.002).
- Adjiman and Floudas (2008). “alphaBB Algorithm”. In: *Encyclopedia of Optimization*. New York: Springer, pp. 61–73. DOI: [10.1007/978-0-387-74759-0_11](https://doi.org/10.1007/978-0-387-74759-0_11).
- Androulakis, Maranas, and Floudas (1995). “alphaBB: A global optimization method for general constrained nonconvex problems”. In: *J. Glob. Optim.* 7.4, pp. 337–363. DOI: [10.1007/bf01099647](https://doi.org/10.1007/bf01099647).
- Applegate et al. (1995). *Finding Cuts in the TSP (A Preliminary Report)*. Tech. rep. AT&T Bell Labs.
- Belotti (2019). *Couenne: a user’s manual*. URL: <https://www.coin-or.org/Couenne/couenne-user-manual.pdf> (visited on May 13, 2024).
- Benders (1962). “Partitioning procedures for solving mixed-variables programming problems”. In: *Numer. Math.* 4.1, pp. 238–252. DOI: [10.1007/BF01386316](https://doi.org/10.1007/BF01386316).
- Birge and Louveaux (2011). *Introduction to Stochastic Programming*. New York: Springer. DOI: [10.1007/978-1-4614-0237-4](https://doi.org/10.1007/978-1-4614-0237-4).
- Bompadre and Mitsos (2011). “Convergence rate of McCormick relaxations”. In: *J. Glob. Optim.* 52.1, pp. 1–28. DOI: [10.1007/s10898-011-9685-2](https://doi.org/10.1007/s10898-011-9685-2).
- Bongartz et al. (2018). *MAiNGO: McCormick based Algorithm for mixed integer Nonlinear Global Optimization*. Tech. rep. <http://permalink.avt.rwth-aachen.de/?id=729717>. The open-source version is available at <https://git.rwth-aachen.de/avt-svt/public/maingo>. The corresponding Python package `maingopy` is available at <https://pypi.org/project/maingopy>. Process Systems Engineering (AVT.SVT), RWTH Aachen University. (Visited on June 10, 2024).
- Cao, Song, and Khan (2019). “Convergence of Subtangent-Based Relaxations of Nonlinear Programs”. In: *Processes* 7.4, p. 221. DOI: [10.3390/pr7040221](https://doi.org/10.3390/pr7040221).
- Cao and Zavala (2019). “A scalable global optimization algorithm for stochastic nonlinear programs”. In: *J. Glob. Optim.* 75.2, pp. 393–416. DOI: [10.1007/s10898-019-00769-y](https://doi.org/10.1007/s10898-019-00769-y).
- Carøe and Schultz (1999). “Dual decomposition in stochastic integer programming”. In: *Oper. Res. Lett.* 24.1-2, pp. 37–45. DOI: [10.1016/S0167-6377\(98\)00050-9](https://doi.org/10.1016/S0167-6377(98)00050-9).
- Chachuat et al. (2015). “Set-Theoretic Approaches in Analysis, Estimation and Control of Nonlinear Systems”. In: *IFAC-PapersOnLine* 48.8, pp. 981–995. DOI: [10.1016/j.ifacol.2015.09.097](https://doi.org/10.1016/j.ifacol.2015.09.097).
- Clarke (1990). *Optimization and Nonsmooth Analysis*. SIAM. DOI: [10.1137/1.9781611971309](https://doi.org/10.1137/1.9781611971309).
- Csallner, Csendes, and Markót (2000). “Multisection in Interval Branch and Bound Methods for Global Optimization – I. Theoretical Results”. In: *J. Glob. Optim.* 16.4, pp. 371–392. DOI: [10.1023/a:1008354711345](https://doi.org/10.1023/a:1008354711345).
- Dantzig and Wolfe (1960). “Decomposition Principle for Linear Programs”. In: *Oper. Res.* 8.1, pp. 101–111. DOI: [10.1287/opre.8.1.101](https://doi.org/10.1287/opre.8.1.101).
- Du and Kearfott (1994). “The Cluster Problem in Multivariate Global Optimization”. In: *J. Glob. Optim.* 5.3, pp. 253–265. DOI: [10.1007/bf01096455](https://doi.org/10.1007/bf01096455).
- Dür and Horst (1997). “Lagrange Duality and Partitioning Techniques in Nonconvex Global Optimization”. In: *J. Optim. Theory Appl.* 95.2, pp. 347–369. DOI: [10.1023/a:1022687222060](https://doi.org/10.1023/a:1022687222060).
- Fiacco, ed. (1983). *Introduction to sensitivity and stability analysis in nonlinear programming*. Elsevier. DOI: [10.1016/s0076-5392\(08\)x6041-2](https://doi.org/10.1016/s0076-5392(08)x6041-2).
- Füllner, Kirst, and Stein (2020). “Convergent upper bounds in global minimization with nonlinear equality constraints”. In: *Math. Programm.* 187.1–2, pp. 617–651. DOI: [10.1007/s10107-020-01493-2](https://doi.org/10.1007/s10107-020-01493-2).
- Geoffrion (1972). “Generalized Benders Decomposition”. In: *J. Optim. Theory Appl.* 10.4, pp. 237–260. DOI: [10.1007/BF00934810](https://doi.org/10.1007/BF00934810).
- Ginchev, Torre, and Rocca (2009). “ $C^{k,1}$ Functions, Characterization, Taylor’s Formula and Optimization: A Survey”. In: *Real Anal. Exchange* 35.2, pp. 311–342.
- Gleixner et al. (2016). “Three enhancements for optimization-based bound tightening”. In: *J. Glob. Optim.* 67.4, pp. 731–757. DOI: [10.1007/s10898-016-0450-4](https://doi.org/10.1007/s10898-016-0450-4).
- Kannan (2018). “Algorithms, analysis and software for the global optimization of two-stage stochastic programs”. PhD thesis. Massachusetts Institute of Technology. URL: <https://dspace.mit.edu/handle/1721.1/117326> (visited on May 13, 2024).
- Kannan and Barton (2017a). “Convergence-order analysis of branch-and-bound algorithms for constrained problems”. In: *J. Glob. Optim.* 71.4, pp. 753–813. DOI: [10.1007/s10898-017-0532-y](https://doi.org/10.1007/s10898-017-0532-y).

- Kannan and Barton (2017b). “The cluster problem in constrained global optimization”. In: *J. Glob. Optim.* 69.3, pp. 629–676. DOI: [10.1007/s10898-017-0531-z](https://doi.org/10.1007/s10898-017-0531-z).
- Karmakar, Mahato, and Bhunia (2009). “Interval oriented multi-section techniques for global optimization”. In: *J. Comput. Appl. Math.* 224.2, pp. 476–491. DOI: [10.1016/j.cam.2008.05.025](https://doi.org/10.1016/j.cam.2008.05.025).
- Karuppiah and Grossmann (2007). “A Lagrangean based branch-and-cut algorithm for global optimization of nonconvex mixed-integer nonlinear programs with decomposable structures”. In: *J. Glob. Optim.* 41.2, pp. 163–186. DOI: [10.1007/s10898-007-9203-8](https://doi.org/10.1007/s10898-007-9203-8).
- Kazazakis (2017). “Parallel computing, interval derivative methods, heuristic algorithms, and their implementation in a numerical solver, for deterministic global optimization”. PhD thesis. Imperial College London.
- Kearfott and Du (1993). “The Cluster Problem in Global Optimization: the Univariate Case”. In: *Computing Supplementum*. Vienna: Springer, pp. 117–127. DOI: [10.1007/978-3-7091-6918-6_10](https://doi.org/10.1007/978-3-7091-6918-6_10).
- Khajavirad and Michalek (2009). “A Deterministic Lagrangian-Based Global Optimization Approach for Quasiseparable Nonconvex Mixed-Integer Nonlinear Programs”. In: *J. Mech. Design* 131.5. DOI: [10.1115/1.3087559](https://doi.org/10.1115/1.3087559).
- Khan (2018). “Subtangent-based approaches for dynamic set propagation”. In: *2018 IEEE Conference on Decision and Control (CDC)* (Miami, FL, USA, Sept. 17–19, 2018), pp. 3050–3055. DOI: [10.1109/cdc.2018.8618872](https://doi.org/10.1109/cdc.2018.8618872).
- Kirst, Stein, and Steuermann (2015). “Deterministic upper bounds for spatial branch-and-bound methods in global minimization with nonconvex constraints”. In: *TOP* 23.2, pp. 591–616. DOI: [10.1007/s11750-015-0387-7](https://doi.org/10.1007/s11750-015-0387-7).
- Langiu, Dahmen, and Mitsos (2022). “Simultaneous optimization of design and operation of an air-cooled geothermal ORC under consideration of multiple operating points”. In: *Comput. Chem. Eng.* 161, p. 107745. DOI: [10.1016/j.compchemeng.2022.107745](https://doi.org/10.1016/j.compchemeng.2022.107745).
- Laporte and Louveaux (1993). “The integer L-shaped method for stochastic integer programs with complete recourse”. In: *Oper. Res. Lett.* 13.3, pp. 133–142. DOI: [10.1016/0167-6377\(93\)90002-X](https://doi.org/10.1016/0167-6377(93)90002-X).
- Li and Grossmann (2019). “A generalized Benders decomposition-based branch and cut algorithm for two-stage stochastic programs with nonconvex constraints and mixed-binary first and second stage variables”. In: *J. Glob. Optim.* 75.2, pp. 247–272. DOI: [10.1007/s10898-019-00816-8](https://doi.org/10.1007/s10898-019-00816-8).
- Li and Li (2015). “Global optimization of an industrial natural gas production network”. In: *IFAC-PapersOnLine* 48.8, pp. 337–342. DOI: [10.1016/j.ifacol.2015.08.204](https://doi.org/10.1016/j.ifacol.2015.08.204).
- Li and Li (2016). “Domain reduction for Benders decomposition based global optimization”. In: *Comput. Chem. Eng.* 93, pp. 248–265. DOI: [10.1016/j.compchemeng.2016.06.009](https://doi.org/10.1016/j.compchemeng.2016.06.009).
- Li and Cui (2024). “A Decomposition Algorithm for Two-Stage Stochastic Programs with Nonconvex Recourse Functions”. In: *SIAM J. Optim.* 34.1, pp. 306–335. DOI: [10.1137/22M1488533](https://doi.org/10.1137/22M1488533).
- Li, Sundaramoorthy, and Barton (2014). “Nonconvex Generalized Benders Decomposition”. In: *Optimization in Science and Engineering*. New York: Springer, pp. 307–331. DOI: [10.1007/978-1-4939-0808-0_16](https://doi.org/10.1007/978-1-4939-0808-0_16).
- Li, Tomaszgard, and Barton (2011). “Nonconvex Generalized Benders Decomposition for Stochastic Separable Mixed-Integer Nonlinear Programs”. In: *J. Optim. Theory Appl.* 151.3, pp. 425–454. DOI: [10.1007/s10957-011-9888-1](https://doi.org/10.1007/s10957-011-9888-1).
- Markót, Csendes, and Csallner (2000). “Multisection in Interval Branch and Bound Methods for Global Optimization – II. Numerical Tests”. In: *J. Glob. Optim.* 16.3, pp. 219–228. DOI: [10.1023/a:1008359223042](https://doi.org/10.1023/a:1008359223042).
- McCormick (1976). “Computability of global solutions to factorable nonconvex programs: Part I - Convex underestimating problems”. In: *Math. Programm.* 10.1, pp. 147–175. DOI: [10.1007/bf01580665](https://doi.org/10.1007/bf01580665).
- Najman, Bongartz, and Mitsos (2021). “Linearization of McCormick relaxations and hybridization with the auxiliary variable method”. In: *J. Glob. Optim.* DOI: [10.1007/s10898-020-00977-x](https://doi.org/10.1007/s10898-020-00977-x).
- Najman and Mitsos (2016). “Convergence analysis of multivariate McCormick relaxations”. In: *J. Glob. Optim.* 66.4, pp. 597–628. DOI: [10.1007/s10898-016-0408-6](https://doi.org/10.1007/s10898-016-0408-6).
- Najman and Mitsos (2019). “Tighter McCormick Relaxations through Subgradient Propagation”. In: *J. Glob. Optim.* 75.3, pp. 565–593. DOI: [10.1007/s10898-019-00791-0](https://doi.org/10.1007/s10898-019-00791-0).
- Ogbe and Li (2019). “A joint decomposition method for global optimization of multiscenario nonconvex mixed-integer nonlinear programs”. In: *J. Glob. Optim.* 75.3, pp. 595–629. DOI: [10.1007/s10898-019-00786-x](https://doi.org/10.1007/s10898-019-00786-x).
- Oliveira et al. (2013). “A Lagrangean decomposition approach for oil supply chain investment planning under uncertainty with risk considerations”. In: *Comput. Chem. Eng.* 50, pp. 184–195. DOI: [10.1016/j.compchemeng.2012.10.012](https://doi.org/10.1016/j.compchemeng.2012.10.012).
- Robertson, Cheng, and Scott (2020). “Convergence Rate Analysis for Schemes of Relaxations in Decomposition Methods for Global Nonconvex Stochastic Optimization” (virtual, Nov. 17, 2020). CAST plenary session of AIChE Annual Meeting 2020.
- Rote (1992). “The convergence rate of the sandwich algorithm for approximating convex functions”. In: *Computing* 48.3–4, pp. 337–361. DOI: [10.1007/bf02238642](https://doi.org/10.1007/bf02238642).

- Ryoo and Sahinidis (1995). “Global optimization of nonconvex NLPs and MINLPs with applications in process design”. In: *Comput. Chem. Eng.* 19.5, pp. 551–566. DOI: [10.1016/0098-1354\(94\)00097-2](https://doi.org/10.1016/0098-1354(94)00097-2).
- Sahinidis (2024). *BARON user manual: v. 24.05.08*. URL: <http://www.minlp.com/downloads/docs/baron%20manual.pdf> (visited on May 8, 2024).
- Schichl and Neumaier (2005). “Interval Analysis on Directed Acyclic Graphs for Global Optimization”. In: *J. Glob. Optim.* 33.4, pp. 541–562. DOI: [10.1007/s10898-005-0937-x](https://doi.org/10.1007/s10898-005-0937-x).
- Scott, Stuber, and Barton (2011). “Generalized McCormick relaxations”. In: *J. Glob. Optim.* 51.4, pp. 569–606. DOI: [10.1007/s10898-011-9664-7](https://doi.org/10.1007/s10898-011-9664-7).
- Smith and Pantelides (1997). “Global optimisation of nonconvex MINLPs”. In: *Comput. Chem. Eng.* 21, S791–S796. DOI: [10.1016/s0098-1354\(97\)87599-0](https://doi.org/10.1016/s0098-1354(97)87599-0).
- Stechlinski, Khan, and Barton (2018). “Generalized Sensitivity Analysis of Nonlinear Programs”. In: *SIAM J. Optim.* 28.1, pp. 272–301. DOI: [10.1137/17m1120385](https://doi.org/10.1137/17m1120385).
- Tawarmalani and Sahinidis (2004). “Global optimization of mixed-integer nonlinear programs: A theoretical and computational study”. In: *Math. Program.* 99.3, pp. 563–591. DOI: [10.1007/s10107-003-0467-6](https://doi.org/10.1007/s10107-003-0467-6).
- Tsoukalas and Mitsos (2014). “Multivariate McCormick relaxations”. In: *J. Glob. Optim.* 59.2-3, pp. 633–662. DOI: [10.1007/s10898-014-0176-0](https://doi.org/10.1007/s10898-014-0176-0).
- Vigerske and Gleixner (2017). “SCIP: Global optimization of mixed-integer nonlinear programs in a branch-and-cut framework”. In: *Optim. Methods Softw.* 33.3, pp. 1–31. DOI: [10.1080/10556788.2017.1335312](https://doi.org/10.1080/10556788.2017.1335312).
- Villanueva (2015). “Set-theoretic methods for analysis estimation and control of nonlinear systems”. PhD thesis. Imperial College London.
- Wechsung (2014). “Global optimization in reduced space”. PhD thesis. Massachusetts Institute of Technology.
- Wechsung, Schaber, and Barton (2014). “The cluster problem revisited”. In: *J. Glob. Optim.* 58.3, pp. 429–438. DOI: [10.1007/s10898-013-0059-9](https://doi.org/10.1007/s10898-013-0059-9).
- Yunt et al. (2008). “Designing man-portable power generation systems for varying power demand”. In: *AIChE J.* 54.5, pp. 1254–1269. DOI: [10.1002/aic.11442](https://doi.org/10.1002/aic.11442).
- Zlobec (2005). “On the Liu-Floudas Convexification of Smooth Programs”. In: *J. Glob. Optim.* 32.3, pp. 401–407. DOI: [10.1007/s10898-004-3134-4](https://doi.org/10.1007/s10898-004-3134-4).